



FACULTEIT LANDBOUWKUNDIGE
EN TOEGEPASTE BIOLOGISCHE
WETENSCHAPPEN



Academiejaar 2002 - 2003

**UREOLYTIC MICROBIAL CALCIUM CARBONATE
PRECIPITATION**

**UREOLYTISCHE MICROBIELE CALCIUMCARBONAAT-
PRECIPITATIE**

door

Frederik Hammes

Thesis submitted in fulfilment of the requirements for the degree of
Doctor (Ph.D.) in Applied Biological Sciences

Proefschrift voorgedragen tot het bekomen van de graad van
Doctor in de Toegepaste Biologische Wetenschappen

op gezag van

Rector: **prof. dr. apr. A. DE LEENHEER**

Decaan:
Prof. Dr. ir. H. VAN LANGENHOVE

Promotoren:
Prof. Dr. ir. W. VERSTRAETE
Prof. Dr. S.D. SICILIANO

Auteur en promotoren geven de toelating dit doctoraatswerk voor consultatie beschikbaar te stellen en delen ervan te kopiëren voor persoonlijk gebruik. Elk ander gebruik valt onder de beperkingen van het auteursrecht, in het bijzonder met betrekking tot de verplichting uitdrukkelijk de bron te vermelden bij het aanhalen van de resultaten van dit werk.

The author and the promoters give the authorization to consult and to copy parts of this work for personal use only. Every other use is subjected to the copyright laws. Permission to reproduce any material contained in this work should be obtained from the author.

Gent, November 2002

Promotoren

Auteur:

Prof. Dr. ir. W. VERSTRAETE

Frederik HAMMES

Prof. Dr. S. SICILIANO

TABLE OF CONTENTS

Notation index

Chapter 1

Introduction	1
--------------------	---

Chapter 2

Microbial calcium carbonate precipitation reviewed	5
--	---

Chapter 3

Species-specific ureolytic microbial calcium carbonate precipitation	31
--	----

Chapter 4

Microbial ecological impact alkaline pH, Ca ²⁺ , and calcium carbonate precipitation ..	58
--	----

Chapter 5

An exploratory study towards Ca ²⁺ removal from industrial wastewater using microbial calcium carbonate precipitation	78
--	----

Chapter 6

Bio-catalytic calcium removal from industrial wastewater – towards industrial application	92
---	----

Chapter 7

Characterisation of the microbial community and precipitation mechanism in a BCC reactor	113
--	-----

Chapter 8

General discussion and perspectives for future research	139
---	-----

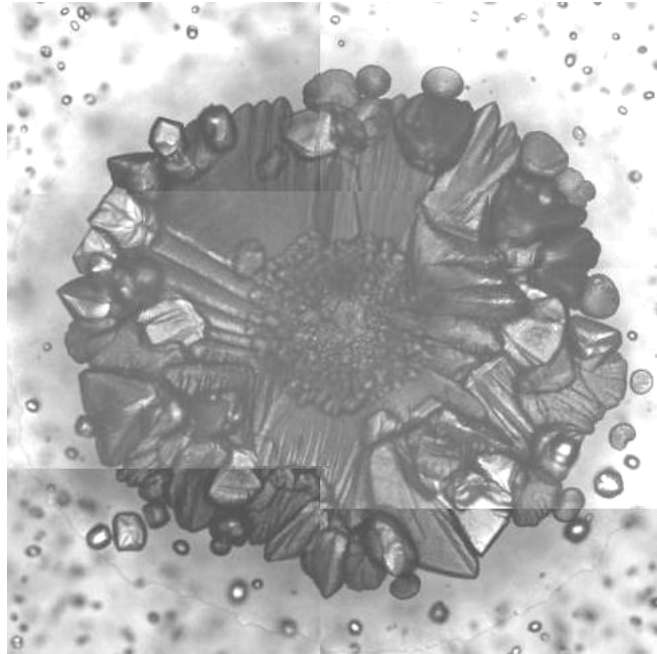
Bibliography **149**

Curriculum vitae

NOTATION INDEX

% G + C	Percent guanine + cytosine
ATP	Adenosine tri-phosphate
Bp	Base pairs (DNA size indicator)
BSA	Bovine serum albumin
CFU	Colony forming units
CNS	Crystal nucleation sites
COD	Chemical oxygen demand
CPB	Calcium precipitating bacteria
DGGE	Denaturing gradient gel electrophoresis
DIA	Digital image analysis
DIC	Dissolved inorganic carbon
DNA	Deoxyribonucleic acid
dNTP	Deoxynucleoside triphosphate
EPS	Extracellular polymeric substances
IAP	Ion activity product
HAP	Hydroxy-apatite
HRT	Hydraulic retention time
Kb	Kilo base pairs (DNA size indicator)
K_H	Henry's constant
K_{SO}	Solubility constant
LMG	Laboratory of Microbiology Gent (Culture collection)
LPS	Lipopolysacharides
LSI	Langelier saturation index
MAP	Magnesium ammonium phosphate
MCP	Microbial $CaCO_3$ precipitation
MLSS	Mixed liquor suspended solids
pCO_2	Partial pressure of CO_2
RSI	Ryznar stability index
SEM	Scanning electron microscopy
SIC	Soil inorganic carbon

TAN	Total ammonium nitrogen
TSS	Total suspended solids
PCR	polymerase chain reaction
Ppm	Parts per million
rDNA	Genes (DNA) coding for rRNA
RNA	Ribonucleic acid
SRB	Sulphate reducing bacteria
SRT	Sludge retention time
SS	Suspended solids
UASB	Up-flow anaerobic sludge bed (reactor)
UV	Ultra violet
VFA	Volatile fatty acids
VSS	Volatile suspended solids
WWT	Wastewater treatment
XRD	X-ray diffraction



In any weather, at any hour of the day or night, I have been anxious to improve the nick of time, and notch it on with my stick too; to stand on the meeting of two eternities, the past and the future, which is precisely the present moment; to toe that line.

Henry David Thoreau, Walden

ACKNOWLEDGEMENTS

Pretoria, 26 February 2003

It is with great joy and lots of nostalgia that I look back today on the last five years in Ghent. Many people contributed towards making these years truly unforgettable. Although the mere completion of this dissertation was probably the minimum expected achievement to show for those years, I do hope in some way it also reflects my utmost appreciation for the friendship, efforts and inputs of everyone.

I am not yet 30 years old, and already I am able to say that I have met, known, and worked with a truly special person. I spent numerous Saturday-morning meetings simply amazed at the unlimited stream of ideas and concepts, which could in somehow be related to my research. For this, all his help, guidance and loads of patience, I thank my promoter, Prof. Willy Verstraete. It is all much appreciated. Many thanks also to my co-promoter Prof. Steven Siciliano. Your endless enthusiasm for research has been inspirational beyond measure during the last 18 months of this work.

I thank the various people involved in the reading and exam commission for taking the time to effort to read this work and for their presence at the examination: Prof. J. Viaene, Prof. J. Vanderdeelen, Prof. P. Vanrolleghem, Prof. E. Vandamme, Prof. M. Verloo, Prof. C. Vandecasteele, Prof. E. Cloete.

A warm word of thanks to every single person at LabMET who, during the last five years, was subjected at one stage or another to yet another theory concerning bacteria, calcium and precipitation, or who just made available a willing ear to absorb some of the unavoidable frustrations of research or homesickness. Specific thanks to some of the guys that got me here: Jan Kielemoes - the best tutor one can ever hope to have had; Philippe Vandevivere; Patrick de Boever; Elke Vincke; Sarah Philips; Geert Rombaut and Youssouf Kalogo. Also specific thanks to people directly involved in my research: Nico Boon,

Arsene Seka, Kris van Hege, Tom Van de Wiele, Mariaan van Wambeke, Els Jolie; Greet Vandevelde; Siska Maertens.

For my two personal secretaries, Kris & Regine: Thank you, thank you and thank you again for everything.

My most sincere appreciation to the D'Haese family, for providing me with a second home in Belgium, and especially Marijke for putting up with me during the last few years. Also to all the guys at Wetteren Rugbyclub, which provided me with some of my fondest memories of Belgium, as well as a broken hand...

Aan Charl. Jy weet goed ek kan nie genoeg dankie se vir al die goeie tye nie. Jy is 'n vriend sonder gelyke. Baie dankie ook vir ma, pa en Johan vir al die ondersteuning, kuiers, rugby videos etc., wat die grrot verlang 'n bietjie minder gemaak het. En dan ook 'n baie baie baie grootste dankie vir Karen, wie se opoffering sekerlik die grootste was.

*Nog 'n najaar in die vreemde
met my drome sonder tal
en ek weet die winter kom weer
met sy sneeu wat ewig val
Maar hier buite sterf die somer
en ek sien die blare val
en ek weet iewers skyn die somer son
op die velde van Transvaal
(Koos du Plessis)*

SUMMARY

Microorganisms are capable of influencing the precipitation of carbonaceous minerals, specifically calcium carbonate (CaCO_3) in a number of ways. For example, microbial cell surfaces act as heterogeneous crystal nucleation sites in super-saturated CaCO_3 solutions. Alternatively, microbes can alter the saturation state of under-saturated solutions, thereby also catalysing mineral precipitation. The latter is the result of common microbial metabolic processes that bring about an increase in the pH and/or the concentration of dissolved inorganic carbon. Examples of such metabolic processes include photosynthesis, organic acid utilisation, and urea hydrolysis, thereby clearly encompassing a wide and diverse range of environments, microorganisms and metabolic processes. As a result, the actual function of bacteria in the precipitation process still remains unresolved today, while the (potential) impacts of microbial precipitation, both in natural environments and in anthropogenic settings, are still largely unexplored. But exactly this diversity also renders microbial mineralisation processes ideal for a number of biotechnological applications. This study investigated the possibility of applying ureolytic microbial CaCO_3 precipitation (MCP) as a novel tool for the removal of calcium from calcium-rich industrial wastewater.

The first part of this work aimed at creating a better understanding of the fundamental principles of ureolytic MCP. Central to this was the enzymatic reaction of bacterial urea hydrolysis, and the impact thereof on the crystallisation of CaCO_3 . It was observed that when pure cultures of ureolytic bacteria were cultivated on agar amended with urea and calcium, morphological different crystal aggregates developed inside colonies of different isolates. Such apparent species-specific precipitation could be of major natural historical significance for example in the characterisation of microbial fossils, or towards specific biotechnological applications of MCP. A novel application of PCR-DGGE was used to study urease gene diversity amongst the isolates. This approach revealed significant differences between the various isolates. In several cases, multiple bands appeared on the DGGE, suggesting the presence of different urease genes in these isolates. This latter

finding was especially of interest, since no previous study was able to indicate the occurrence of urease isozymes within a single bacterium. The majority of the crystallisation differences could be attributed to urease gene diversity, with concomitant variations in the substrate affinity, and maximum hydrolysis rate for the respective isolates. Another interesting result from this section of the work was that for certain isolates, urease activity increased up to 10-fold in the presence of 30 mM calcium, coinciding with characteristic crystal formation for these isolates. This latter result established a first link between the environment (high concentration calcium ions) and the biological process (urea hydrolysis) that results in eventual precipitation. This topic was further explored, and the effect of a typical precipitation environment (high pH and high Ca^{2+} concentration), as well as the direct and indirect effects of CaCO_3 precipitation, on survival and growth of pure cultures was investigated. It was hypothesised that calcium ions become toxic to bacteria under alkaline pH conditions, and that precipitation of CaCO_3 thus could be a cation detoxification process. This hypothesis was vindicated to some extent via comparative growth experiments, and the suggestion was made that the link between environment, bacterium and precipitation is energy (ATP required for detoxification). Not only did this reinforce the previous suggested theories of ATP-driven calcification, but it also suggested a plausible function of this process within the ecology of the precipitating organisms.

The second part of this dissertation concerned the development of a biotechnology for calcium removal from paper-recycling wastewater using ureolytic MCP. Calcium-rich industrial wastewater poses a significant problem to industries, especially those following the current tendency of water circuit-closure. These problems include the malfunctioning of aerobic and anaerobic reactors, and especially severe scale formation in pipelines and on heat exchangers. A laboratory-scale reactor (termed a bio-catalytic calcification reactor (BCC)) was developed, which comprised calcareous sludge (functioning as crystal nucleation sites) with high microbial ureolytic activity. These reactors were fed with wastewater contained about 12 mM Ca^{2+} , and additionally dosed with 8.3 mM urea. Even though the anaerobic wastewater was saturated as such with respect to CaCO_3 , urea addition and hydrolysis were shown to be prerequisites for CaCO_3 precipitation. Almost all (85 – 90 %) of the soluble calcium was precipitated as calcite, and removed through sludge

sedimentation in the treatment reactor. This bio-catalytic process presents an uncomplicated, efficient and economic feasible method for the removal of calcium from industrial wastewater. A pilot plant of this system is currently under construction, which would in time validate the industrial applicability thereof.

In the final part of this work, BCC reactor evolution from initialisation to optimisation over a six-week period was characterised. Denaturing gradient gel electrophoresis of 16S rRNA genes revealed a dynamic evolution in the microbial community structure of the calcareous sludge, eventually dominated by a few species including *Porphyromonas* sp., *Arcobacter* sp. and *Bacteroides* sp. Four to five weeks were required for the establishment of optimal reactor performance, which coincided with 15 times increase in urease activity. Moreover, urease hydrolysis in the optimal period was directly proportional to Ca²⁺ removal. Epi-fluorescence and scanning electron microscopy showed that the calcareous sludge was colonised with living bacteria, as well as the fossilised remains of organisms, thus suggesting that precipitation event is localised in a micro-environment, due to colonisation of the crystal nucleation sites (calcareous sludge) by the precipitating organisms.

This study uncovered several interesting aspects of ureolytic MCP. Most importantly, it elucidated the potential of applying this natural phenomenon in the treatment of complex industrial wastewater, specifically towards calcium removal.

SAMENVATTING

Micro-organismen kunnen de precipitatie van carbonaat mineralen, meer bepaald calcium carbonaat (CaCO_3), op verschillende manieren beïnvloeden. Enerzijds kunnen celoppervlakken optreden als heterogene kristal nucleatiesites voor oververzadigde CaCO_3 -oplossingen en anderzijds kunnen microben ook de verzadigingstoestand van onderverzadigde oplossingen wijzigen waardoor ze eveneens de precipitatie van mineralen katalyseren. Dit is het gevolg van gewone microbiële metabolische processen die een stijging van de pH en/of een stijging van de concentratie van opgeloste anorganische koolstof veroorzaken. Voorbeelden van dergelijke processen zijn fotosynthese, verbruik van organische zuren en hydrolyse van ureum en ze omvatten daarom een uitgebreide en diverse reeks van milieus, micro-organismen en metabolische processen. De eigenlijke functie van de bacteriën in de precipitatieprocessen is nog steeds niet gekend. Ook de (potentiële) impact van microbiële precipitatie, in natuurlijke en antropogene milieus, werd tot nog toe weinig bestudeerd. Door hun grote diversiteit zijn microbiële mineralisatieprocessen ideaal voor een aantal biotechnologische toepassingen. Deze studie onderzoekt de toepassingsmogelijkheden van ureolytische microbiële CaCO_3 -precipitatie (MCP) voor het verwijderen van calcium uit calciumrijk industrieel afvalwater.

In het eerste deel van dit werk worden de fundamentele principes van ureolytische MCP uitgelegd. De enzymatische reactie van de bacteriële ureumhydrolyse en de impact hiervan op de kristallisatie van CaCO_3 stond hierbij centraal. Er werd aangetoond dat wanneer ureum en calcium werden toegevoegd aan zuivere culturen van ureolytische bacteriën, zich morfologisch verschillende kristalaggregaten vormden binnen de kolonies van verschillende isolaten. De precipitatie bleek soort-specifiek te zijn, wat belangrijk kon zijn voor onder andere de karakterisatie van microbiële fossielen of voor specifieke biotechnologische toepassingen van MCP. Een nieuwe toepassing van PCR-DGGE werd gebruikt om de diversiteit van de ureumgenen onder de isolaten te bestuderen. Hieruit bleek dat de verschillende isolaten significant verschillen. In meerdere gevallen vertoonden

de DGGE profielen verscheidene banden, wat wees op de aanwezigheid van verschillende urease genen in deze isolaten. Deze bevinding was van specifiek belang omdat de aanwezigheid van urease isozymen in één afzonderlijke bacterie nog nooit werd aangetoond. In de meeste gevallen konden de verschillen in kristallisatie worden toegeschreven aan de diversiteit in ureasegenen, met de bijhorende variatie in affiniteit voor substraten en de maximale hydrolysesnelheid van de respectievelijke isolaten. Ook kon in dit deel van het werk voor bepaalde isolaten worden aangetoond dat de urease-activiteit werd vertienvoudigd in aanwezigheid van 30 mM calcium. Dit komt overeen met een karakteristieke kristalformatie in deze isolaten. Hier werd voor het eerst het verband gelegd tussen omgevingsfactoren (de hoge concentratie aan calcium ionen) en de biologische processen (ureumhydrolyse) die de precipitatie veroorzaken. Om dit verder te onderzoeken, werd het effect geanalyseerd van een omgeving die typisch is voor precipitatie (hoge pH en hoge Ca^{2+} -concentratie) en de directe en indirecte effecten van CaCO_3 -precipitatie op het overleven en de groei van pure culturen. Er werd verondersteld dat calciumionen toxisch werden voor de bacteriën bij alkalische pH, waarop de precipitatie van CaCO_3 een kationisch detoxificatieproces kon zijn. Deze veronderstelling werd gedeeltelijk bevestigd door vergelijkende groei-experimenten. Er werd daarbij ook gesuggereerd dat energie (ATP nodig voor detoxificatie) de link vormt tussen omgeving, bacterie en precipitatie. Dit versterkt de theorieën van ATP-gestuurde calcificatie en de mogelijke functie van deze processen in de ecologie van de precipiterende organismen.

Het tweede deel van deze thesis behandelt de ontwikkeling van een biotechnologie voor het verwijderen van calcium in afvalwater van de recyclage van papier door gebruik te maken van ureolytische MCP. Vele industriële bedrijven hebben problemen met industrieel afvalwater dat rijk is aan calcium (vooral ook omdat de bedrijven steeds meer werken met gesloten watercircuits). Problemen die kunnen optreden zijn het slecht functioneren van aërobe en anaërobe reactoren en vooral scaling van pijpleidingen en warmtewisselaars. Er werd een reactor op laboschaal ontwikkeld (de bio-catalytische calcificatie reactor (BCC)) die calciumrijk slib bevatte met een hoge microbiële ureolytische activiteit, functionerend als kristal nucleatiesite. De reactoren werden voorzien van afvalwater met gemiddeld 12 mM Ca^{2+} , waaraan 8,3 mM ureum werd toegevoegd. De toevoeging en hydrolyse van ureum bleken nodig om de CaCO_3 -

precipitatie op gang te brengen, ook al was het anaëroob afvalwater verzadigd ten aanzien van CaCO_3 . Vijfentachtig tot negentig procent van het opgeloste calcium werd neergeslagen als calciëet, en werd verwijderd door de slibsedimentatie in de reactor. Dit bio-catalytisch proces is een eenvoudig, efficiënt en economisch haalbare methode om calcium te verwijderen uit industrieel afvalwater. Een pilootopstelling van het systeem is op dit ogenblik in aanbouw en kan op termijn de industriële toepasbaarheid van het concept valideren.

In het laatste deel van dit werk wordt de overgang van de BCC reactor van initialisatie tot optimalisatie (periode van zes weken) gekarakteriseerd. De dynamische evolutie van de microbiële structuur in het kalkrijke slib werd aangetoond door DGGE van 16S rRNA genen. Uiteindelijk bestond de microbiële gemeenschap in het slib uit enkele *Porphyromonas sp.*, *Arcobacter sp.* en *Bacteroides sp.* Vier tot vijf weken waren nodig om het niveau te bereiken waarop de reactor optimaal werkt, waarbij de ureaseactiviteit steeg tot 15 keer de initiële activiteit. De urease hydrolyse in de optimale periode was recht evenredig met het verwijderen van Ca^{2+} . Epifluorescentie en scanning elektronen microscopie toonden aan dat het kalkrijke slib werd gekoloniseerd door levende bacteriën en gefossiliseerde overblijfselen van organismen. Dit veronderstelt dat de precipitatie zich voordoet in een micro-omgeving, door de kolonisatie van de kristal nucleatiesites (kalkrijke slib) door de precipiterende organismen.

Deze studie bespreekt een aantal interessante aspecten van het ureolytische MCP. Het toont eveneens het potentieel aan van het gebruik van deze natuurlijke processen in de behandeling van complex industrieel afvalwater, vooral voor het verwijderen van calcium.

Chapter

1

INTRODUCTION

INTRODUCTION

Bacteria are primary agents of geochemical change due to their high surface area to volume ratio, widespread and abundant distribution, evolutionary adaptiveness, and incredible diverse enzymatic and nutritional possibilities (Warren and Haack, 2001). Carbonaceous minerals are commonly found in oceans, soils and geological formations, and as such, represent a significant fraction of the global carbon pool. For example, Eswaran *et al.* (2000) estimated the quantity of the soil inorganic carbon pool (referring mainly to carbonates) at between 700 and 900 Pg (= 10^{15} g), while it is believed that carbonate minerals constitute as much as 7 % of the global terrestrial mass (Boughriet *et al.*, 2000). Though mineral carbonates have a rather low turnover rate, they are regarded as amongst the most reactive minerals on earth, and as such are constantly involved in the processes of dissolution and precipitation, thereby fulfilling a dynamic component of the global carbon cycle (Figure 1.1). More than sixty carbonate minerals are known, most commonly represented by calcium carbonate (CaCO_3) (Deer *et al.*, 1960).

Initially absent from Figure 1.1 though, was the underestimated role of microorganisms in the precipitation of mineral carbonate. Microbiological involvement in CaCO_3 precipitation has come to prominence at the beginning of the previous century (Feldmann, 1997; Drew, 1914), yet for decades it remained mostly restricted to geological and

geomicrobiological characterisations of natural carbonate rocks. However, the last two decades witnessed a noticeable progression in this field of study, which can be attributed to:

- (1) An increased recognition of the global contribution of microbes to carbon cycling, specifically within the context of global warming (Whalen *et al.*, 2002; McGenity and Sellwood, 1999);
- (2) The suggestion that microbial precipitates can be used to study past-life, also from extra-terrestrial samples (McKay *et al.*, 1996);
- (3) The development of innovative technological applications involving microbial precipitation (Castanier, 1995; Ferris and Stehmeier, 1993);
- (4) Advances in microbiological research techniques, noticeably microscopy and molecular microbiology (McGenity and Sellwood, 1999);

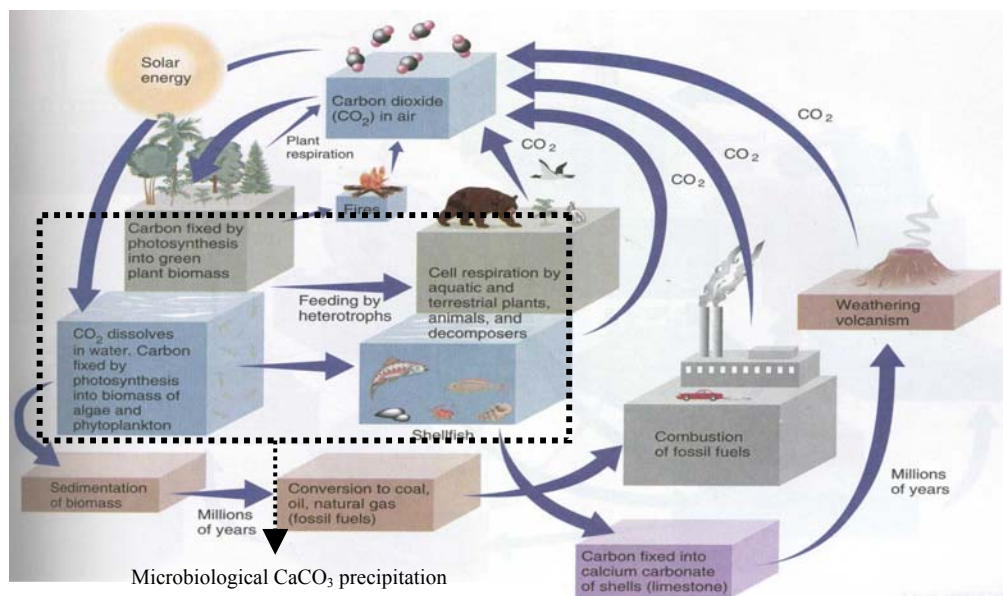


Figure 1.1. The carbon cycle (adapted from Nebel and Wright, 1998)

Microbiological CaCO₃ precipitation (MCP) have been linked to numerous microbial species, representing extremely diverse environments. This has led to a large degree of uncertainty still surrounding the actual role of bacteria in the precipitation process (Camoin, 1999; McGenity and Sellwood, 1999). Part of the diversity in opinions is caused by the fact that MCP often involves a combination of several research disciplines such as

geology, crystal chemistry, aquatic chemistry, microbial ecology and microbial technology, and studies often lack the interdisciplinary approach that is essential to this field of research (McGenity and Sellwood, 1999).

HYPOTHESIS AND AIMS A completely un-exploited, certainly under-studied, possible application field for MCP was identified in the wastewater industry, namely for the precipitation-removal of calcium (as CaCO_3) from Ca^{2+} -rich industrial wastewater. From the multitude of possible MCP mechanisms/pathways (discussed in Chapter 2), urea hydrolysis was chosen as best suited for both research and industrial purposes. The primary aim of this dissertation was to assess and develop an industrial-orientated calcium removal/recovery technology, based on ureolytic MCP. However, the importance of improving the fundamental understanding of various aspects (microbiology, ecology, enzymology, and chemistry) of this process, had not gone unnoticed, and formed the secondary aims of this research.

OVERVIEW CHAPTER 2 provides a broad review of the most important literature concerning MCP. The aims of this chapter were to (1) underpin the basic chemical principles governing CaCO_3 precipitation; (2) position CaCO_3 precipitation within the wider field of microbial mineral formation; (3) elucidate the dynamics (environments, pathways, species) within this field; and (4) contextualize ureolytic MCP amongst these. Furthermore, recently developed biotechnological applications involving MCP are also discussed. CHAPTER 3 presents a detailed study of some of the major aspects of ureolytic MCP based on precipitation in synthetic media by pure cultures of natural isolates. In this chapter, specific focus is given to the apparent observation of species-specific CaCO_3 precipitation, and the primary parameters that can contribute to this phenomenon. In CHAPTER 4, the effects of precipitation environments and CaCO_3 precipitation as such on the microbial ecology of the precipitating organisms was determined. Whether bacteria precipitate minerals with ecological “intention”, or whether this is an unwanted side-reaction which still affects the micro-organisms positively or adversely, is not only of major fundamental interest, but also critical towards any biotechnological application of this phenomenon. CHAPTER 5 presents the results from the first laboratory-scale study concerning the application of ureolytic MCP in the treatment of calcium-rich industrial

wastewater. The sole purpose of this chapter was to assess whether sufficient potential exists to warrant further investigation along this line of research. That indeed being the case, CHAPTER 6 presents the development of a laboratory-scale sequential batch reactor for calcium removal from industrial wastewater. These reactors are termed bio-catalytic calcification (BCC) reactors. In this chapter, the emphasis was on the practical wastewater parameters and engineering aspects of this process, while some theoretical modelling and a brief economic assessment of the process are also included. CHAPTER 7 completes the BCC study with an investigation into the microbiological component thereof. This includes a study of the adaptation of the microbial population and urease genes in the reactor, which thereby links up with the pure culture work done in Chapter 3. In CHAPTER 8, a succinct overview of the most important findings of the various chapters is presented, and these are placed within context of one another and the global study on microbial carbonate precipitation. Perspectives on future research possibilities within this field are also given.

ACKNOWLEDGEMENTS The application section of this research was carried out with financial support and collaboration from VPK (Oudegem, Belgium) and AVECOM NV (Belgium). I am specifically indebted to J-P. Van Eeckhoorn (VPK), A. Deschildre (VPK), Mariane van Wambeke, Els Jolie and Greet Vandevelde for technical assistance. For research assistance, I sincerely thank Prof. J. De Villiers (University of Pretoria, South Africa), Prof. E. Van Ranst (RUG), Prof J. Vanderdeelen (RUG), Dr. Nico Boon, Dr. Arsene Seka, Stefaan de Knijff and Maarten Tavernier. [Link to Contents](#) [Link to Chapter 2](#)

MICROBIAL CALCIUM CARBONATE PRECIPITATION REVIEWED

Redrafted from:

- (1) F. Hammes and W. Verstraete. 2002. Key roles of pH and calcium metabolism in microbial carbonate precipitation. *Re/Views in Environmental Science & Bio/Technology* 1, 3-7.

ABSTRACT *Numerous microbial species from vastly diverse environments have previously been associated with calcium carbonate (CaCO₃) precipitation, resulting in much controversy about the actual role of bacteria in the precipitation process. This chapter describes the basic chemical principles of CaCO₃ precipitation, and shows that it concerns essentially four key factors: (1) the concentration of dissolved inorganic carbon, (2) the pH, (3) the concentration calcium ions (Ca²⁺), and (4) crystal nucleation site development. Several microbial metabolic processes directly influence the first three factors, while the physical and chemical characteristics of bacterial cells render them ideal crystal nucleation sites. These microbial influences on CaCO₃ precipitation are reviewed, along with emerging biotechnological applications of this phenomenon.*

THE BASIC PRINCIPLES OF CaCO₃ PRECIPITATION

Dissolved inorganic carbon (DIC)

Carbon dioxide (CO₂) is an abundant molecule in the earth's atmosphere ($p\text{CO}_2 = 10^{-3.4}$ atm), which continuously and dynamically interact with aqueous systems by dissolving as aqueous CO₂, followed by further speciation as bicarbonate (HCO₃⁻) and carbonate (CO₃²⁻) depending on several environmental factors (Equation 2.1). For the purpose of this study, the various dissolved CO₂ species will collectively be referred to as dissolved inorganic carbon (DIC).



The knowledge of only a few parameters of an aquatic system allows for rather accurate computations of individual DIC species (Stumm and Morgan, 1981). This data is in turn useful, for example, in the calculation of the likeliness of dissolution/precipitation reactions to occur, or the quantification of pH changes to a carbonate-buffered system, or (as is the case in this work) to demonstrate the impact of a biological process on such a system. Comprehensive and detailed literature on speciation modelling is available (Morse and Arvidson, 2002; Stumm and Morgan, 1981). Depending on the required accuracy, these calculations can indeed become extremely complex, and should in such a case be done with either self-programmed computer software, or commercially available speciation software. Examples of the latter include MINEQL (<http://www.mineql.com>), ChemEQL, CHESS, JESS, EQ3/6 (<http://chess.ensmp.fr/chemsites.html>).

On the other hand, simplified calculations can be used for indicative purposes. Such an approach is described in this section, where ion activity coefficients were disregarded (thus assigned a value of “1”), which means that the system is governed only by the species concentration and the activity coefficients. Two possible scenarios are considered: (1) a closed system and (2) an open system.

A closed system implies the absence of gaseous CO₂ exchange with the atmosphere, and thus that the total carbon concentration (C_T) of the system remains constant and can be expressed as the sum of the individual DIC-species' concentrations (Equation 2.2).

$$C_T = [\text{CO}_{2(\text{aq})}] + [\text{H}_2\text{CO}_3] + [\text{HCO}_3^-] + [\text{CO}_3^{2-}] \quad (\text{Eq. 2.2})$$

The equilibrium reactions and constants governing DIC speciation in a closed aquatic system are shown in Table 2.1. Note that the brackets indicate ion activities, but that this will be interpreted as ion concentrations. This is in fact only accurate if the ion activity coefficients are equal to one, which is the case when the ionic strength of the solution is lower than 0.01 mol.L⁻¹.

Table 2.1. Chemical equilibrium reactions and constants governing the dissolution of CO₂ in aqueous media (Nillson and Sternbeck, 1999; Stumm and Morgan, 1981).

Equilibrium reaction	Constant	log K (25 °C, 1 atm)	
$\text{OH}^- + \text{H}^+ \rightleftharpoons \text{H}_2\text{O}$	$K_w = (\text{OH}^-)(\text{H}^+)$	= - 14.0	(Eq. 2.3)
$\text{CO}_{2(\text{aq})} + \text{H}_2\text{O} \rightleftharpoons \text{H}_2\text{CO}_3^*$	$K = \frac{(\text{CO}_{2(\text{aq})})}{(\text{H}_2\text{CO}_{3(\text{aq})}^*)}$	= - 2.84	(Eq. 2.4)
$\text{H}_2\text{CO}_3^* \rightleftharpoons \text{HCO}_3^- + \text{H}^+$	$K_1 = \frac{(\text{HCO}_3^-(\text{aq}))(\text{H}^+)}{(\text{H}_2\text{CO}_3^*(\text{aq}))}$	= - 6.352	(Eq. 2.5)
$\text{HCO}_3^- \rightleftharpoons \text{CO}_3^{2-} + \text{H}^+$	$K_2 = \frac{(\text{CO}_3^{2-}(\text{aq}))(\text{H}^+)}{(\text{HCO}_3^-(\text{aq}))}$	= - 10.329	(Eq. 2.6)

Note: $\text{H}_2\text{CO}_3^* = \text{CO}_{2(\text{aq})} + \text{H}_2\text{CO}_3$

The equilibrium constants are temperature dependant, and can be calculated according to Equations 2.7 – 2.9 (temperature in °F). Simply stated, these equations mean that if the temperature increase, then log K₁ and log K₂ values will also increase.

$$\log K_1 = -356.3094 - 0.06091964.T + 21834.37/T + 126.8339 \log T - 1684945/T^2 \quad (\text{Eq. 2.7})$$

$$\log K_2 = -107.8871 - 0.03252849.T + 5151.79/T + 38.9256 \log T - 563713.9/T^2 \quad (\text{Eq. 2.8})$$

Integration of Equations 2.2 – 2.6 allows the determination of ion fractions using the α values as defined in Equations 2.9 – 2.11.

$$[\text{H}_2\text{CO}_3^*] = \alpha_0.C_T \quad \alpha_0 = \left(1 + \frac{K_1}{[\text{H}^+]} + \frac{K_1K_2}{[\text{H}^+]^2}\right)^{-1} \quad (\text{Eq. 2.9})$$

$$[\text{HCO}_3^-] = \alpha_1.C_T \quad \alpha_1 = \left(\frac{[\text{H}^+]}{K_1} + 1 + \frac{K_2}{[\text{H}^+]}\right)^{-1} \quad (\text{Eq. 2.10})$$

$$[\text{CO}_3^{2-}] = \alpha_2.C_T \quad \alpha_2 = \left(\frac{[\text{H}^+]^2}{K_1K_2} + \frac{[\text{H}^+]}{K_2} + 1\right)^{-1} \quad (\text{Eq. 2.11})$$

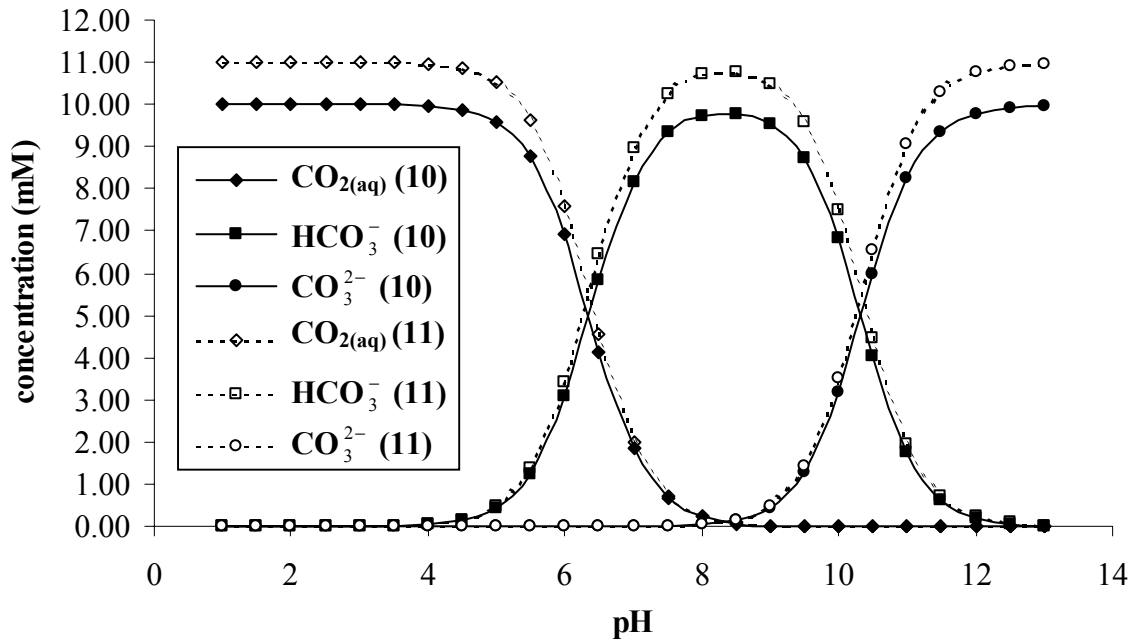


Figure 2.1. Dissolved inorganic carbon speciation as a function of the pH, calculated for a closed system containing 10 mM and 11 mM DIC respectively at 25 °C.

Thus, if the pH, C_T and temperature of a system are known, the various DIC species can be calculated. Figure 2.1 shows the graphical plot of such calculations, for a system containing respectively 10 mM and 11 mM DIC at 25 °C and various pH levels. At least two important logical deductions can be made from this image: (1) if the pH increases, the

concentration CO_3^{2-} increases; (2) if the concentration DIC increases in a buffered system, the CO_3^{2-} also increases.

An open system implies that exchange between gaseous CO_2 in the atmosphere and the solution is possible, which means that the partial pressure of CO_2 ($p\text{CO}_2$) should be taken into account. Using Henry's law constant (K_H), the concentration of aqueous CO_2 can be calculated according to Equations 2.12 - 2.14. Similarly, the combination of Equation 2.14 with Equations 2.9 – 2.11 allows the prediction of the various other DIC fractions (Equation 2.15 – 2.17).

$$\text{CO}_{2(g)} \rightleftharpoons \text{CO}_{2(aq)} \quad K_H = \frac{(\text{CO}_{2(aq)})}{(\text{CO}_{2(g)})} \quad (-\log K_H = -1.468) \quad (\text{Eq. 2.12})$$

$$\log K_H = 108.3865 + 0.01985076 \cdot T - 6919.53/T - 40.45154 \log T + 669365/T^2 \quad (\text{Eq. 2.13})$$

$$[\text{CO}_{2(aq)}] \approx [\text{H}_2\text{CO}_3^*] = K_H \cdot p\text{CO}_2 \quad (\text{Eq. 2.14})$$

$$C_T = \frac{1}{\alpha_0} K_H \cdot p\text{CO}_2 \quad (\text{Eq. 2.15})$$

$$[\text{HCO}_3^-] = \frac{\alpha_1}{\alpha_0} K_H \cdot p\text{CO}_2 = \frac{K_1}{[H^+]} K_H \cdot p\text{CO}_2 \quad (\text{Eq. 2.16})$$

$$[\text{CO}_3^{2-}] = \frac{\alpha_2}{\alpha_0} K_H \cdot p\text{CO}_2 = \frac{K_1 K_2}{[H^+]^2} K_H \cdot p\text{CO}_2 \quad (\text{Eq. 2.17})$$

Figure 2.2 depicts DIC speciation in an open system at 25 °C and atmospheric pressure ($p\text{CO}_2 = 10^{-3.4}$ atm). It is clear that the DIC of the system is only dependant on the partial pressure of CO_2 . Essentially, two important conclusions arise from this image. In a system sealed off from the atmosphere, for example an anaerobic reactor, a higher $p\text{CO}_2$ would mean a higher concentration of CO_3^{2-} . Similarly, if such water (over-saturated with DIC with respect to atmospheric $p\text{CO}_2$) were exposed to air, CO_2 stripping would occur to obtain equilibrium, which would imply a pH increase (Sawyer *et al.*, 1994).

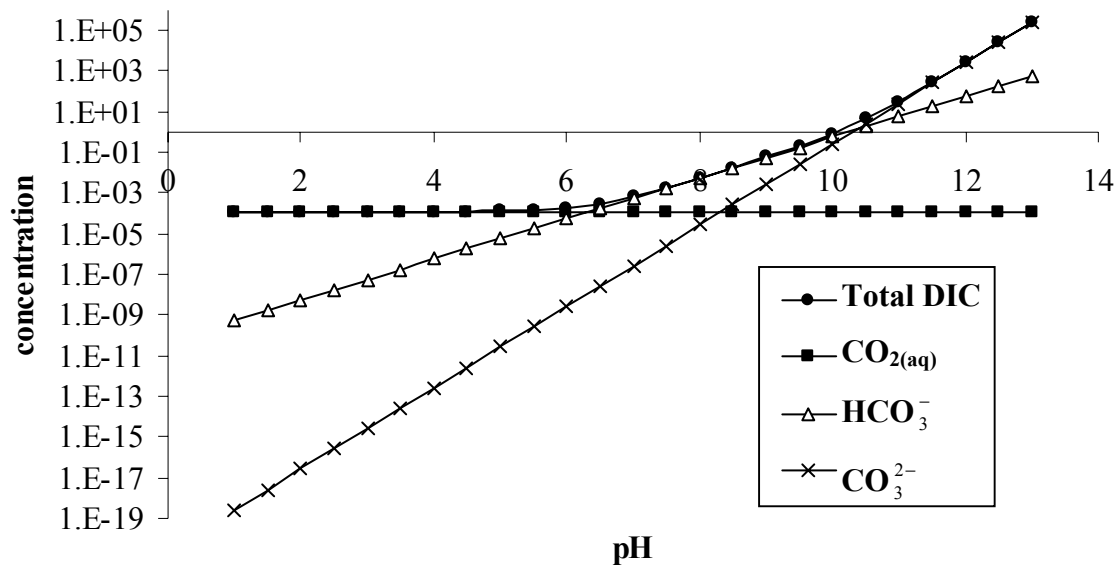


Figure 2.2. Dissolved inorganic carbon speciation in an open system as a function of the pH at 25 °C and atmospheric pressure.

Calcium ions and CaCO₃ precipitation

Calcium ions (Ca²⁺) are common in low concentrations (0 - 50 ppm) in almost all surface waters, wastewater, groundwater and soils. In higher concentrations (100 – 2000 ppm), it is found in oceans, saline lakes and saline soils (Grobe and Machel, 2002). Anthropogenic sources or water rich in calcium (500 – 1500 ppm) includes effluents from reverse osmosis, bone processing and paper recycling industries, and also even drinking water supplies (Habets and Knelissen, 1997; Van Langerak *et al.*, 1997). Calcium ions can precipitate in a number of mineral forms such as calcium carbonate (CaCO₃), hydroxyapatite (Ca₅OH(PO₄)₃) and carbonate-apatite (Ca₅(PO₄)₃CO₃). Biological influences on such precipitation are well known e.g. mollusc shells, vertebrate teeth and bones, and coral reefs (Suzuki *et al.*, 2002; Hunter, 1996). Calcium containing minerals can also dissolve naturally, or under biological influence, for example sulphuric acid corrosion of concrete, driven by *Thiobacillus* species (Monteny *et al.*, 2000).

These biologically influenced precipitation and dissolution processes are equilibrium reactions, governed by solubility constants. The solubility constant for CaCO_3 is temperature dependent and defined by Equation 2.19 (Van Haandel and Lettinga, 1994). The interpretation of Equation 2.19 is that a higher temperature results in a higher K_{SO} value, thus favouring the precipitation reaction. Note also that several authors interpret K_{SO} values as a function of the complexity of the system: in seawater and anaerobic effluent for example, K_{SO} values of respectively 6.2 and 6.7 have been reported (Van Haandel and Lettinga, 1994; Stumm and Morgan, 1981). Although this approach is erroneous – it is in fact the ion activities which change and not the K_{SO} values – it does allow for simplistic calculations of speciation in such environments. Comparison of the ion activity product (IAP) (Equation 2.20) with the solubility constant can define the saturation state (Ω) of a system (Equation 2.21) (Morse and Arvidson, 2002).



$$K_{\text{SO}} = [\text{Ca}^{2+}][\text{CO}_3^{2-}] = 4.83 \times 10^{-9} \quad (\text{calcite, } 25^\circ\text{C}) \quad (\text{Eq. 2.19})$$

$$\text{IAP} = (\text{Ca}^{2+})(\text{CO}_3^{2-}) \quad (\text{Eq. 2.20})$$

$$\Omega = \text{IAP}/K_{\text{SO}} \quad (\text{Eq. 2.21})$$

$\text{IAP} > K$: over-saturated system (precipitation is likely)

$\text{IAP} = K$: equilibrium

$\text{IAP} < K$: under-saturated system (dissolution is likely)

As stated earlier, the ion activities will be disregarded for the purposes of this study, and therefore the CO_3^{2-} concentration (Equations 2.11 or 2.17) will be used directly together with the soluble calcium concentration for the estimation of the saturation state of a given system.

Crystal nucleation site (CNS) development and crystal growth

Above, it was shown that the saturation state of a Ca^{2+} - H_2O - CO_2 system could be calculated and defined. However, over-saturation represents only the first step in a series of

events leading to eventual crystal formation (Stumm and Morgan, 1981). Even if the concentration of mineral ions in a solution gradually increases and exceeds the solubility product of a solid mineral phase, insoluble precipitates will not normally form until a certain degree of super-saturation has been achieved. Stable nuclei can only be formed after an activation energy barrier has been surmounted. The process during which the maximum free energy is attained is known as nucleation, and involves the growth of critical nuclei which are unstable relative to re-solution (Ferris and Stehmeier, 1993). Nucleation may occur either homogeneously or heterogeneously. In homogeneous nucleation reactions, critical nuclei are formed by random collisions of ions or atoms in solution. Conversely, heterogeneous nucleation involves the formation of critical nuclei on surfaces of foreign solids which enhance nucleation (Ferris and Stehmeier, 1993; Stumm and Morgan, 1981).

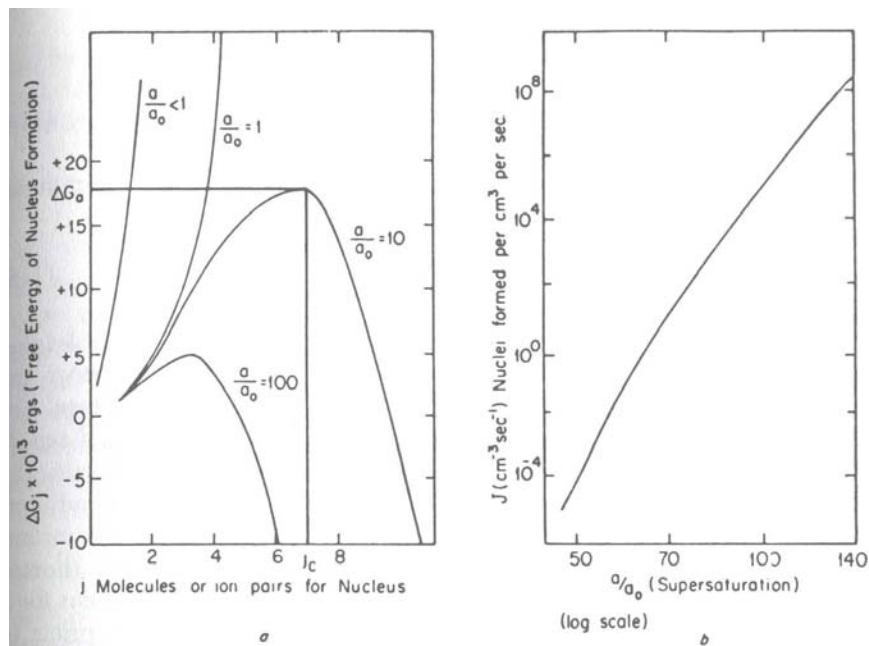


Figure 2.3. The effect of saturation on the free energy barrier during homogenous nucleation (left) and the resulting impact thereof on the rate of nucleation (right) (Stumm and Morgan, 1981).

Figure 2.3 illustrates the effect of over-saturation on homogeneous nucleation. Simply stated, it means that saturation of at least 100 times above the K_{SO} values is required before crystallisation proceeds at a detectable rate.

Once the critical nucleus is formed, further increases in the number of ions (associated with the nucleus) are accompanied by a decrease in free energy. This process is generally referred to as crystal growth, during which material is deposited on the crystal surface. This may include foreign material such as other divalent cations (Mg^{2+} , Sr^{2+}), anions (e.g. PO_4^{3-}) or organic macromolecules that can be incorporated in the crystal lattice. These inclusions may have an inhibitory effect on crystal growth (Kawaguchi and Decho, 2002). The final step is ripening, during which small crystallites convert to large crystals (Stumm and Morgan, 1981).

More than 60 different carbonate minerals are known, which include calcite (CaCO_3), dolomite ($\text{CaMg}(\text{CO}_3)_2$), magnesite (MgCO_3), rhodochrosite (MnCO_3) and siderite (FeCO_3). CaCO_3 is one the most common, and can exist as five polymorphs. Aragonite and calcite are the most dominant forms found in natural environments (Figure 2.4), while vaterite forms at normal temperature and pressure but is metastable. The two other forms are calcite II and calcite III, which are synthetic CaCO_3 forms, known only to exist at high pressure (Deer *et al.*, 1966). Aragonite is often associated with biological precipitation, but calcite is less soluble and thus thermodynamically favourable, meaning that aragonite in time rearrange to form calcite. The specific K_{SO} values for aragonite can be determined from the free energy of formation thereof (Equation 2.18):

$$\Delta G_f^0(\text{aragonite}) = -1127.8 \text{ kJ}\cdot\text{mol}^{-1}$$

$$\Delta G_f^0 = -553.54 \text{ kJ}\cdot\text{mol}^{-1} - 52729 \text{ kJ}\cdot\text{mol}^{-1} - (-1127.8 \text{ kJ}\cdot\text{mol}^{-1}) = 46.36 \text{ kJ}\cdot\text{mol}^{-1}$$

$$\text{and } \Delta G_f^0 = RT \ln K_{\text{SO}}$$

$$K_{\text{SO}} = 7.24 \times 10^{-9}$$

Similarly, using a ΔG_f^0 (calcite) value of $-1128.8 \text{ kJ}\cdot\text{mol}^{-1}$, a K_{SO} value for calcite of 4.83×10^{-9} is obtained.

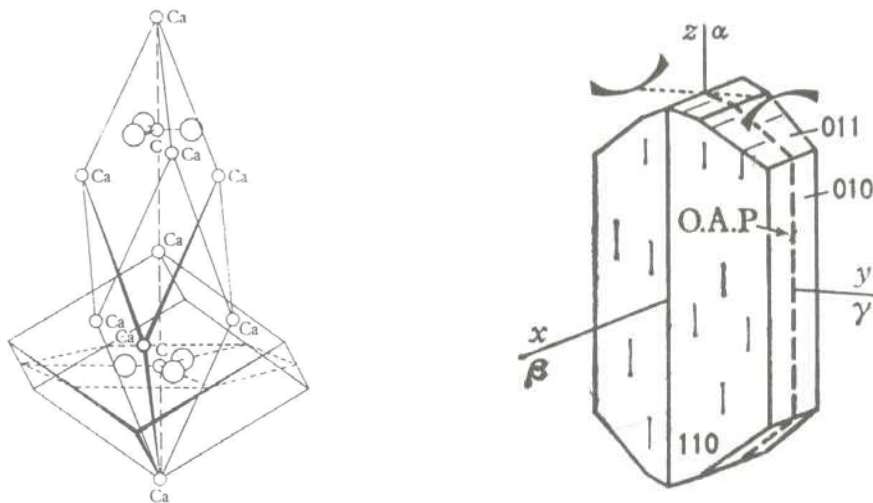


Figure 2.4. The crystal structure of calcite (left) and aragonite (right). The elongated cell represents the true rhombohedral unit cell of calcite (Deer et al., 1966)

Polymorphism is not the only aspect bringing about differentiation amongst CaCO_3 crystals. For example, calcite can form numerous different shapes by combining the basic forms of the positive rhombohedron, negative rhombohedron, steeply, moderately and slightly inclined rhombohedrons, various scalahedrons, prism and pinacoid to name a few of the more common forms. There are more than 300 crystal forms identified in calcite and these forms can combine to produce the thousand different crystal variations (<http://mineral.galleries.com>).

MICROBIOLOGICAL INFLUENCES ON CaCO_3 PRECIPITATION

Microbes can influence precipitation through altering almost any of the precipitation parameters discussed above, either separately, or in various combinations with one another. This may include the production of metabolic by-products influencing the saturation state of the system. It can also be a result of nucleation catalysis, with bacteria acting as

nucleation sites, while microbes can also affect crystal growth habit and polymorph selectivity (Castanier *et al.*, 1999; Douglas and Beveridge, 1998; Hunter, 1996).

Microbial production of DIC

Microbes continuously affect the saturation state of a given system by increasing the DIC concentration. Bacterial heterotrophic metabolism usually results in the complete oxidation of the organic carbon and electron donor, resulting in the production of CO₂ or HCO₃⁻ (Braissant *et al.*, 2002; Dawes and Sutherland, 1992). This has led to the generalised conclusion that most microorganisms are capable of precipitating CaCO₃ (Knorre and Krubein, 2000; Boquet *et al.*, 1973). This “mechanism” was also used to explain calcite precipitation by *Escherichia coli* and *Staphylococcus aureus* pure cultures in a nutritious medium with defined pH levels (Katkova and Rakin, 1994). Though CO₂ as such is acidic, it was demonstrated (Figure 2.1) that an increase of this component within a closed or buffered system would lead to an increase in the concentration of CO₃²⁻. For example, in up-flow anaerobic sludge bed (UASB) reactors, it is not uncommon to obtain DIC concentrations of up to 30 mM, due to microbial conversion of organic matter to CO₂ within a closed reactor system (Van Langerak, 1997; Van Haandel and Lettinga, 1994).

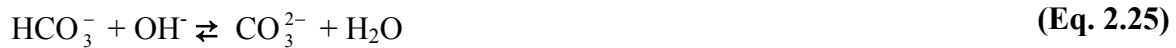
pH increase through autotrophic CO₂ utilisation

As shown in Figures 2.1 and 2.2 an increase in the pH of a system would directly imply an increase in the CO₃²⁻ concentration, leading to more favourable precipitation conditions. Autotrophic microorganisms consume CO₂ for the production of biomass. As depicted in Equation 2.22, this entails the removal of the acidic component (CO₂) from the system, which in turn would induce a re-active shift in the bicarbonate equilibrium towards carbonate, thereby resulting in a subsequent increase in the pH (Equation 2.23) (Erlich, 1998; Dawes and Sutherland, 1992).





Ferris and Thompson (1996) as well as Douglas and Beveridge (1996) described essentially similar reactions, in which hydroxyl ions are released as a result of microorganisms using bicarbonate ions intracellular as a carbon source. The hydroxyl ions are subsequently exchanged for bicarbonate ions over the cell membrane, where they react extracellularly with bicarbonate ions, producing carbonate ions (Equations 2.24 and 2.25).



Under such circumstances, precipitation could occur if soluble calcium ions are present in the system. A further model concerning photosynthetic induced precipitation is advocated by McConnaughey and Whelan (1997), specifically linking calcium transport to the above-mentioned reactions. This “pathway” is dealt with in a later section.

Castanier *et al.* (1999) distinguished between three types of autotrophic microorganisms utilising CO_2 : (1) methanogenic archaeobacteria, (2) sulphurous or non-sulphurous purple/green photosynthetic bacteria, and (3) cyanobacteria. Photosynthetic algae (e.g. *Nannochloris atomus* (Yates and Robbins, 1997)) and some aquatic plants (e.g. *Potamogeton* (McConnaughey and Whelan, 1997)) can also precipitate CaCO_3 via this pathway, but for the purpose of this study primarily bacteria will be discussed. Oxygenic photosynthesis is regarded as being by far the most prevalent precipitation-inducing reaction in natural environments (Douglas and Beveridge, 1996). This reaction is found in aqueous environments such as marine locations (Yan *et al.*, 1999), microbial mats of thermal hot springs (Arp *et al.*, 1999), and freshwater biofilms (Erlich, 1998; McConnaughey and Whelan, 1997). Bacteria which have been linked with this process include the cyanobacteria *Synechococcus* (Southam, 2000; Douglas and Beveridge, 1996; Ferris and Thompson, 1996), *Synechocystis* and *Scytonema* (McConnaughey & Whelan, 1997), and *Schizothrix* sp. (Kawaguchi and Decho, 2002).

Microbial processes increasing both the pH and DIC

(a) Organic acid utilisation

Some common species of soil bacteria use organic acids as their sole source of carbon and energy. Such acids include acetate, citrate, oxalate, acetate, glyoxylate, succinate, and malate and the consumption of these acids results in a pH increase for the system, together with a DIC increase, thereby leading to precipitation in the presence of calcium ions (Equations 2.26 – 2.28) (Braissant *et al.*, 2002; Knorre and Krubein, 2000).



Table 2.2. Examples of precipitation through organic acid utilisation

Microorganism	Acid	Mineral phase	Reference
<i>Pseudomonas fluorescence</i>	Citrate	Calcite and Vaterite	Anderson <i>et al.</i> (1992)
<i>Ralstonia eutropha</i> & <i>Xanthobacter autrophicus</i>	Ca-citrate Ca-oxalate	Calcite and Vaterite	Braissant <i>et al.</i> (2002)
<i>Flavobacter sp.</i> <i>Acinetobacter sp.</i>	Acetate		Ferrer <i>et al.</i> (1988)
<i>Vibrio spp.</i>	Ca-acetate	Mg-calcite	Rivadeneira <i>et al.</i> (1994)
<i>Nesterkonia halobia</i>	Ca-acetate	Dolomite, aragonite and calcite	Rivadeneira <i>et al.</i> (2000)
<i>Halomonas eurihalina</i>	Ca-acetate	Aragonite, calcite and Mg-calcite	Rivadeneira <i>et al.</i> (1998)
Heterotrophic microbial mat isolates	Ca-acetate	Calcite	Knorre and Krumbein (2000)

Organic acid utilisation is commonly used in microbial CaCO₃ precipitation experiments. Table 2.2 summarises some of the microbial strains, crystal types and organic acids which have been reported for this mechanism of precipitation during experiments under defined laboratory conditions. In all these examples, precipitation of CaCO₃ went together with an increase in the pH (up to 9.5 in some cases) in the precipitation medium. Evidently, numerous heterogeneous bacterial groups are linked to this precipitation mechanism. This has led Braissant *et al.* (2002) to speculate that this pathway might be extremely common in natural environments, due to the abundance of such low molecular weight acids in soils (produced by fungi and plants). It has also been suggested to be one of the main causes of calcite precipitation in biofilms exposed to landfill leachate rich in acetic acid (Cooke *et al.*, 1999).

(b) Dissimilatory sulphate reduction

Dissimilatory sulphate reduction, which is carried out by sulphate reducing bacteria (SRB), actually represents a combination of biological and chemical reactions to achieve an increase in both the DIC concentration and the pH. This reaction typically occurs in anaerobic environments rich in sulphate and organic matter (Castanier *et al.*, 1999). The reaction usually starts as a result of the dissolution of gypsum (CaSO₄·2H₂O/CaSO₄), which is a pure physico-chemical process (Equation 2.29), and which releases both sulphate and calcium ions. Under these circumstances, organic matter can be consumed by SRB carrying out sulphate reduction, and sulphide and metabolic CO₂ is released (Equation 2.30) (Peckman *et al.*, 1999; Wright, 1999).



However, as such the reaction leads to acidification (and thus in fact inhibition of precipitation) due to H₂S production (Machel *et al.*, 2001). Castanier *et al.* (1999) showed that removal of the produced hydrogen sulphide (H₂S) is a prerequisite for carbonate precipitation to occur. Discharge of the gaseous H₂S is a physico-chemical process that can

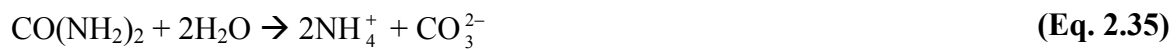
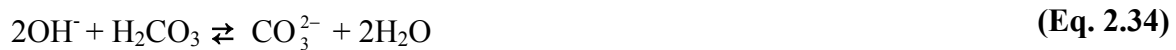
bring about the pH change. Also, in natural environments, sulphide will combine instantaneously with iron to produce pyrite and/or pyrrhotite, and this reaction is reportedly quite common during biological sulphate reduction in the presence of iron (Machel *et al.*, 2001; Wright, 1999). Microbiologically, H₂S can be converted by anoxygenic sulphide phototrophic bacteria to elemental sulphur (Castanier *et al.*, 1999), also leading to a pH increase, and subsequent precipitation. However, Machel (2001) argued that sulphate reduction most often occurs in environments that are buffered by chemical species other than DIC, thus leading to precipitation only as a result of the increase in DIC.

CaCO₃ precipitation via this pathway occurs in seawater, geological formations (Machel, 2001; Peckman *et al.*, 1999), in landfill leachates (Maliva *et al.*, 2000) and even during the biological treatment of acid mine drainage (Kaufman *et al.*, 1996). In geological formations, this often results in the characteristic “invasive” replacement of gypsum with CaCO₃ (Machel, 2001). Interestingly, in several of the described examples for this pathway, dolomite and aragonite, instead of calcite, seem to be the most predominant minerals to precipitate (Machel, 2001; Warthmann *et al.* 2000; Peckman *et al.*, 1999; Wright 1999). Dolomite formation is most interesting: up to date, only a few laboratory-scale simulations of microbial dolomite formation have been reported (Feldmann, 1997). While the governing processes of bacterial dolomite formation are not yet fully underpinned, Wright (1999) hypothesised that a key factor in this could be the accumulation of magnesium on bacterial cell walls. In a rather significant finding, Machel (2001) reported that it was possible to distinguish visually between CaCO₃ precipitated through biological sulphate reduction, compared to precipitates as a result of thermo-chemical sulphate reduction.

(c) Nitrogen conversion processes

Another heterotrophic pathway involves the nitrogen cycle, and more specifically the ammonification of amino acids, nitrate reduction, and urea degradation. These three mechanisms have in common the production of metabolic CO₂ and ammonia (NH₃), the latter leading to a pH increase (Castanier *et al.*, 1999; Abdelouas *et al.*, 1998). Urea or uric

acid hydrolyses is the most common form. The reaction takes place according to Equations 2.31 – 2.34, which are combined in Equation 2.35 (Burne and Chen, 2000; Wright, 1999).



This pathway is more often associated with precipitation in soils, groundwater and geological sediments (Fujita *et al.*, 2001; Abdelouas *et al.*, 1998), as well as precipitates linked to the urinary tract (Hedelin, 2002; Kramer *et al.*, 2000). Urea is the major nitrogenous waste product of most terrestrial animals, humans included. Human blood serum contains between 1 – 10 mM urea, and human urine up to 500 mM (Burne and Chen, 2000). The pathway of urea hydrolysis is the basis of the research presented in this thesis, and detailed information concerning the molecular, biochemical and enzymatic aspects of this process is presented in the relevant chapters.

A wide variety of microorganisms produce the urease gene. Ureolytic bacteria that have been associated with CaCO_3 (usually calcite) precipitation include *Bacillus pasteurii* (Stocks-Fischer *et al.*, 1999; Ferris and Stehmeier, 1993), *Pseudomonas* spp. and *Variovorax* spp. (Fujita *et al.*, 2001), and *Leuconostoc mesenteroides* (Ferris and Stehmeier, 1993). Abdelouas *et al.* (1998) associated the nitrifiers *Pseudomonas aeruginosa* and *P. stutzeri* with calcite and aragonite precipitation in natural groundwater.

In complex natural environments, the different metabolic pathways can also contribute together to induce precipitation. Wright (1999) described a specific case of dolomite precipitation in Australia involving microorganisms of all three major pathways discussed above. Dead photosynthetic cyanobacteria, together with other organic matter, were degraded by sulphate reducing bacteria, which resulted in the production and release of

DIC and ammonia (from amino-acid degradation). The latter was the principle cause of an increase in pH and thus in carbonate levels, which eventually lead to precipitation.

Microorganisms as crystal nucleation sites

Ferris and Stehmeier (1993) suggested that there is considerable geological evidence that microorganisms might function as crystal nucleating agents during mineral precipitation. Apart from the metabolic processes discussed above, microbes also specifically catalyse the nucleation of CaCO_3 by reducing the required activation energy barrier (for nucleus formation). Stumm and Morgan (1981) stated that the essence of this catalysis is that the surface of the heteronucleus (in this case the bacteria) should match well with that of the crystal. In other words, the interfacial energy between the bacteria and the crystal should be smaller than the interfacial energy between the crystal and the solution.

Due to the high surface-to-volume ratio of bacteria, they are ideal for crystal nucleation sites (Warren and Haack, 2001). A bacterium's ability to interact with metals is dependent on the types and the densities of functional groups, which are in turn affected by the cell wall composition, and the presence of S-layers, sheaths, capsules or extracellular polymeric substances (EPS). Gram-negative bacteria have cell membranes which are dominated by the presence of carboxylate groups, as well as phosphate moieties, resulting in a net-negative charge (Schultze-Lam *et al.*, 1996). Gram-positive bacteria have lipopolysaccharide (LPS) and peptidoglycan, also having a net-negative charge. The overall anionic nature of bacterial cells in most aquatic environments is a result of the pK_a values of the carboxyl and phosphoryl groups (4 – 7) (Warren and Haack, 2001; Ferris and Beveridge, 1985). Under normal conditions, divalent cations (Ca^{2+} ; Mg^{2+}) contribute to the stability of teichoic and teichuronic acid polymers, LPS, and S-layers. This reaction (binding of divalent cations to the cell wall) is the beginning of crystallisation (Southam, 2000). The formation of CaCO_3 moieties on the cell surface correlates with the moieties on a CaCO_3 crystal surface (Nilsson and Sternbeck, 1999), so that the heteronucleus (bacteria) does indeed match up with the crystal. Not only does the cell surface features of the bacteria contribute to crystal nucleation site formation, but also the influences of cellular processes on the immediate surroundings of the bacteria (Schultze-Lam *et al.*,

1996). As a result of an extremely low Reynold's number, microorganisms are always surrounded by a thin watery layer, which physically creates a micro-environment (Warren and Haack, 2001; Schultze-Lam *et al.*, 1996). This layer forms an interface between the microbial cell and the outside environment, in which concentrations of chemical species different to those of the outside environment can prevail. Figure 2.5 shows how the micro-environment principle was applied by Monger and Gallegos (2000) to explain classically observed filament encrustation in soil microbiota. This micro-environment concept can also be extended to include biofilm micro-domains or single bacterial colonies on plates (Schultze-Lam *et al.*, 1996; Merz-Preiß, 2000). Both Wright (1999) and McConnaughey and Whelan (1997) reported the potential of microorganisms to concentrate cations, while EPS are known to slow down diffusion of ions (HCO_3^- , CO_3^{2-} , Ca^{2+}), thus resulting in elevated localised concentrations (Kawaguchi and Decho, 2002). The result thereof is a localised effect on the saturation state of the solution, which is an essential component in overcoming the activation energy barrier during nucleation.

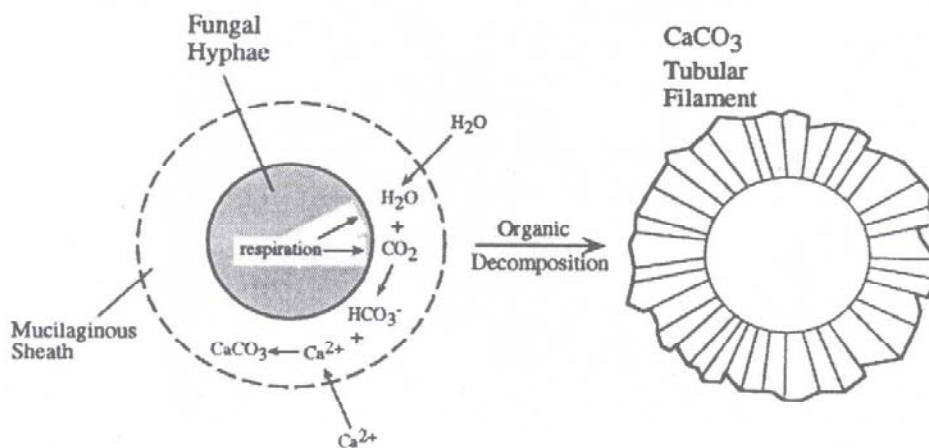


Figure 2.5. Fungal hyphae encrustation (Monger and Gallegos, 2000)

Stocks-Fischer *et al.* (1999) attributed much of the complexity surrounding microbial CaCO_3 precipitation to this cell-associated precipitation, while Arp *et al.* (1999) suggested that acting as crystal nucleation sites is the primary precipitating role of bacteria during mineral formation in super-saturated thermal hot-springs. However, these same authors also attributed no functional role to micro-environments and even indicated that EPS might

rather act inhibitory towards precipitation in that it slows down calcium transport towards the nucleation sites (in a super-saturated macro-environment). This latter view was shared by Knorre and Krumbein (2000). These authors reported that many bacteria are in fact poor crystal nucleation sites, and bacteria would rather tend to avoid precipitation, as this process would be detrimental to the cells.

Influences on crystal growth and maturation

The wide variation observed in the nucleation, growth habit and polymorph selectivity of biogenic CaCO₃, and the striking differences between these and synthetic CaCO₃, could be attributed to a high degree of control exerted by the organic matrix (extracellular polymers and associated proteins) (Brown *et al.*, 2000; Hunter, 1996). This impact is specifically ascribed to the interaction of biological macro-molecules with the crystal planes. For example, Hunter (1996) reported that the nucleation of calcite and aragonite commonly involves proteins with closely spaced aspartic acid residues. It was also shown that the binding of proteins and also polysaccharides to specific crystal faces inhibits the growth of the crystal in the direction perpendicular to that face, while similarly, polymorph selectivity has been attributed to the organic matrix. Experimental evidence for this phenomenon is not lacking. As early as 1960, Watube and Wilbur (1960) showed that the specific formation of aragonite in mollusc shells were a function of the protein matrix. More recently, Braissant *et al.* (2002) detected the specific formation of vaterite (in stead of calcite) during organic acid consumption by *X. autotrophicus*, which coincided with excessive slime production by this organism. These authors argued that the observed polymorphism could have been a result of viscosity changes due to slime formation, or specific components of the slime (in this case the slime contained mostly glucuronic acid). In a similar finding, Kawaguchi and Decho (2002) found aragonite formation by the marine cyanobacteria *Schizothrix* sp. to be directly related to EPS components. These authors emphasized the role of acidic proteins during aragonite formation, specifically proteins rich in aspartic acid and glutamic acid residues (Kawaguchi and Decho, 2002).

An ongoing argument of “active” versus “passive” precipitation

The diverse opinions on the role of bacteria in the CaCO₃ precipitation process are further flamed by theories of so-called “active” and “passive” precipitation. The extent of the controversy can be seen from the various definitions (or lack thereof), concerning “active” and “passive” precipitation. For example, Southam (2000) suggested a simple and logic approach by defining “passive” microbial mineralisation as being mineralisation as a result of bacterial cells acting as crystal nucleation sites, and “active” precipitation as that resulting from the production of metal-re-active by-products by bacteria. Knorre and Krumbein (2000), Novitsky (1981), and Boguet *et al.* (1973) all argued that even this should not be termed “active” precipitation, since the precipitation event is in essence unrelated to the microorganisms. The only function of the microorganisms is the provision of metabolic CO₂ and OH⁻ in their aqueous environment. In stark contrast to this, Ferrer *et al.* (1988), Rivadeneyra *et al.* (1998) and Morita *et al.* (1980), proposed “active” precipitation to occur, for example based on observations of polymorphism selectivity during laboratory scale experiments with selected pure cultures. These authors did not specify any mechanisms, apart from arguing that precipitation was not only an unwanted side-effect of microbial metabolism. Castanier *et al.* (1999) vaguely proposed a mechanism for this by defining “active” precipitation as a process linked to cation transport (presumably Ca²⁺) across cellular membranes, and “passive” precipitation all the above processes where metabolic products are formed. McConnaughey and Whelan (1997) concurred with this viewpoint, and hypothesised that algae and cyanobacteria used active calcium metabolism, coupled with photosynthetic MCP for the purpose of generating protons to assist the organisms in nutrient and bicarbonate uptake (Equations 2.36 and 2.37).



Merz-Preiß (2000) highlighted several other potential benefits for the precipitating organisms as a result of cyanobacterial calcification, arguing that this reaction is not

merely a side-effect of photosynthesis. Firstly, a 1:1 ratio of photosynthesis to calcification reduces alkalisation and depletion of dissolved CO₂ around the cells, thus serving as a pH buffer. A second possibility is that precipitation protects the bicarbonate pump, which could be inhibited by carbonate ions, while some attention has also been given to the possibility that a crystal layer might be a protective layer against UV radiation (Merz-Preiß, 2000).

These theories inevitably highlight the essential point to the argument: whether bacterial precipitation is an unwanted and accidental by-product of microbial metabolism (Knorre and Krumbein, 2000), or a specific process with ecological benefits for the precipitating organisms (Merz-Preiß, 2000; McConnaughey and Whelan, 1997). Knorre and Krumbein, (2000) reported that the precipitation process is detrimental to bacterial cells. Southam (2000) elaborated on the causes of this adverse effect, claiming that mineralisation affects the surface available for nutrient uptake and disrupts the proton motive force eventually. Apparently it often happens in mineralising environments that some bacteria are more extensively involved in the mineralisation process than others, and that the non-mineralising bacteria subsequently tend to persist in these environments (Southam, 2000). On the other hand, cellular defensive mechanisms against the detrimental effects of precipitation have been described. For example, Ferris and Beveridge (1985) reported a case where bacteria tended to produce an S-layer specifically in the presence of toxic metals. The result was that precipitation occurred on the S-layers, which were subsequently shed off by the organisms, guaranteeing ongoing survival. Southam (2000) reported a similar case for *Bacillus licheniformis*, which produce an anionic capsule to protect it against toxic metals through localised precipitation.

For the purpose of this study, the viewpoint is taken that MCP is indeed no more than the result of chemical reactions by metabolic cell products, or specific cell wall characteristics catalysing precipitation, unless the precipitation, or the control/inhibition thereof, holds some ecological benefits for the organism involved. A closer look at this is taken in Chapters 3 and 4.

IMPLICATIONS AND BIO-TECHNOLOGICAL APPLICATIONS OF MICROBIAL CaCO₃ PRECIPITATION

Biofilm formation, biofouling and biocorrosion

The impacts of microbiological processes on mineral dissolution/corrosion processes have been properly characterised for both anthropogenic and natural scenarios (Roberts *et al.*, 2002; Warscheid and Braams, 2002). However, only recently have scientists started to consider microbial mineral precipitation within this context, and initial reports seem to suggest that the contribution of microorganisms towards mineral precipitation might have been largely underestimated up to now (Braissant *et al.*, 2002; Castanier *et al.*, 2000). As is the case with biological corrosion processes in anthropogenic settings, unwanted mineral deposition could hold far reaching economic implications.

Biofilms are complex microbial associations consisting of bacteria and EPS, and which form on almost any exposed man-made surface (Stolz, 2000). Mineral precipitation in biofilms is a result of the trapping of sediments in the EPS, specific concentration of cations, and also due to the numerous possible microbial metabolic processes (as described above) (Decho, 2000; Stolz, 2000). A well-known example is the precipitation of ferromanganese deposits in water pipelines (Decho, 2000). In fact, in water (drinking, sewage, industrial effluents) distribution pipelines, biofilms are exposed to various concentrations of calcium ions, as well as sulphates, and nitrogenous compounds which may well give rise to CaCO₃ precipitation. The result would be excessive clogging of pipelines, and scale formation on mechanical equipment, resulting in process failure. Folk (1999) suggested a specific (but undefined) interaction between nanobacteria (0.03 – 0.3 µm) and aragonite scaling in water pipelines. Other common industrial examples include calcite and Mg-calcite precipitation during landfill leachate treatment (Maliva *et al.*, 2000; Cooke *et al.*, 1999).

Another consequence of mineral deposition in biofilms could be corrosion of stainless steel. Decades ago, directed CaCO₃ precipitation in water distribution systems were

considered a plausible corrosion inhibition technique (Langelier, 1937). This was based on the argument that homogenous CaCO_3 precipitation would bring about a protective layer on the steel surface. Biofilm associated precipitation would, however, not be homogenous, and recent studies have highlighted the role of patchiness, or micro-domains, in the onset of corrosion (Decho, 2000; Kielemoes *et al.* 2000).

Figure 2.6 shows a microscope photograph of a biofilm formed on stainless steel (type 316L) during 30 days exposure to Ghent city tap water and inoculated with *Leptothrix sp.* CaCO_3 deposits on the filamentous *Leptothrix* organisms can clearly be seen. Also note the resemblance between this CaCO_3 deposition and the model presented in Figure 2.5.

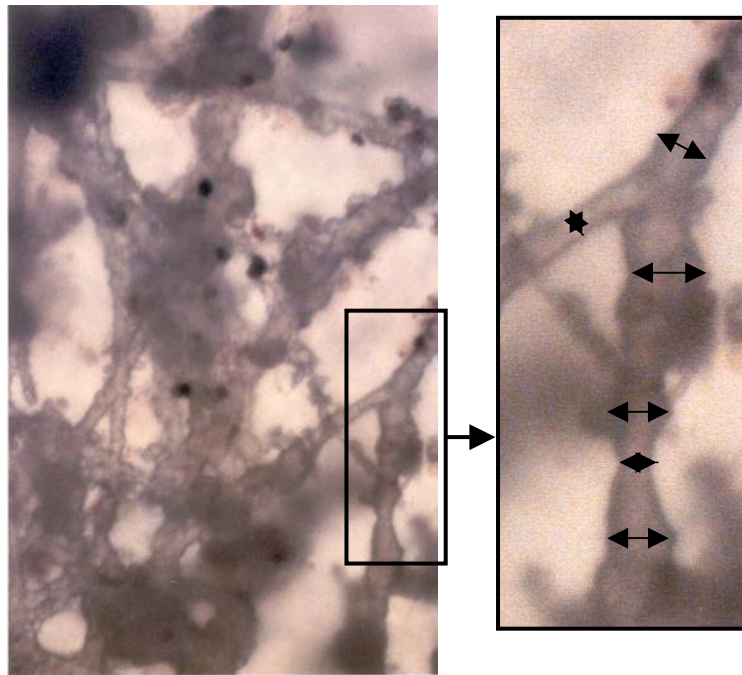


Figure 2.6. Microscopic image of the completely calcified filaments of a *Leptothrix sp.* biofilm growing on stainless steel (316L) surface exposed to Ghent city tap water ($\pm 110 \text{ mg}\cdot\text{L}^{-1} \text{ Ca}^{2+}$).

Mineral deposition in biofilms has specifically been characterised to occur on catheters inserted in the urinary track of humans during medical procedures (Hedelin, 2002). In this

instance, the environment (urine) contains calcium ($\pm 10 \text{ mg}\cdot\text{L}^{-1}$), magnesium ($\pm 5 \text{ mg}\cdot\text{L}^{-1}$), phosphorus ($\pm 20 \text{ mg}\cdot\text{L}^{-1}$), and especially urea ($\pm 200 \text{ mg}\cdot\text{L}^{-1}$), thereby favouring urease driven precipitation (Hedelin, 2002; Kramer, 2000). In fact, several studies have linked ureolytic precipitation to the initial formation of kidney stones in humans (Bichler *et al.*, 2002; Bradbury, 1998), while a recent study has also identified this mechanism to be at the basis of calcite and calcium-phosphate deposition (called calculus formation) in plaque-biofilms on teeth (Burne and Chen, 2000; Wong *et al.*, in press). In this case, the source of urea is saliva (1 – 20 mM) produced at about $1 \text{ L}\cdot\text{day}^{-1}$ by humans, while calcium ions could even arise from tooth decay (Burne and Chen, 2000).

Monument and building surfaces tend to accumulate inorganic and organic pollutants from the environment. The result is that bacteria use the organic pollutants as nutrients, forming natural biofilms on exposed building surfaces, which eventually results in the formation of crusts (up to several mm thick) and patinas on the surface (Urzi *et al.*, 1999; Rodriques-Navarro *et al.*, 1997). The impact of this can range from aesthetic damage to actual structural damage. The positive side to these adverse effects is that observations and understanding of the precipitation process have lead to the emergence of a variety of biotechnological applications.

MCP used for the restoration of sandstone monuments/buildings

Biominalisation has been developed as a useful tool in the restoration of sandstone/limestone buildings and monuments (Castanier *et al.*, 2000; Le Métayer-Levrel *et al.*, 1999). A first patented application in this field concerned the protection of such surfaces through the microbiological deposition of a protective CaCO_3 layer (Adolphe, 1990). This process works as follows: a layer of selected bacteria is sprayed on the surface, together with specific nutrients and calcium ions. Over time, this layer is fed repeatedly with the nutrient medium, and CaCO_3 is precipitated (Le Métayer-Levrel *et al.* 1999). Results from full-scale applications of this treatment demonstrated effective working as well as sustainability of the protective application (Castanier *et al.*, 2000; Le Métayer-Levrel *et al.*, 1999). A second patented application concerns the use of a biological mortar or cement, specifically for application in larger cracks and fissures (Castanier *et al.*, 1995). The concept of this is similar, except that the bacteria and nutrient medium are in this case

mixed with grounded limestone or sand grains. An innovative addition to this application is that natural pigments can be added to the mixture and incorporated in the final CaCO₃ crystals, to obtain a desired colour effect (Castanier *et al.*, 2000; Le Métayer-Levrel *et al.*, 1999). Due to the commercial application of this process, only limited information concerning the microbial strains and the nature of the precipitation medium is provided. The main advantage of this treatment above synthetic treatments is the fact that the *in situ* biologically precipitated CaCO₃ is most likely to resemble the original mineral surface in aesthetic and structural characteristics (Castanier *et al.*, 2000; Le Métayer-Levrel *et al.*, 1999).

A different research group studied a similar application, employing MCP through urea hydrolysis using *B. pasteurii* in the precipitation reaction (Bachmeier *et al.*, 2002; Bang *et al.*, 2001; Ramachandran *et al.*, 2001). These authors specifically extended the application to include common concrete surfaces. While it was shown that a mortar treatment significantly improved strength and stiffness values of treated concrete cracks, Ramachandran *et al.* (2001) commented that excessive microbial presence in such mortars compromised the structural integrity of the mortar itself. Moreover, Bachmeier *et al.* (2002) found that concrete surfaces posed additional challenges to the process, in that the pH of the surface is too high (up to pH 12) to support microbial activity. A proposed innovation to overcome this problem was the immobilisation of only the urease enzyme on poly-urethane foam, and the application as such (Bachmeier *et al.*, 2002). Current full-scale applications of this process include restoration work on the Empire State building (New York, USA), and on the Mount Rushmore statues (<http://ssbang.sdsmt.edu>).

Tiano *et al.* (1999) also investigated CaCO₃ on sandstone, but specifically focussing on the changes to structural characteristics such as porosity and strength. These authors employed the precipitation mechanism of organic acid (calcium acetate) utilisation and a strain of *Micrococcus sp.* and *B. subtilis* respectively. Contrary to the findings reported above, Tiano *et al.* (1999) reported only a limited positive effect of the treatment, while warning against additional adverse effects such as the formation of stained patches, and side-reactions of the added chemicals or formed products with the original surface.

Control of groundwater and pollutant transport in sub-soil

Another application of ureolytic driven MCP was patented, concerning the precipitation plugging of pores and permeable channels in sub-surface geological formations (Ferris and Stehmeier, 1993). As patented, this process employs urease-positive microbial strains such as *B. pasteurii* and *Leuconostoc mesenteroides*, fed with a nutrient medium containing urea and calcium. Both Gollapudi *et al.* (1995) and Stocks-Fischer *et al.* (1999) confirmed the efficient working of this process on laboratory scale. The initial intention of the application was to enhance the recovery of oil from oil reservoirs or to control the flow of a spilled contaminant in a reservoir (Ferris and Stehmeier, 1993). However, recent advances in this field also highlighted an additional advantage of this towards the treatment of groundwater contaminated with heavy metals and radionuclides. Ferris *et al.* (1995) and Abdelouas *et al.* (1998) reported the co-precipitation of respectively strontium (Sr) and uranium (UO₂) with microbiologically produced calcite in natural environments. Warren *et al.* (2001) and Fujita *et al.* (2001) subsequently tested the specific application of ureolytic MCP for this purpose, and positive initial reports certainly warrants further investigation. A natural evolution of this technology seems to be the treatment (removal and recovery) of contaminated wastewater through microbiological precipitation. Loydd and Lovley (2001) argued that such processes could have numerous advantages over conventional chemical treatment processes. The development of such a technology was the driving force behind the work presented in this thesis, and practical, microbiological and economical aspects thereof are therefore discussed in the relevant chapters.

CONCLUSION

Microbial CaCO₃ precipitation involves various microorganisms, pathways and environments. Urea hydrolysis presents a straightforward common microbial process, which causes mineral precipitation in natural environments, and which can be (and is) used in biotechnological applications.

[Link to Contents](#) [Link to Chapter 3](#)

SPECIES-SPECIFIC MICROBIAL CALCIUM CARBONATE PRECIPITATION

Redrafted from:

- (1) F. Hammes, N. Boon, J. de Villiers, S. D. Siciliano and W. Verstraete. Strain-specific ureolytic microbial calcium carbonate precipitation by different isolates from the *Bacillus sphaericus* group. Submitted to Applied and Environmental Microbiology (October 2002).

ABSTRACT *During a study of ureolytic microbial calcium carbonate (CaCO₃) precipitation by bacterial isolates collected from different environmental samples, morphological differences were observed in the large CaCO₃ crystal aggregates that precipitated within bacterial colonies grown on agar. Based on these differences, twelve isolates were selected for further study. Sequencing of 16S rDNA showed that all isolates were phylogenetically closely related to the *Bacillus sphaericus* group. Urease gene diversity amongst the isolates was examined using a novel application of PCR-DGGE. This approach revealed significant differences between the isolates. In several isolates multiple bands appeared on the DGGE, suggesting the presence of different urease genes in these isolates. The substrate affinity, and maximum hydrolysis rate of crude enzyme extracts differed considerably between the 16S rDNA taxonomic clusters. For certain isolates, urease activity increased up to 10-fold in the presence of 30 mM calcium and resulted in characteristic crystal formation for these isolates.*

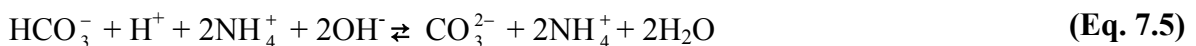
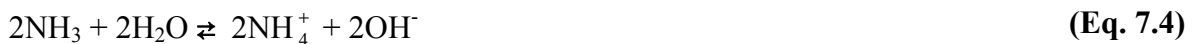
INTRODUCTION

Numerous and diverse microbial species participate in the precipitation of mineral carbonates in various natural environments including soils, geological formations, freshwater biofilms, oceans and saline lakes (Rivadeneira *et al.*, 2000; Peckman *et al.*, 1999; Douglas and Beveridge, 1998; Rivadeneira *et al.*, 1998). Such natural precipitates often can be viewed as the fossil records or “fingerprints” of bacterial activity (Trewin and Knoll, 1999; Westfall, 1999). This process was at the heart of the debate as to whether mineral sediments on the ALH84001 Martian meteorite represent proof of life in outer space (Vecht and Ireland, 2000; Westfall, 1999; McKay *et al.*, 1996). In addition to its natural historical importance, microbial carbonate precipitation (MCP) is the basis of innovative applications in both the building sector and wastewater industry (Stocks-Fischer *et al.*, 1999; Ferris and Stehmeier, 1993; Refer to Chapters 5 – 7 in this work).

The precise role of microbes in the carbonate precipitation process is still not clear. Boquet *et al.* (1973) suggested that almost all bacteria are capable of CaCO₃ precipitation. Knorre and Krumbein (2000) concluded MCP occurred as by-product of common microbial metabolic processes such as photosynthesis, urea hydrolysis and sulphate reduction. These metabolic processes increase the alkalinity (increase in pH and dissolved inorganic carbon (DIC)) of the environment, and thereby favour CaCO₃ precipitation (Castanier *et al.*, 1999; Douglas and Beveridge, 1998). Alternatively, it is possible that there are specific attributes of certain bacteria that promote and affect CaCO₃ precipitation. The negatively charged nature of microbial cell walls favours the binding of divalent cations (Ca²⁺; Mg²⁺), thereby making microorganisms ideal crystal nucleation sites (Rivadeneira *et al.*, 1998; Schultze-Lam *et al.*, 1996). Microbial extracellular polymeric substances (EPS) are also an important factor in precipitation, either through trapping and concentration of calcium ions, or as a result of specific proteins influencing precipitation (Kawaguchi and Decho, 2002). These authors suggested that specific proteins in biological EPS causes the formation of different CaCO₃ polymorphs. A third hypothesis combines the common metabolism and strain specificity hypotheses to suggest that CaCO₃ precipitation, possibly influenced by

intracellular calcium metabolism, might play in the ecology of the precipitating organism (Castanier *et al.*, 1999; McConnaughey and Whelan, 1997; Anderson *et al.*, 1992).

Enzymatic hydrolysis of urea presents a straightforward model for studying microbial CaCO₃ precipitation. The urease enzyme (urea amidohydrolase; EC 3.5.1.5) is common in a wide variety of micro-organisms. It can be readily induced by adding an inexpensive substrate and is involved in several biotechnological applications (Stocks-Fischer *et al.*, 1999; Ferris and Stehmeier, 1993). Urea is hydrolysed intracellular to one mole ammonia and one mole carbamate (Equation 7.1), which spontaneously hydrolyse forming a further mole of ammonia and carbonic acid (Equation 7.2) (Burne and Chen, 2000). These products subsequently equilibrate in water to form bicarbonate, and two moles of ammonium and hydroxide ions (Equations 7.3 and 7.4). The latter give rise to a pH increase, which in turn can shift the bicarbonate equilibrium resulting in the formation of carbonate ions (Equation 7.5), which in the presence of soluble calcium ions, precipitate as CaCO₃ (Equation 7.6) (Burne and Chen, 2000; Castanier *et al.*, 1999).



During laboratory work over the past few years, we found that different bacterial isolates precipitated visually different crystal aggregates in a repeatable manner when cultivated on semi-solid media under similar growth conditions. The aim of this chapter was to characterise the mechanisms responsible for this diversity in crystal aggregate morphology. Such information would be of interest to those investigating carbonate precipitation as a fossil record and those investigating carbonate precipitation as a potential biotechnology.

MATERIALS & METHODS

Isolation

CaCO₃ precipitating strains were isolated from two soils (garden soil and landfill soil, Ghent, Belgium), a freshly cut concrete surface (Portland, CEM I 42.5 R), and from calcareous sludge from a bio-catalytic calcification (BCC) reactor. The latter treats calcium-rich industrial wastewater through ureolytic microbial carbonate precipitation (Refer to Chapters 5, 6, 7). The above samples were suspended in sterile physiological solution (8.5 g·L⁻¹ NaCl), diluted appropriately, and plated on precipitation agar containing per litre: 3 g nutrient broth (Oxoid), 20 g urea (Riedel-de Haën), 2.12 g NaHCO₃ (Sigma), 10 g NH₄Cl (Sigma), and 30 mM CaCl₂·2H₂O (Sigma) (Stocks-Fischer *et al.*, 1999; Ferris and Stehmeier, 1993). Incubation was done at 28 °C. Colonies were assessed every 5 days with a stereo microscope (Wild, Heerbrugg) and selected as positive, based on visual crystal formation within 10 days. Positive isolates were purified through repetitive dilution and plating (as described above). The purified strains were deposited in the BCCMTM/LMG - Culture Collection (Ghent, Belgium).

Microscopy and phase identification

Crystal precipitating colonies were studied after 5 days and 10 days cultivation with light microscopy using an Axioskop II plus (Zeiss) microscope, and stereo microscopy (Wild, Heerbrugg). Digital images were captured with a 1-CCD camera (Hamamatsu Photonics GmbH, Hersching, Germany). A total of 12 isolates were selected based on visual differences in the precipitate morphology. Large crystal aggregates that precipitated within single colonies of these isolates were subsequently harvested from the agar surface, washed in sterile water, and dried (28 °C, 3 days). The dried aggregates were ground to the appropriate particle size for XRD analysis, (< 10 µm), using a McCrone micronising mill. The milled samples were then mounted in a sample holder and analysed using a Siemens D-501 diffractometer. Phase identification was done after background subtraction using the Bruker EVA software. The operating parameters are given below.

Instrument and data collection parameters:

Radiation	Cu $K\alpha$ (1.5418 Å)
Temperature	25°C
Specimen	flat-plate, rotating (30 RPM)
Power Setting	40 kV, 40 mA
Soller slits	2° (diffracted beam side)
Divergence slits	1°
Receiving slits	0.05°
Monochromator	secondary, graphite
Detector	scintillation counter
Range of 2θ	15-70° 2θ
Step width	0.04° 2θ
Time per step	1.5 seconds

Urease activity, location and Ca^{2+} :urea assay

In a first experiment all the isolates were tested for urease activity, as well as the location thereof. This was done by streaking the purified cultures on urease test agar (BBL, Becton Dickinson & Company, Sparks, USA), and inoculating urease test broth (as above) with viable liquid cultures as well as the filtrates (0.22 μm , Millipore) of the liquid cultures. A change in coloration following incubation (5 days, 28 °C) was recorded as a urease-positive reaction. The Ca^{2+} :urea assay studied the relation between urea hydrolysis and CaCO_3 precipitation. Liquid medium was prepared containing nutrient broth (1 $\text{g}\cdot\text{L}^{-1}$), Ca^{2+} (30 mM as CaCl_2), NaHCO_3 (2 mM) and urea (100 mM). The pH of the medium was set at 7.00 (1 N HNO_3) and the medium was filter sterilised (Millipore 0.22 μm). The isolates were cultivated (28 °C, shaking) in nutrient broth (13 $\text{g}\cdot\text{L}^{-1}$) supplemented with urea (20 $\text{g}\cdot\text{L}^{-1}$), harvested at mid-log phase, concentrated (5000 g, 15 min.), and washed twice in sterile physiological solution. 50 mL samples of sterile medium were inoculated separately with each of the isolates to final concentrations between 10^7 and 10^8 $\text{cfu}\cdot\text{mL}^{-1}$. The latter was determined by serial dilution (sterilised physiological solution) and plating (nutrient agar + urea). A negative control was sterile media without inoculation. The assay commenced upon inoculation, and total ammonium nitrogen (TAN) was determined by

measuring the amount of ammonium released after 10 minutes spectrophotometrically (425 nm), according to the Nessler assay method (Greenberg *et al.*, 1992). This was done regularly as an indication of hydrolysed urea. On two separate time periods, when the TAN corresponded with between 10 – 20 mM hydrolysed urea, soluble Ca^{2+} was measured as well. The latter was done following appropriate dilution (milliQ water) and acidification (1 N HNO_3), using flame atomic absorption spectrometry (Perkin Elmer Flame AAS, Überlingen, Germany). All experiments were done in triplicate, while all dilutions and measurements were done in duplicate.

Polymerase chain reaction (PCR) amplification of 16S rRNA genes

DNA template for PCR-amplification from pure cultures was obtained by extracting total genomic DNA according to the manufacturer's instructions (Wizard® Genomic DNA Purification Kit, Promega, Leiden, The Netherlands). The PCR mastermix contained 500 nM of each primer, 200 μM of each deoxynucleoside triphosphate, 1.5 mM MgCl_2 , 10 μl of Thermophilic DNA Polymerase 10X Reaction Buffer (MgCl_2 -free), 2.5 U of Taq DNA Polymerase (Promega, Madison, WI, USA), 400 ng/ μl of bovine serum albumin (Boehringer), and DNase and RNase free filtersterile water (Sigma-Aldrich Chemie, Steinheim, Germany) to a final volume of 100 μl . One μl of DNA template was added to 24 μl of mastermix. The 16S rRNA gene fragments were obtained by amplifying the 16S rRNA gene with primers P63f (5'-CAGGCCTAACACATGCAAGTC-3') and P1378r (5'-CGGTGTGTACAAGGCCCGGGAACG-3'). PCR was performed in a 9600 thermal cycler (Perkin-Elmer, Norwalk, CT, USA) with a program consisting of: 10 min. 95 °C; 30 cycles of 1 min. 94 °C, 1 min. of 53 °C, 2 min. at 72 °C; and a final elongation for 10 min. at 72 °C.

DNA sequencing and sequence analysis

DNA sequencing of the PCR fragments was carried out by ITT Biotech-Bioservice (Bielefeld, Germany). Analysis of DNA sequences and homology searches were completed with standard DNA sequencing programs and the BLAST server of the National Center for Biotechnology Information (NCBI) (www.ncbi.nlm.nih.gov) using the BLAST algorithm

(Altshul *et al.*, 1997) and specifically the “blastn” program for the comparison of a nucleotide query sequence against a nucleotide sequence database. A phylogenetic tree was constructed by using the RDP Phylip 3.5c Interface (Maidak *et al.*, 2001). Distance matrix analyses were done with the Jukes and Cantor (Jukes and Cantor, 1969) correction and tree construction was done by the neighbour-joining method (Saitou and Nei, 1987).

PCR-Denaturing gradient gel electrophoresis (DGGE) of the *ureC* gene

The DNA extraction and PCR-mastermix composition was identical as described above. *Bacillus pasteurii* (ATCC 6453) was included as positive control for ureolytic microbial CaCO₃ precipitation (Stocks-Fischer *et al.*, 1999; Ferris and Stehmeier, 1993). To amplify the genes encoding for the *ureC* subunit of the urease enzyme, PCR was performed with primers UreC-F (5'-TGGGCCTTAAAATHCAYGARGAYTGGG-3') and UreC-R (5'-GGTGGTGGCACACCATNANCATRTC-3') as previously described by Reed (2001). The length of the expected amplified fragment was 382 bp. To examine the diversity of the partial *ureC* DNA fragments by DGGE, a GC clamp (5'-CGCCCGCCGCGCGCGGGCGGGGCGGGGGCACGGGGGG-3') of 40 bp (Muyzer *et al.*, 1993) was attached to the 5' end of the UreC-F primer. The applied PCR conditions were as follow: 94 °C for 5 min., followed by 35 cycles of 92 °C for 1 min., 50 °C for 1 min., and 72 °C for 2 min. A final extension was carried out at 72 °C for 10 min. DGGE was performed with the Bio-Rad D Gene System (Hercules, CA, USA). PCR samples were loaded onto 7 % (wt/vol.) polyacrylamide gels in 1xTAE (20 mM Tris, 10 mM acetate, 0.5 mM EDTA, pH 7.4). The polyacrylamide gels were made with a denaturing gradient ranging from 40 % to 60 %, with 7 M urea and 40 % formamide as 100 % denaturing agent. The electrophoresis was run for 16 hours at 60 °C and 45 V. The resulting gels were stained with SYBR GreenI nucleic acid gel stain (1:10,000 dilution; FMC BioProducts, Rockland, ME, USA) and photographed (Boon *et al.*, 2000). The processing of the DGGE gels was done with the Bionumerics software 2.0 (Applied Maths, Kortrijk, Belgium). The calculation of the similarities was based on the Dice correlation coefficient and results in a distance matrix. The UPGMA clustering algorithm was used to calculate the dendrograms of the DGGE gel. Putative *ureC* gene fragments were excised from the DGGE gel, re-amplified and send for sequencing (as above). The resulting

nucleotide sequences were translated to protein sequences using the “blastx” software (BLAST; NCBI) and these sequences were compared with a protein sequence database.

Nucleotide sequence accession numbers

The near full sequences (800 - 1300 kb) of 16S rDNA for all isolates have been deposited in GenBank database under accession numbers AF548874 - AF548885. Six nucleotide sequences (\pm 300 kb) of urease genes were also deposited as no. AY178982 - AY178987.

Protein extraction

Isolates were cultivated in 1 L nutrient broth (Oxoid) with $20 \text{ g}\cdot\text{L}^{-1}$ urea for 48 h at $30 \text{ }^\circ\text{C}$ with shaking (100 rpm). Bacterial cells were harvested by centrifuging (8000 g, 30 min), washing the pellet in extraction buffer (100 mM NaH_2PO_4 , 1 mM EDTA, pH 7.0), followed by centrifuging (15000 g, 10 min) and re-suspension in extraction buffer (see above). Crude enzyme was extracted by bead-beating (three times 90 seconds with 10 second pauses in between). Protein concentration was determined by following the procedure of Bradford (1976). This encompassed adding 200 μL of commercial Bio-Rad protein assay solution to 800 μL of appropriately diluted sample, and measuring the colour development spectrophotometrically at 595 nm. Bovine serum albumin was used as the standard.

Urease activity assay

Urease activity was assayed in 1 mL buffer containing 100 mM NaH_2PO_4 , 1 mM EDTA and pH 8.0. Ten different substrate concentrations were used, varying between 5 and 100 mM urea. Both the crude enzyme and the reaction mixtures were incubated for 5 min at $25 \text{ }^\circ\text{C}$ prior to the urease assay. The reaction was initiated upon addition of the crude enzyme and urease activity was determined by measuring the amount of ammonium released after 10 minutes spectrophotometrically at 425 nm, according to the Nessler assay method (Greenberg *et al.*, 1992). One unit of urease is defined as the amount of enzyme hydrolyzing one μmol urea per min. Michaelis-Menten kinetic constants, K_m and V_{max} ,

were estimated by graphing the data in a Lineweaver-Burk plot. In a further assay for the effect of pH on the urease activity, the method above was repeated with 50 mM urea solutions at pH 7 and 8 (in 100 mM phosphate buffer), and pH 9 (in 100 mM TRIS buffer). In both assays, commercial urease from Jack beans (Sigma; Type III from Jack Beans) was used as the positive control.

Effect of calcium on urease activity

The respective isolates were cultivated and concentrated as described above. Sterile solutions were prepared comprising urea (100 mM), nutrient broth (1 g·L⁻¹) and NaHCO₃ (10 mM) at pH 7 (1 N HNO₃), and inoculated with the respective isolates to final concentrations of 10⁷ – 10⁸ cfu·mL⁻¹. Similar solutions containing additionally 30 mM CaCl₂ were also inoculated. These solutions were all incubated (25 °C, stirring) and sampled every 30 minutes. TAN was measured as above, and the results expressed as the urease activity in the presence of calcium, divided by the urease activity in the absence of calcium. All experiments were done in triplicate, all measurements were done in duplicate.

Principle component analysis, multivariate analysis of variance, and discriminant analysis

Principle component analysis (PCA) was carried out, using Bionumerics software, and incorporating as parameters for each isolate the (i) number of urease bands from the DGGE, (ii) the Ca²⁺:urea ratio values, (iii) the respective K_m and (iv) V_{max} data, and (v) the calcium-urease activity data. This was done to establish a statistical correlation between the various parameters and the morphological differences observed between the crystal aggregates. Multivariate analysis of variance (MANOVA), and discriminant analysis were further used to identify the primary contributing parameter(s) to these morphological differences. Three different groups were defined based on the PCA: (i) CPB 1 – CPB 4, (ii) CPB 5 – CPB 6, (iii) CPB 7 – CPB 12. Accounting for covariance structure and relative character importance were both used in the discriminant calculations.

RESULTS

About 10 % of all bacterial colonies isolated from various sources induced crystallisation on the precipitation agar. Precipitation commenced with a darkening in the centre of the bacterial colony, which is attributed to amorphous CaCO_3 formation (between 20 h and 5 days, depending on the isolate), followed by crystallisation and crystal maturation in time (Figure 3.1(a-e)). The precipitate always formed within the bacterial colony on the agar surface, thereby also capturing bacteria within the crystal structure (not shown). The conversion of amorphous CaCO_3 to the crystal phase is a rapid-occurring event, taking usually only two to five hours for completion.

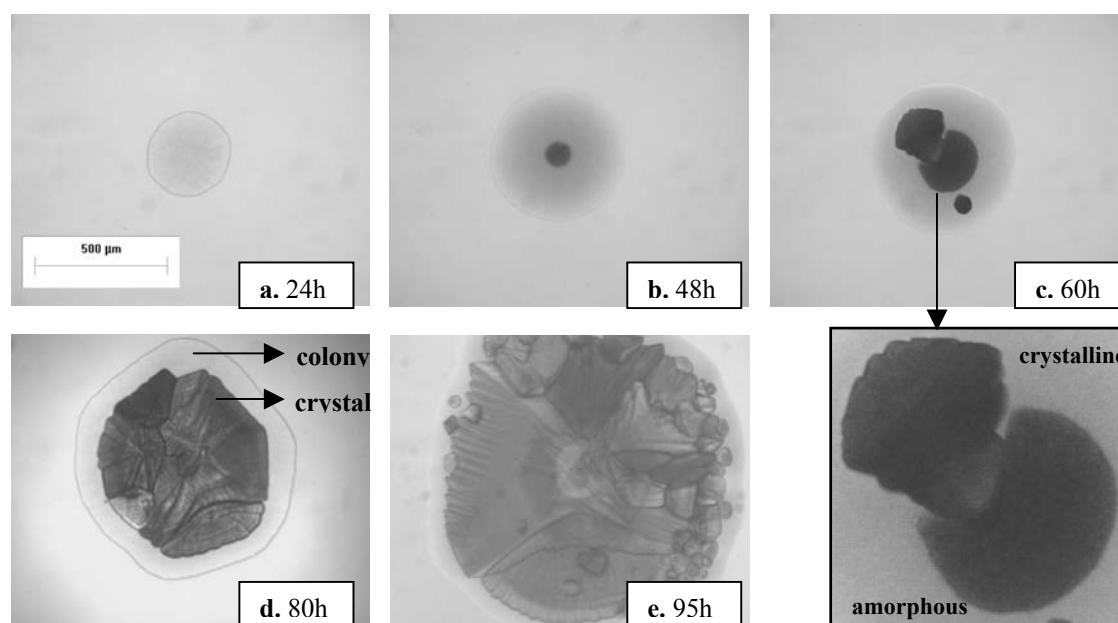


Figure 3.1(a-e). A typical ureolytic CaCO_3 precipitation sequence, commencing with the formation of amorphous CaCO_3 , followed by crystallisation (enlargement from Figure 3.1c) and crystal maturation. Figure 3.1d shows the position of the crystal inside the bacterial colony on the agar surface.

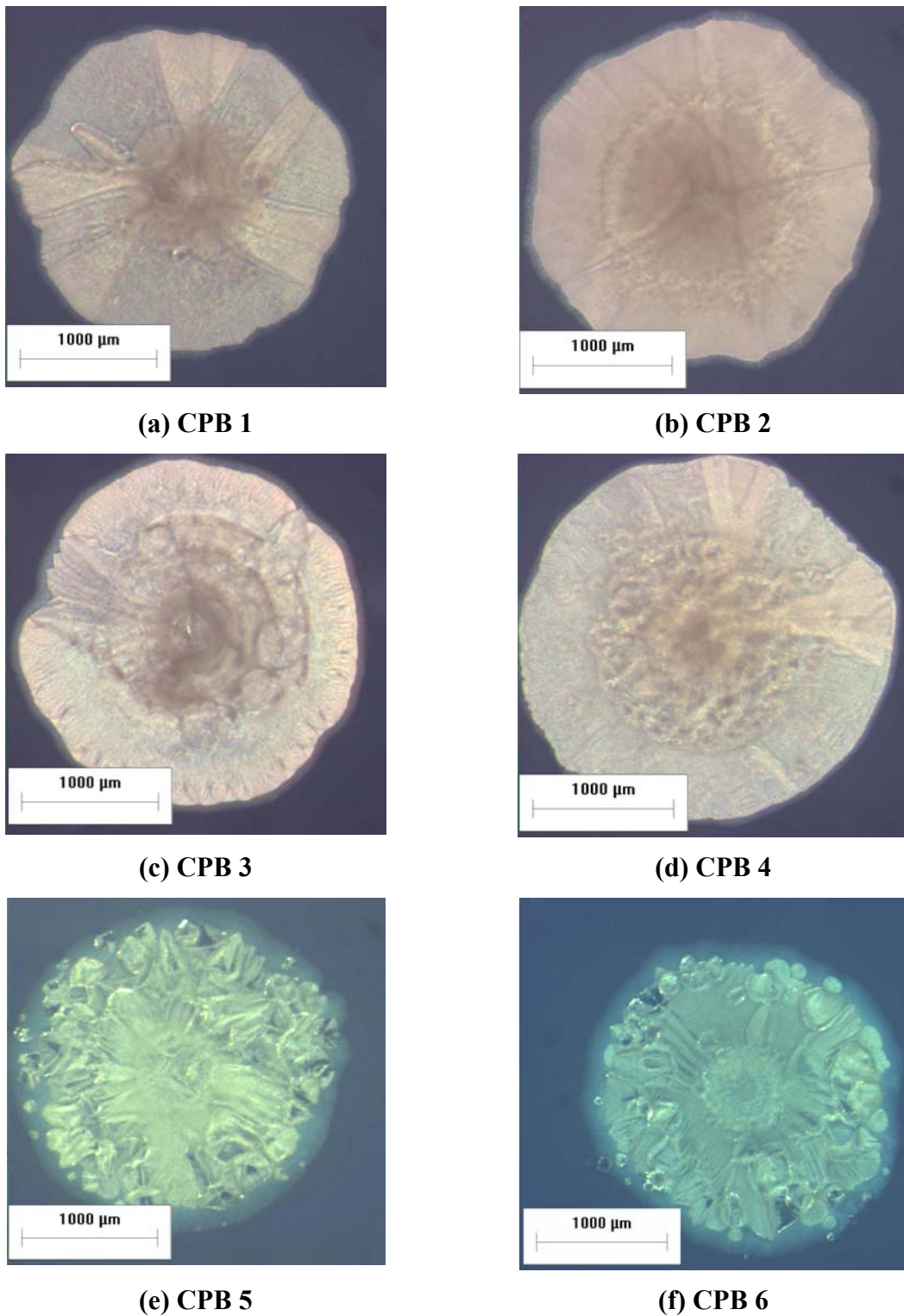
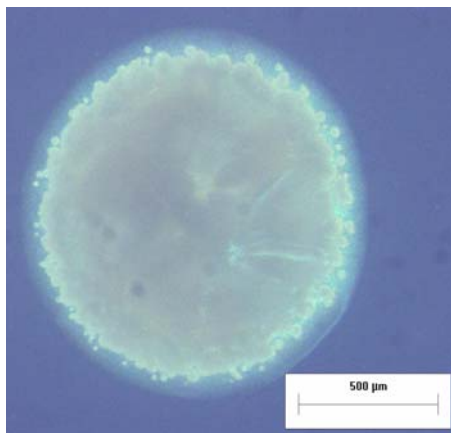
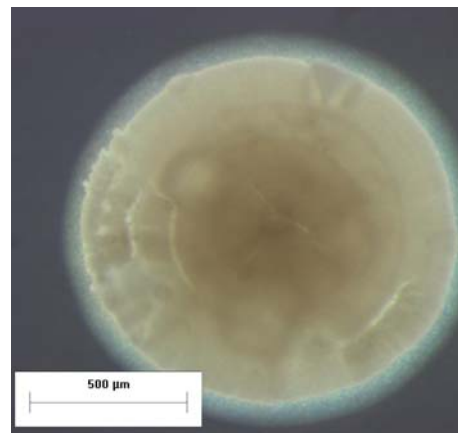


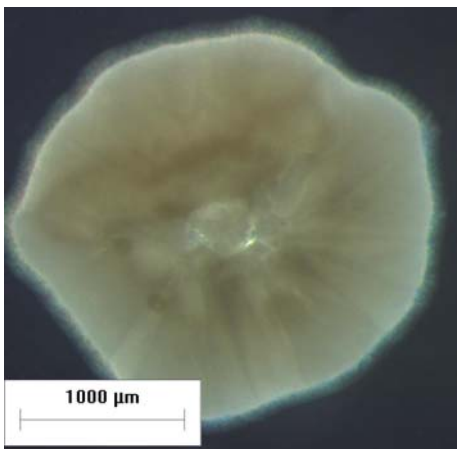
Figure 3.2(a-f). Stereo microscope images of calcium carbonate crystals precipitated within bacterial colonies on semi-solid growth media, and classed according to morphological differences



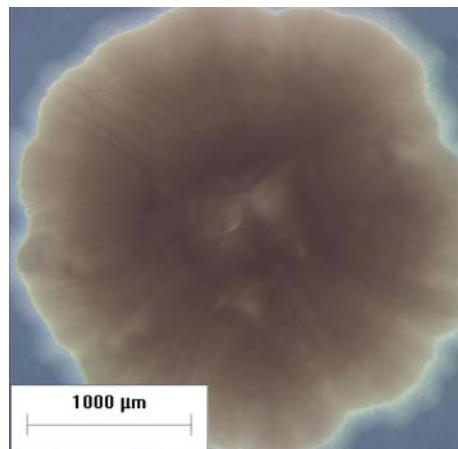
(g) CPB 7



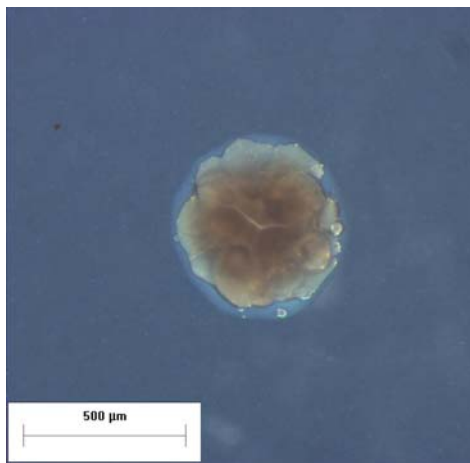
(h) CPB 8



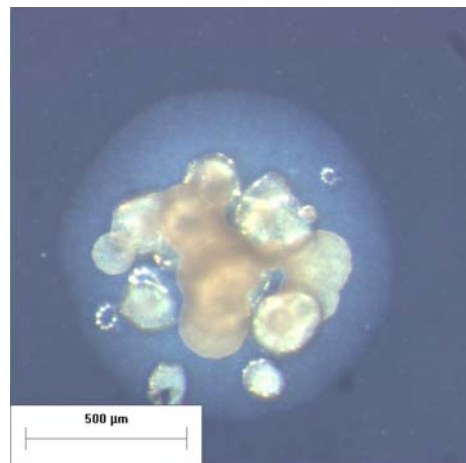
(i) CPB 9



(j) CPB 10



(k) CPB 11



(l) CPB 12

Figure 3.1(g-l). Stereo microscope images of calcium carbonate crystals precipitated within bacterial colonies on semi-solid growth media, and classed according to morphological differences

Twelve such isolates were selected for further study, based on morphological differences observed in the large crystal aggregates which were precipitated within single colonies on the precipitation agar (Figure 3.2). The isolates were termed calcium-precipitating bacteria (CPB 1 – 12). Four basic morphologically distinct groups of crystal aggregates were distinguished: CPB 1 – 4 all produced large, light-brown structures which formed rapidly (20 – 48 h for crystallisation), with aggregates taking up as much as 98 % of the total colony surfaces (Figure 3.2). CPB 5 and 6 precipitated at similar rates, but in this case the result was distinctly sharp, whitish and transparent crystal aggregates. CPB 7 – 10 precipitated at noticeably slower rates than the first strains (about 3 - 5 days for crystallisation). The resulting precipitates were thick, brown aggregates, almost amorphous in appearance. CPB 11 and 12 required between 5 – 10 days for crystallisation, and were characterised by the initial formation of separate, small, spherical crystals, only coalescing after a couple of days.

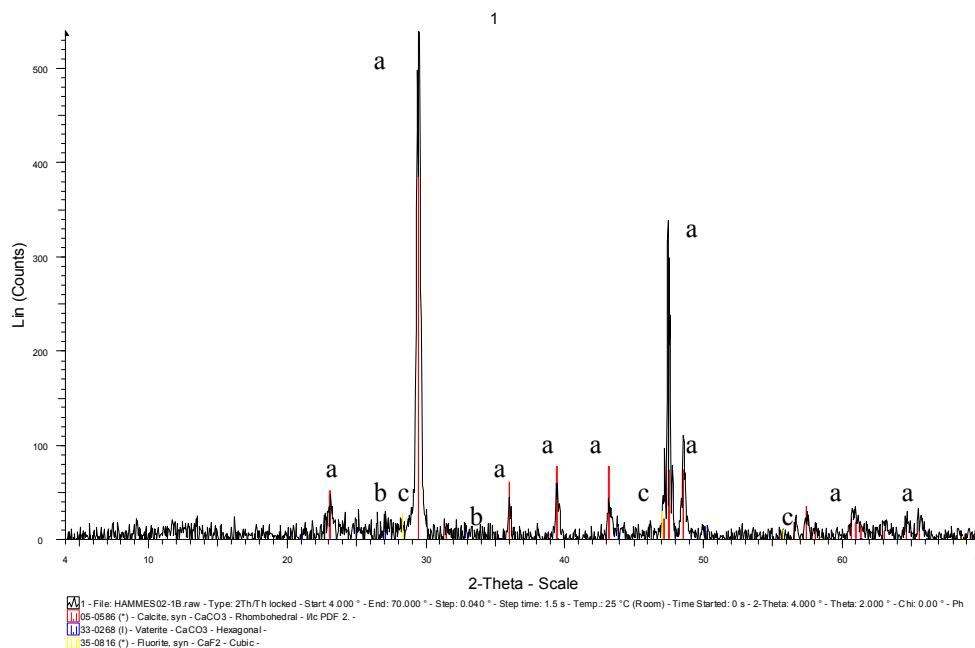


Figure 3.3. An example of the XRD data of CaCO_3 precipitated by isolate CPB 1. The crystal forms are indicated: a = calcite, b = vaterite, c = fluorite.

Note that the different crystal groups neither reflected the initial isolation origin of the isolates (Table 3.1), nor their cell morphology, since all isolates were rod-shaped between 1 and 3 μm in length. X-ray diffraction (XRD) analysis of the crystals characterised the primary crystal component of all the classes as rhombohedral calcite, though hexagonal vaterite was detected in some cases as well. Figure 3.3 shows an example of the XRD data from CPB 1, while the complete data for each isolate is presented in Table 3.1. The XRD data was not quantified.

Table 3.1. *Initial origin, and XRD results of the different isolates*

Isolate	Origin	XRD data
CPB 1	Soil sample A	Calcite (rhombohedral); Vaterite (hexagonal); Fluorite (cubic)
CPB 2	Soil sample B	Data not available
CPB 3	BCC reactor	Calcite (rhombohedral); Vaterite (hexagonal); Fluorite (cubic)
CPB 4	BCC reactor	Calcite (rhombohedral); Vaterite (hexagonal)
CPB 5	Soil sample A	Data not available
CPB 6	Soil sample B	Calcite (rhombohedral); Vaterite (hexagonal)
CPB 7	Concrete	Calcite (rhombohedral); Fluorite (cubic)
CPB 8	Concrete	Calcite (rhombohedral)
CPB 9	Soil sample B	Calcite (rhombohedral); Vaterite (hexagonal); Fluorite (cubic)
CPB 10	Soil sample B	Calcite (rhombohedral); Vaterite (hexagonal); Fluorite (cubic)
CPB 11	Soil sample B	Calcite (rhombohedral)
CPB 12	Concrete	Calcite (rhombohedral); Vaterite (hexagonal)

Urease presence, location and Ca^{2+} :urea assay

In all cases, urease activity was cell-associated. All 12 isolates produced a urease-positive coloration when grown on urease test-agar, or when inoculated into urease test-broth. None of the filtrates of liquid cultures gave a positive reaction. Table 3.2 shows the results from the Ca^{2+} :urea assay. Some notable differences are evident: for example CPB 5 and CPB 9 display noticeably high Ca^{2+} :urea ratios, while that recorded for CPB 4 was exceptionally

low. However, in general it appears that a value of about 0.75 – 0.8 was typical for most of the isolates, with little difference between aggregate morphology classes, with Class 1 having a ratio of 0.733 (n=3), Class 2, 0.84 (n=1), Class 3, 0.80 (n=4) and Class 4, 0.75 (n=2).

Table 3.2. Comparison between the amount of calcium precipitated (mM) and the amount of urea hydrolysed (mM) by the different isolates. Standard deviation ($n = 3$) is indicated.

Isolate	Crystal class	Ca ²⁺ (mM)/urea(mM)
CPB 1	1	n.a.
CPB 2	1	0.77 ± 0.48
CPB 3	1	0.74 ± 0.1
CPB 4	1	0.69 ± 0.07
CPB 5	2	0.84 ± 0.02
CPB 6	2	n.a.
CPB 7	3	0.74 ± 0.03
CPB 8	3	0.75 ± 0.01
CPB 9	3	0.93 ± 0.05
CPB 10	3	0.78 ± 0.18
CPB 11	4	0.76 ± 0.06
CPB 12	4	0.75 ± 0.05

n.a.: data not available

Identification and sequencing

All isolates were closely related to one another and to cultured bacteria from the *Bacillus sphaericus* group. BLAST results suggested the closest relatives of this group to be *Bacillus pasteurii* (CPB 1 – 4), *Bacillus psychrophilus* (CPB 5 – 7), *Planococcus okeanokoites* (CPB 8) and *Bacillus globisporus* (CPB 9 – 12), while another closely related species to all isolates was *Filibacter limicola*. A phylogenetic tree (neighbour-joining) was constructed, using *Escherichia coli* and *B. subtilis* as outgroups (Figure 3.4). Although all

isolated CPB are related to the *Bacillus sphaericus* group, there was still sufficient diversity in the 16S rDNA to distinguish the isolates in different clusters. The largest cluster contains CPB 1 – 4 and CPB 7 & 8 and is closely related to *B. pasteurii*. The second cluster contains CPB 11 & 12, and the third contains CPB 10. CPB 9 is situated between the second and third clusters. The fourth cluster contains CPB 5 & 6 and is noticeably distant from the others.

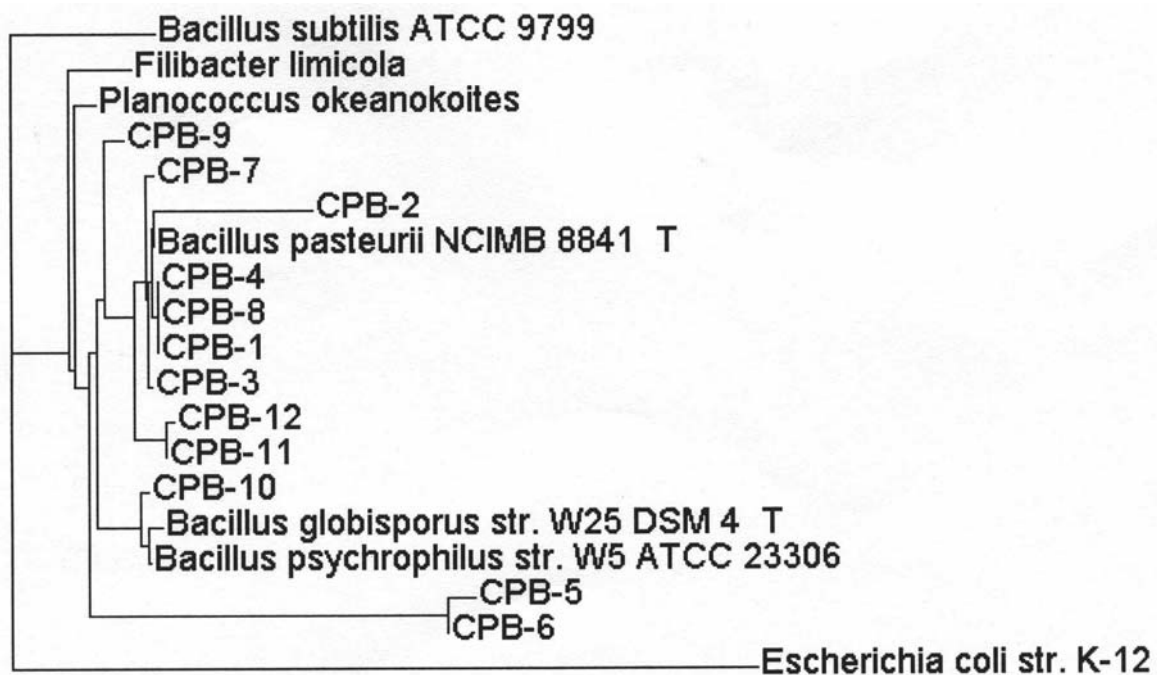


Figure 3.4. A neighbour-joining tree, based upon partial 16S rRNA gene sequences of the 12 isolates and closest relatives. *E. coli* was used as out-group. Sequence analysis was done as described in the text, 402 base positions were included in the calculations.

Urease gene diversity

PCR-DGGE, using *UreC* primers, revealed bands differing in position and number between isolates (Figure 3.5). A cluster analysis based on band position, showed two large groupings as well as four completely ungrouped isolates (CPB 7, 8, 10, 12). The first grouping includes CPB 1 & 2 (100 % similarity), CPB 11, and CPB 3 & 4. The second

grouping includes CPB 5 & 6 (100 % similarity) and CPB 9, as well as *B. pasteurii*. All the bands were excised from the DGGE, but only six bands (as indicated in Figure 3.5), were successfully purified, amplified and sequenced. In all cases, amino-acid sequences were related to the alpha subunit (*UreC*) of previously described ureases, thus indicating that the PCR amplification was indeed specific. The highest degree of similarity was found with sequences from *Bacillus halodurans* (NP 241120.1), *Corynebacterium glutamicum* (NP 599339.1), *Bacillus pasteurii* (S 47104) and *Haemophilus influenzae* (NP 438697.1). The similarities between the isolate sequences and these corresponding sequences ranged between 66 % and 90 %, and amongst one another between 81 and 95 % (see Table 3.3 for similarity details).

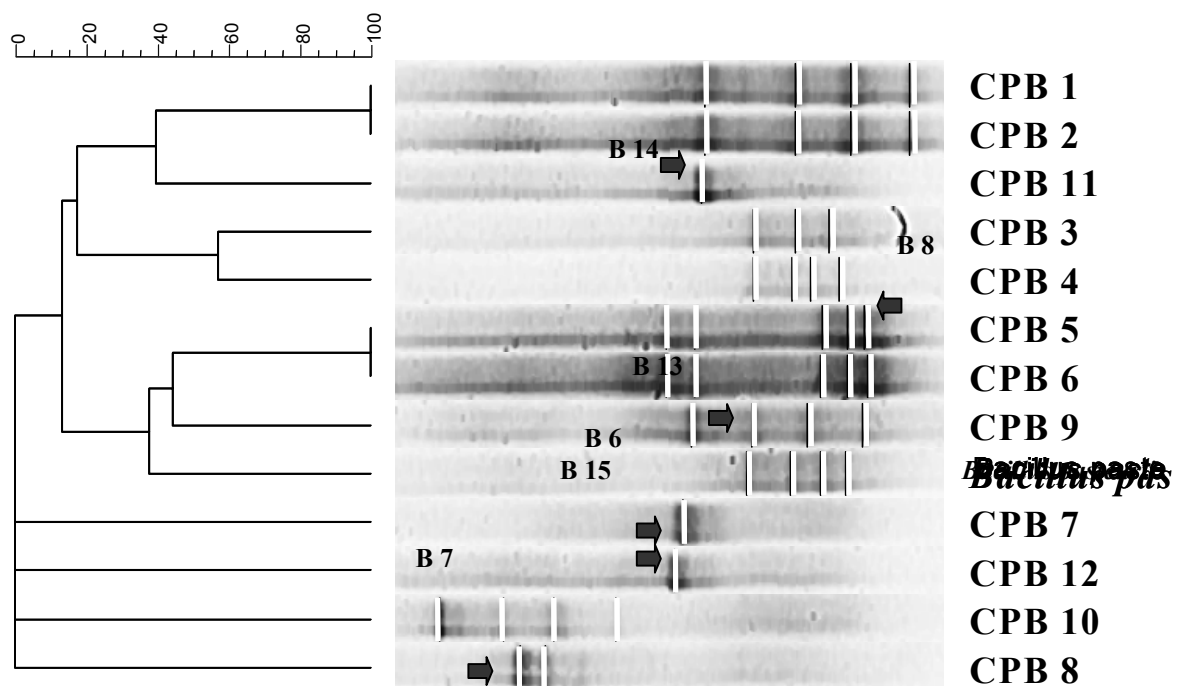


Figure 3.5. DGGE separation of selectively amplified urease PCR products from the different isolates, with *B. pasteurii* as positive control. White lines represent bands, and individual bands indicated with arrows were excised and sequenced, as described in the text.

Table 3.3. Comparison of the translated amino-acid sequences from the DGGE gel with one another (B) and with known sequences (F). Top right shows identities, bottom left shows positives.

	B6	B7	B8	B13	B14	B15	F1	F2	F3	F4
B6	*	92	86	82	81	78	77	75	75	78
B7	95	*	85	88	83	77	82	82	79	79
B8	93	90	*	89	82	76	77	75	75	78
B13	91	95	94	*	81	75	78	73	75	73
B14	91	91	93	90	*	67	74	74	70	74
B15	84	86	86	85	81	*	68	64	66	57
F1	87	89	90	92	89	82	*	-	-	-
F2	87	89	90	85	88	81	-	*	-	-
F3	85	88	90	86	87	82	-	-	*	-
F4	86	87	88	86	87	66	-	-	-	*

F1 = *B. halodurans* (α subunit of urease gene); F2 = *C. glutamicum* (α subunit of urease gene); F3 = *B. pasteurii* (urease gene); F4 = *H. influenzae*

(α subunit of urease gene)

Urease activity

There were distinct differences amongst the isolates for both the substrate affinity (K_m) and rate (V_{max}) values (Table 3.4). Isolates CPB 1, CPB 3, CPB 4, CPB 5 and CPB 6 showed high urea affinity, while isolates CPB 7 – 12 displayed remarkably low affinities (> 30 mM urea). More variation was detected in the specific rates. CPB 5, 6 and 12 showed rather high rates, while CPB 7, 9, 11 showed very low rates. The activity of the crude enzyme extract was more adversely affected by lower pH regimes than by higher pH regimes with isolates CPB 7 – 12 being most sensitive to lower pH values. The high urea-affinity isolates (CPB 3 – 6) were also the least affected by pH 7 (Figure 3.6).

Table 3.4. Michaelis-Menton kinetic values (K_m and V_{max}) determined on crude enzyme extracts from the various ureolytic calcium-precipitating isolates. Standard deviations indicated.

Isolate	Crystal class	K_m		V_{max}	
		(mM substrate)		(mM urea min ⁻¹ mg ⁻¹ protein)	
CPB 1	1	12.1	± 4.2	9.9	± 1.1
CPB 2	1	21.0	± 1.3	16.7	± 0.6
CPB 3	1	11.9	± 0.1	8.0	± 0.1
CPB 4	1	11.7	± 1.6	10.3	± 0.5
CPB 5	2	7.3	± 0.1	30.0	± 0.2
CPB 6	2	6.6	± 0.4	23.7	± 0.5
CPB 7	3	34.8	± 1.4	1.7	± 0.1
CPB 8	3	53.9	± 14.8	12.3	± 1.9
CPB 9	3	36.3	± 0.4	5.4	± 0.1
CPB 10	3	38.1	± 0.5	8.1	± 0.0
CPB 11	4	35.9	± 1.8	1.7	± 0.1
CPB 12	4	45.3	± 3.6	22.4	± 1.3

Effect of calcium on urease activity

Figure 3.7 shows the comparison between urease activity of the isolates (live, intact cells) with and without calcium addition to the medium. CPB 1 – 4 displayed large increases in urease activity (4 – 10 times) in the presence of calcium ions compared to that in the absence of calcium. The other isolates displayed either no differences or slight adverse effects of calcium on their respective urease activities.

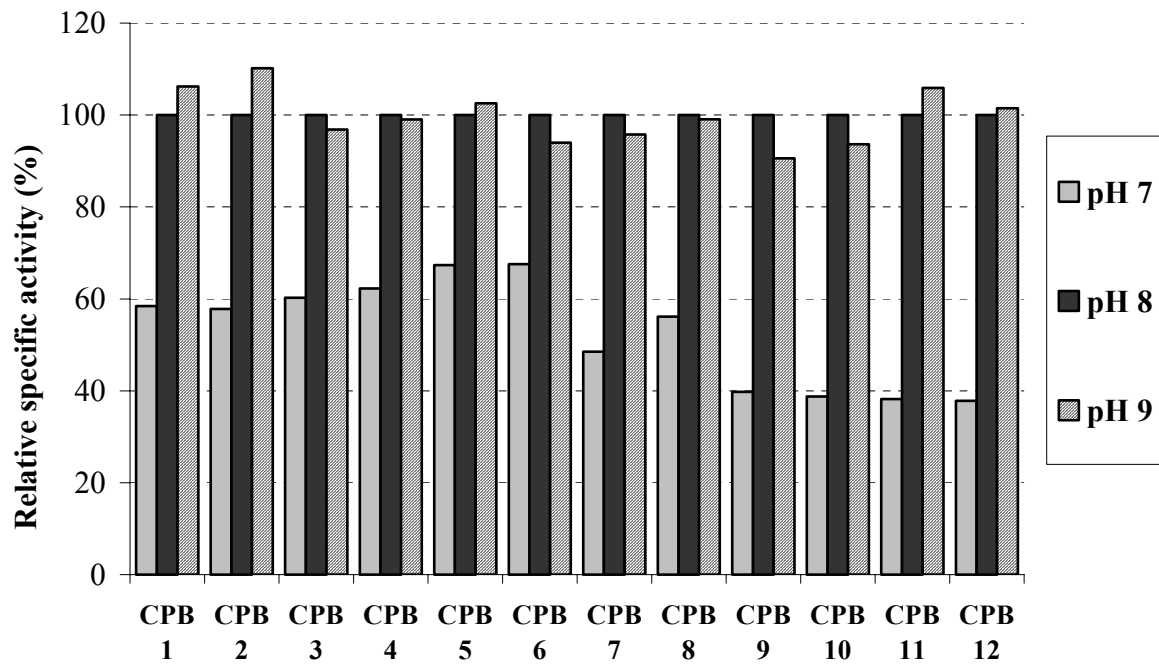


Figure 3.6. The effect of pH on the specific urease activity of the various pure cultures relative to the specific activity at pH 8 (100 %) as determined from a 50 mM urea assay.

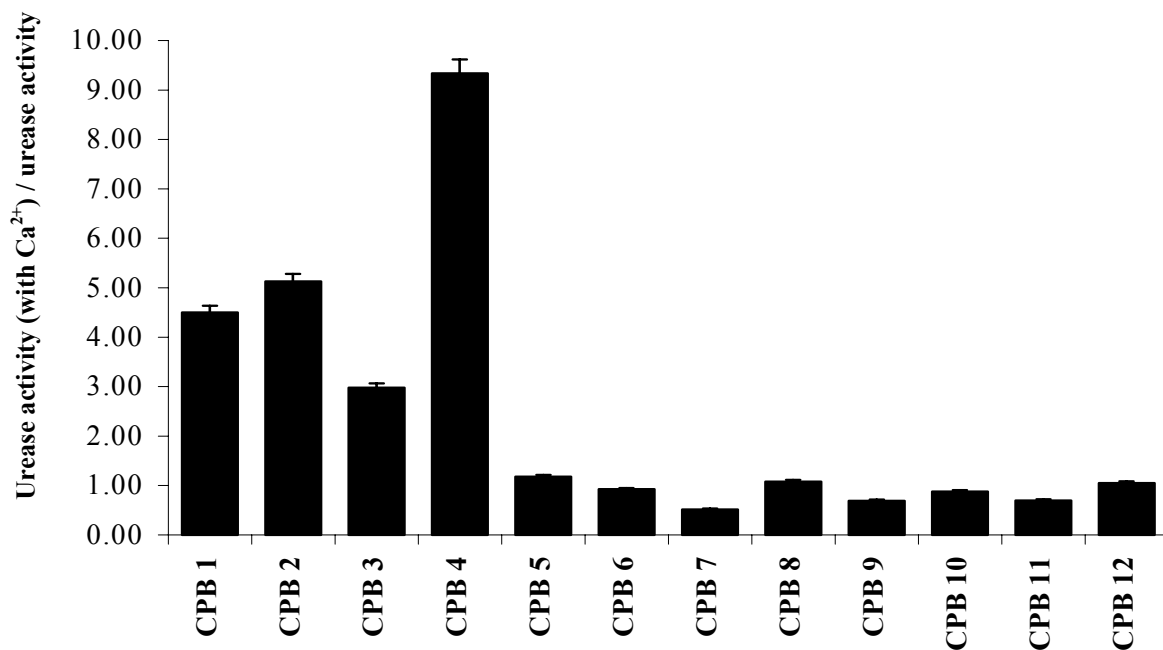


Figure 3.7. The effect of calcium ions (30 mM) on the specific urease activity (100 mM urea assay) of the various isolates, expressed as urease activity with calcium over urease activity without calcium present. Error bars indicate standard deviation.

Principle component analysis (PCA)

PCA confirmed that at least three crystal groupings could be explained with the various urease data, thereby verifying that the differences in precipitation could largely be ascribed to diversity in the urease gene fragments of the various isolates, with resulting biochemical differences in urease activities of the various isolates (Figure 3.8). The first two principal components (PC) explained most of the total variation 99.7 % (PC 1 = 79.4 %; PC 2 = 18.9 %). The PCA did, however, not separate the different crystal-aggregate groups completely, most notably CPB 11 and 12 clustered together with CPB 7 – 10 (see Figure 3.2). Based on the PCA, three groups were included in the discriminant analysis. The results showed that for the first discriminant (accounting for 91 % discrimination) in descending order of importance, the substrate affinity (K_m) had a positive contribution, while the maximum hydrolysis rate (V_{max}) and the number of bands both had negative contributions ($p = 0.008$ %).

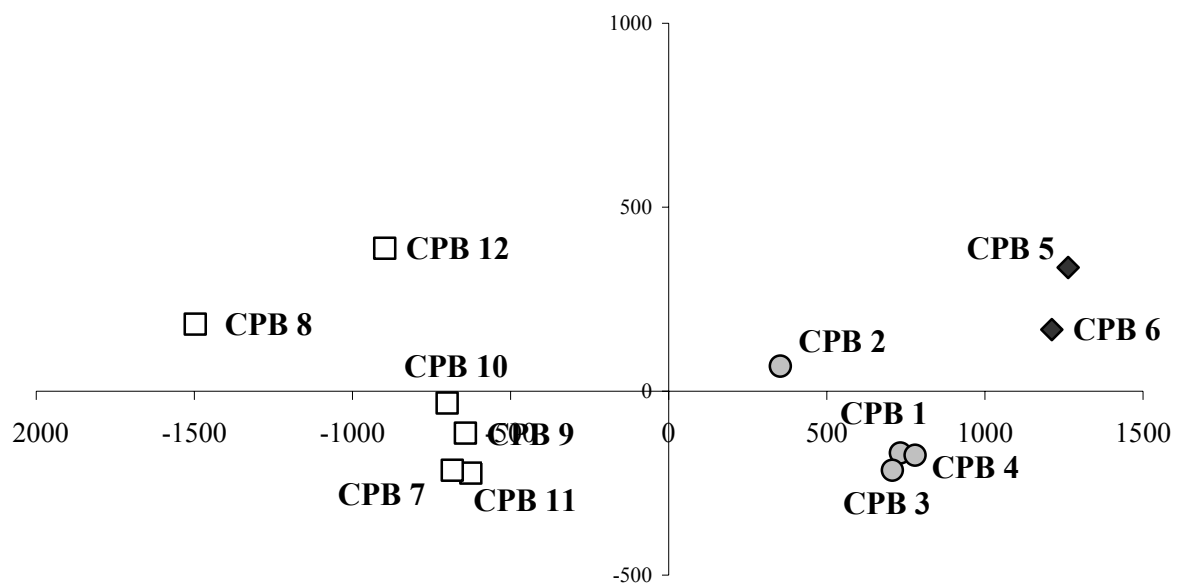


Figure 3.8. Principle component analysis incorporating biochemical and molecular urease data, and revealing at least three major clusters.

DISCUSSION

The aim of this study was to investigate the mechanisms causing apparent differences in crystal aggregate formation during ureolytic microbial calcium carbonate precipitation (MCP). Precipitation within microbial colonies on agar presents a unique opportunity to study this natural phenomenon within a specific localised microenvironment created by the micro-organisms (Figure 3.1). Previous studies have used X-ray diffraction (XRD) data to suggest species-specific precipitation (Kawaguchi and Decho, 2002; Rivadeneyra et al, 2000) but others contend that species-specific differences are due primarily to environmental rather than microbial factors (Knorre and Krumbein, 2000). Although morphological differences in crystallisation were evident (Figure 3.2), XRD analysis showed in all cases rhombohedral calcite to be the primary component, with vaterite and also fluorite only detected in some cases. Fluorite detection was surprising in the sense that none of the culture media components contained any fluorine to our knowledge. That aside, the precipitation of fluorite as a result of microbial ureolytic activity has been described to occur in dental plaque biofilms (Wong *et al.*, in press). Vaterite detection was also interesting, as vaterite is metastable at normal temperature and atmospheric pressure. It was suggested previously that the metastable polymorphs form initially, and subsequently converts to a stable polymorph e.g. calcite (Vecht and Ireland, 2000). In fact, enzymatic precipitation experiments using liquid solutions of urea and CaCl_2 at room temperature found the sequence of precipitation to be first amorphous CaCO_3 , then vaterite, and finally calcite (Sondi and Matijevic, 2001). Though calcite is commonly precipitated during ureolytic carbonate precipitation (Bachmeier *et al.*, 2002; Bang *et al.*, 2001; Stocks-Fischer *et al.*, 1999), microbes precipitate other polymorphs such as aragonite (Kawaguchi and Decho, 2002; Rivadeneyra et al, 2000). The fact that all the samples displayed very similar XRD results, while clear morphological differences were evident, suggests that the differences were a result of variations in crystal growth rates along different planes of the crystal structure. This could have been a result of the colony growth rate and/or actual urease activity, thereby influencing the rate of supply of chemical species required for precipitation (Sondi and Matijevic, 2001). Alternatively, crystal growth can be inhibited or altered by the adsorption of proteins, organic matter or

inorganic components to specific crystallographic planes of the growing crystal (Kawaguchi and Decho, 2002; Rivadeneyra et al, 1998; Schultze-Lam *et al.*, 1996). Organic matrix effects on crystallisation was, in the case of ureolytic MCP under the conditions studied herein, thought to be secondary to enzyme-related effects.

The results showed urease activity to be present in all the isolates and that the location of the urease enzymes were not extracellular for any of the isolates, concurring with most of the literature concerning this point (Burne and Chen, 2000; Stocks-Fischer *et al.*, 1999; Mobley and Hausinger, 1989). The purpose of the Ca^{2+} :urea assay was to eliminate the effects of growth rate and specific urease activity, and then establish whether any quantitative differences could be found between the amount of calcium precipitated compared to the amount of urea hydrolysed. All samples were inoculated with high cell numbers, representing both sufficient urease proteins and crystal nucleation sites. Equations 3.1 – 3.5 show how one mole of urea can account for the formation of one mole calcium carbonate in theory, bar the loss of carbonate through bicarbonate equilibrating reactions, and the requirement for crystal nucleation sites. Previous work suggested that biological factors such as intracellular active calcium metabolism (McConnaughey and Whelan, 1997), cation-cell membrane interactions (Schultze-Lam *et al.*, 1996), or extracellular polymeric substance (EPS), could all enhance CaCO_3 precipitation. However, the results from the Ca^{2+} :urea assay (Table 3.2) did not support cellular-based specific precipitation, as it did not correspond with the crystal groupings. The fact that a similar Ca^{2+} :urea ratio was detected for most of the isolates suggests that individual urease activity is probably the governing factor in the evidenced precipitation differences in this specific case.

Several ureolytic CaCO_3 precipitating species have been characterised before, including *B. pasteurii* (Stocks-Fischer *et al.*, 1999; Ferris and Stehmeier, 1993), *Pseudomonas* spp. and *Variovorax* spp. (Fujita *et al.*, 2000), and *Leuconostoc mesenteroides* (Ferris and Stehmeier, 1993). It is therefore emphasized that the isolation and identification results presented herein do not necessarily represent a unique group of calcium-precipitating bacteria, but rather organisms that proliferate and express the urease gene under the given cultivation conditions. However, the close relation of the various isolates from this study

within the *Bacillus sphaericus* group is remarkable. To some extent this predominance of a specific phylogenetic group can be attributed to environments from which the isolates were sampled. Both the soils and the concrete surface represent dry conditions in which spore-forming organisms such as *Bacillus* species proliferate. In this regard Felske *et al.* (1998) for instance showed with fluorescent *in situ* hybridisation (FISH) that at least 40 % of all bacteria in a Dutch soil belonged to *Bacillus* species and some other low-G+C-content organisms. The isolation and cultivation conditions could also have had a selective influence: nutrient broth with urea addition is a preferred growth medium of ureolytic *Bacillus* species (Stocks-Fischer *et al.*, 1999; Ferris and Stehmeier, 1993).

A new approach to study the diversity of functional genes is analysis of PCR products of these genes with DGGE (Boon *et al.*, 2001; Rosado *et al.*, 1998). To our knowledge, this is the first study that has used DGGE to examine the diversity of a urease gene fragment. The first noticeable result from the urease DGGE is the apparent presence of isozymes. Though the occurrence of urease isoforms within a single organism has been described previously, no molecular proof for the occurrence of multiple isozymes within a single bacterium has yet been presented (Burne and Chen, 2000; Mobley and Hausinger, 1989). The results presented in this study are interesting, but also inconclusive. DGGE examination of PCR products amplified with degenerated primers often reveals more than one band from a single unique starting template (Kowalchuck *et al.*, 1997). The generation of multiple bands was, however, not entirely consistent, since not all CPB-DNA templates did result in multiple bands (Figure 3.5). As a consequence, in some of the CPB strains isolated, the possible existence of different isozymes should certainly not be excluded. The DGGE also shows distinct differences as well as evident resemblances between the various isolates, which were highlighted by the cluster analysis (Figure 3.5). Interestingly, some correlation between the clustering and the crystal groupings could be detected. For example, the 100 % similarities between CPB 1 & 2 and CPB 5 & 6 respectively, coincide with their distinct and almost identical respective crystallisation patterns (Figure 3.2). On the other hand, *B. pasteurii* clustered with CPB 5, 6 and 9, in contrast with its phylogenetic clustering (Figure 3.4). These results confirm previous literature reports that a definite degree of divergence exists in the genetic make-up of microbial ureases (Mobley *et al.*, 1995; Mobley and Hausinger, 1989). DGGE makes it possible to reveal this urease diversity, since this

technique allows the separation of a 1-bp difference between two sequences (Felske *et al.*, 1999). This DGGE approach, applied to total DNA extracted from various environmental habitats, could be especially useful for further investigation of the diversity of urease genes in microbial communities without prior cultivation of the urease positive organisms. Given the high urease affinity present in some organisms and the induction of urease activity in these isolates by calcium, the relationship between 16S rDNA and urease divergence may highlight some of the ecological roles of urease in environmental isolates.

In general, the isolates displayed low urea affinity and high specific rates. The first deduction from this could be that the isolates are not scavengers for urea, but responds well to high concentrations thereof. K_m values for urease enzymes ranging between 0.1 and 100 mM urea have been reported for bacteria (Mobley and Hausinger, 1989). Typical examples are: *B. pasteurii* = 40 – 130 mM; *Proteus mirabilis* = 13 mM; *Ureaplasma urealyticum* = 2.5 mM (Mobley and Hausinger, 1989). Stocks-Fischer *et al.* (1999) reported a V_{max} value for *B. pasteurii* urease of 1.72 – 3.55 mM·min⁻¹·mg⁻¹_{protein} (depending on the pH). Standard reported V_{max} values range between 1 – 5.5 mM·min⁻¹·mg⁻¹_{protein} for purified microbial enzymes, while *U. urealyticum* was shown to have values between 33 – 180 mM·min⁻¹·mg⁻¹_{protein} (Mobley and Hausinger, 1989). Crude enzyme extracts should be used comparatively rather than as being reflective of the actual urease activity of an organism, as the latter is significantly affected by trans-membrane transport of urea (via urea permease enzymes), ammonia and protons. Usually, experiments with crude enzyme extracts results in higher than actual values for urease rates. Nonetheless, the activity results from Table 3.4 do explain to some extent the differences seen in crystallisation. Isolates CPB 1 - 6 all showed moderate to high substrate affinities and specific rates, thus resulting in rapid crystallisation as well as CaCO₃ precipitates, which are more crystalline in appearance. This was especially the case for class CPB 5 & 6. Isolates CPB 7 and CPB 8 are somewhat intermediate concerning their activity values, which also accounts for their indifferent classification. Isolates CPB 8 - 12, representing classes 5 and 6 displayed low substrate affinities and low specific rates (with the exception of isolate CPB 12 on the latter). This as such could explain the slower crystal formation, allowing for more colony growth, and thus interference by the sorption of organic matter in the crystal structure. The results further suggest that most of the enzymes displayed activity optima between pH 8

and 9. Stocks-Fischer *et al.* (1999) reported a similar pH trend for *B. pasteurii*. This apparent alkaline affinity of the enzymes could be attributed to the conditions of growth (and subsequent expression). The isolates are cultivated in medium of which the initial pH is between 7 and 8, but upon urea hydrolysis, this rapidly increases to pH 9.3 (Stocks-Fischer *et al.*, 1999).

The urease data sheds more light on the physiological role of urea hydrolysis (which causes the eventual CaCO₃ precipitation). Bacteria can use urea to (1) increase the pH of an environment (Burne and Marquis, 2000; Stocks-Fischer *et al.*, 1999), (2) as source of nitrogen (Moblely and Hausinger, 1989), and (3) as source of ATP (Burne and Chen, 2000; Mobley and Hausinger, 1989). The fact that the urease optima was in the alkaline pH range suggests that the function thereof was not a pH effect, since that would rather apply to acidic conditions (Burne and Marquis, 2000; Wong *et al.*, in press). The low urea affinity of several of the crude extracts also contradicts expected results from organisms that use urea as nitrogen source, as this would require the hydrolysis of often very low environmental concentrations. This leaves ATP synthesis as a possibility, and the high specific rates detected for some of the isolates do concur with this.

The presence of calcium modulated urease activity of live, intact bacterial cells. An adverse modulation was expected. Southam (2000) suggested that surface associated mineralisation would result in limitations of nutrient transport and eventual disruption of the proton-motive force, thereby suggesting that precipitation resulting from urea hydrolysis may be detrimental to bacterial cells, and thus to further urease activity. Figure 3.7 shows that for most of the isolates no difference was detected between urease activity in the presence or absence of calcium. However, isolates CPB 1 – 4 displayed remarkable increases in urease activity in the presence of soluble calcium. If the 5 to 10-fold increases detected here are considered together with the specific rates from Table 3.4, urease activities to the order of 50 – 100 mM·min⁻¹·mg⁻¹_{protein} are implied, which is well within range of the highest urease activities ever detected for bacteria (Moblely and Hausinger, 1989). This coincided with similar characteristic macro-crystallisation by these four isolates (Figure 3.2(a-d)). To our knowledge, calcium ions have not previously been associated with increased urease activity. While Ca²⁺ could theoretically facilitate better

trans-membrane transport, or improve intracellular signalling processes, it should be expected that these processes occur in all related organisms, such as the case is here. An alternative explanation may be a detoxification response of the bacteria to high calcium concentrations (McConnaughey and Whelan, 1997; Anderson *et al.*, 1992). Active calcium metabolism requires energy (ATP) (McConnaughey and Whelan, 1997), and several microorganisms (e.g. *B. pasteurii*) have previously been shown to produce ATP through urea hydrolysis (Burne and Chen, 2000; Mobley and Hausinger, 1989). At least for some strains, these results support the above suggestion that urease may be utilised as ATP source. The fact that some strains displayed such a pronounced effect warrants further research on the possibilities of an ATP-driven calcification process.

CONCLUSION

In conclusion, this paper clearly shows strain-specific precipitation to occur during ureolytic microbial CaCO₃ precipitation. Cell wall or matrix-associated influences were not analysed. Nonetheless, principle component analysis confirmed that the differences in crystal aggregate formation could largely be ascribed to diversity in the urease gene fragments of the various isolates, with resulting biochemical differences in the urease activities of the various isolates.

[Link to Contents](#) [Link to Chapter 4](#)

ACKNOWLEDGEMENTS

The authors would like to thank Dr Sabine Verryn, who performed the XRD analyses and phase identification, Prof. R. Hausinger for comments on the urease molecular results, and Vanessa Vermeiren, Hanne Lievens and Sofie Dobbelaere for critical reading of the manuscript.

MICROBIAL ECOLOGICAL IMPACT OF ALKALINE pH, Ca^{2+} AND CALCIUM CARBONATE PRECIPITATION

Redrafted from:

- (1) **F. Hammes and W. Verstraete.** 2002. Key roles of pH and calcium metabolism in microbial carbonate precipitation. *Re/Views in Environmental Science & Bio/Technology* 1, 3-7.
- (2) **F. Hammes, N. Boon and W. Verstraete.** 2001. Calcium interaction with bacteria at alkaline pH regimes. In: Abstracts "9th International Symposium on Microbial Ecology (ISME-9)", Amsterdam, The Netherlands. p. 137.

ABSTRACT *The effect of a typical precipitation environment (high pH and high Ca^{2+} concentration), as well as the direct and indirect effects of calcium carbonate (CaCO_3) precipitation, on survival and growth of pure cultures was investigated. It is hypothesised that calcium ions become toxic to bacteria under alkaline pH conditions, and that precipitation of CaCO_3 thus could be a cation detoxification process. This chapter considers the potential ecological benefits and drawbacks of microbial CaCO_3 precipitation.*

INTRODUCTION

Although microbiological calcium carbonate precipitation (MCP) has been investigated extensively both in natural environments and under defined laboratory conditions, the exact mechanisms of precipitation and the function of this process within the microbial ecology of the precipitating organism remains unresolved (Yates and Robbins, 1999; Rivadeneyra *et al.*, 1994; Ferrer *et al.*, 1988). Nonetheless, the primary metabolic role of bacteria in the precipitation of CaCO₃ has been ascribed to their ability to create an alkaline environment through various physiological activities including urea hydrolysis, photosynthesis, etc. (Castanier *et al.*, 1999; Douglas and Beveridge, 1998). The fact that these metabolic processes lead to mineral precipitation has been largely ascribed as to being a side-event, or even an unwanted process, that has little or nothing to do specifically with the precipitating organism (Knorre and Krumbein, 2000; Boquet *et al.* 1973). Higher organisms such as algae, coral, and molluscs for example all gain ecological advantages from precipitation, most noticeably in the form of protective layers. But the fact is that up to date, no bacterium has been shown to precipitate CaCO₃ with specific ecological “intention” or benefit. However, McConnaughey and Whelan (1997) have argued theoretically that photosynthetic microorganisms could gain an ecological advantage from CaCO₃ precipitation, in that they produce protons this way which are necessary to improve the uptake of nitrogen and bicarbonate by these organisms (Equation 4.1 and 4.2).



This theory of McConnaughey and Whelan (1997), is based entirely on active Ca²⁺ metabolism by the microorganisms, leading to supersaturated micro-environments. More evidence exists for an important role of calcium metabolism in the precipitation process. Castanier *et al.* (1999) suggested that “active” CaCO₃ precipitation could be linked to ion transport (specifically Ca²⁺) across cellular membranes, while Yates and Robbins (1999) used radioactive labelled Ca²⁺ to indicate that extracellular precipitated calcium originated from inside the precipitating organisms.

Calcium metabolism

Compared to higher organisms, calcium interaction with, and regulation in, bacteria have received very little research attention and thus remain much of a black box today (for review, see Norris *et al.*, 1996). Apart from playing some part in the formation of heat resistant spores (Raeymaekers *et al.*, 2002), calcium was thought to be an element not likely to be used by bacteria, and of which the primary role with regards to bacteria was binding with the membranes (Stocks-Fischer *et al.*, 1999). Only recently has the important function of calcium as a signal molecule in bacteria similar to that in plants been reported, and has it emerged that calcium metabolism is a vital component of bacterial physiology (Holland *et al.*, 1999; Herbaud *et al.*, 1998). Calcium is indeed not likely to be used by bacteria, but rather tightly regulated. Calcium regulation in bacterial cells comprises of influxes and effluxes as a result of active and/or passive transport mechanisms. Since calcium is a rather large molecule, trans-membrane transport is usually protein-assisted. The latter (passive transport) is common in bacteria and is facilitated by antiporters (Ca²⁺/2H⁺, Ca²⁺/2Na⁺) (Holland *et al.*, 1999; Desrosiers *et al.*, 1996), protein-based channels and non-proteinaceous channels (Norris *et al.*, 1996). Transport via these systems can be bi-directional, depending on the specific system, but requires the existence of an electrochemical gradient (i.e. from high gradient to low gradient). Due to the fact that normal intracellular calcium concentrations are usually up to 10³-times lower than extracellular concentrations, passive transport usually accounts for calcium influx (Desrosiers *et al.*, 1996; Norris *et al.*, 1996). Primary or active calcium transport on the other hand is facilitated by ATP-dependent ion pumps based on plant-like Ca²⁺-ATPase enzymes. These systems are able to transport calcium against an electrochemical gradient but at the expense of energy (ATP) (Desrosiers *et al.*, 1996).

Hypothesis

A typical carbonate precipitation environment comprises high extracellular calcium concentrations (up to 10,000 times higher than the cytoplasmic Ca²⁺ concentration (Anderson *et al.*, 1992)) and low extracellular (compared to intracellular) proton

concentrations (as a result of alkaline pH regimes). Figure 4.1 schematises the hypothesised chain-of-events under such conditions.

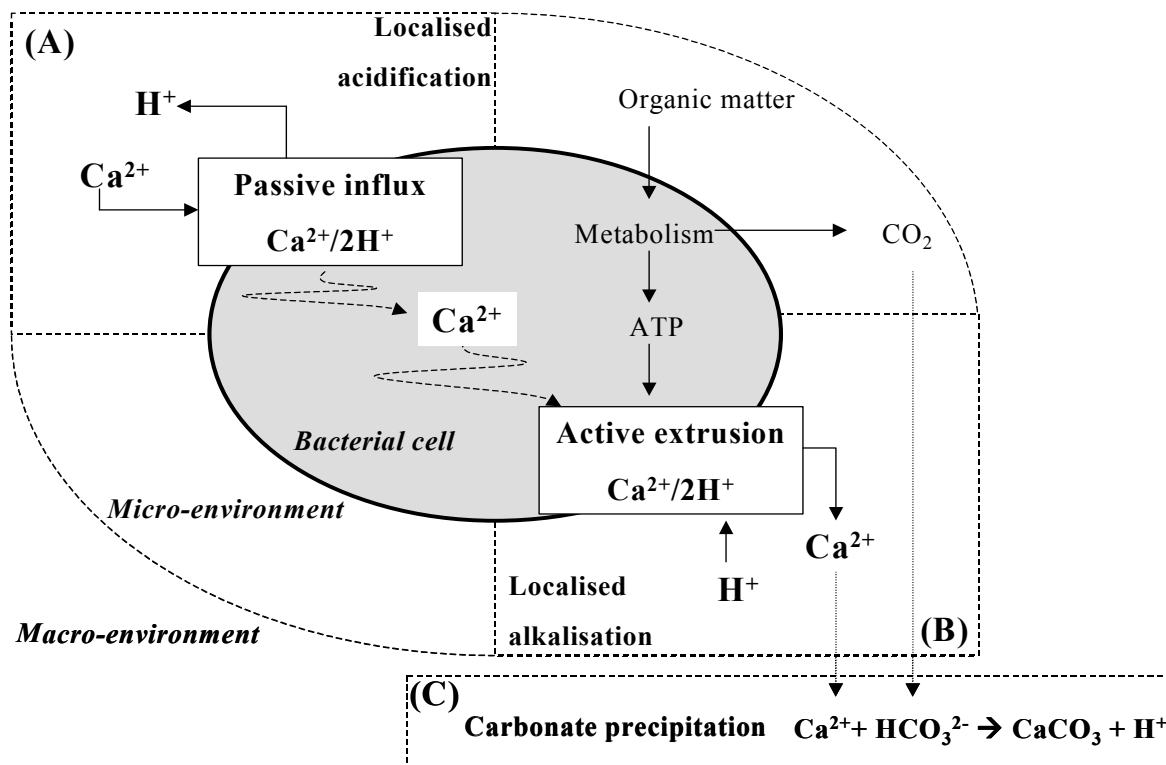


Figure 4.1. Hypothesised chain of events following the exposure of a bacterial cell to an alkaline environment rich in calcium ions.

The combination of an extracellular alkaline pH and calcium ions pose an inevitable stressful environment for bacteria: passive calcium influx as a result of the complimentary Ca²⁺/2H⁺ electrochemical gradients will lead to intracellular calcium build-up and excessive proton loss (Figure 4.1, section A). At the cellular level, this event could result in irreversible damage due to the (1) disruption of intracellular calcium-regulated signal processes, (2) alkalisation of intracellular pH and (3) depletion of the proton pool required for numerous other physiological processes (Norris *et al.*, 1996; Anderson *et al.*, 1992). Survival under such conditions requires active export of intracellular calcium, e.g. via the described ATP-dependent calcium pumps, which would reduce intracellular calcium ions and simultaneously compensate the proton loss (Figure 4.1, section B) (Anderson *et al.*, 1992). The latter event could result in a localised increase in pH, due to proton uptake, in

the same region as the calcium ion increase, which would form an ideal localised precipitation micro-environment (Figure 4.1, section C) (McConnaughey and Whelan (1997)). Even if spatial limitations restrict the formation of localised micro-environments, survival of the organism is dependent on active calcium metabolism. To accomplish this, energy is required, of which metabolic CO₂ is a natural by-product. Thus, survival and proliferation will lead to an increase the extracellular DIC concentrations, which would affect the solubility product of CaCO₃, eventually favouring precipitation. Moreover, Figure 4.1 shows how carbonate precipitation will theoretically alter the extracellular environment (decrease soluble Ca²⁺ and increase acidity) so that it becomes more favourable for bacterial proliferation. Thus, to summarise, in this chapter it is hypothesised that CaCO₃ precipitation is a result of calcium ion detoxification through active ATP dependant calcium extrusion under conditions of high extracellular calcium concentration and a high pH.

Understanding the microbial ecological impacts of CaCO₃ precipitation is important. Fundamentally it addresses a major question as to whether microbial-catalysed CaCO₃ precipitation is an ecological beneficial reaction for the bacteria, or merely an unrelated side-event of metabolism. Moreover, this process is used in biotechnological applications, and knowledge of the effect of the reaction on the optimal function of the biocatalyst, would therefore contribute to successful application and operation thereof. The aim of this chapter is to investigate some of the factors of this hypothesis, specifically in relation to ureolytic precipitation.

MATERIALS & METHODS

Bacterial cultures

Myroïdes odoratus (LMG 4028; ATCC 29979), previously *Flavobacterium odoratum* (Desrosiers *et al.*, 1996; Vancanneyt *et al.*, 1996), was acquired from the BCCM/LMG culture

collection (Ghent, Belgium), while a certified culture of *Delftia acidovorans* (Boon *et al.*, 2000) was present in the laboratory. Both these pure cultures were cultivated and maintained on nutrient agar (Oxoid) at 28 °C. Two strains of ureolytic calcium precipitating bacteria, belonging to the *Bacillus sphaericus* group were isolated from soil and a concrete surface respectively (CPB 4 and CPB 12; this study, Chapter 3), and maintained on nutrient agar supplemented with 20 g·L⁻¹ urea (Riedel-de Haën).

Ca²⁺ effect on bacterial survival/proliferation at different pH

Liquid growth media were prepared consisting of 2.5 g·L⁻¹ nutrient broth of which the pH was fixed at 8, 8.5 and 9 respectively (1 N NaOH) before sterilisation. After sterilisation, 10 mM Ca²⁺ (as CaCl₂) was added aseptically (0.22 Whatman filters) to some of the samples, resulting in media at all three pH levels with and without calcium added. The sterilised media were inoculated with pre-cultivated samples of *M. odoratus* and *D. acidovorans* (see above), and incubated (28 °C, 100 rpm) for 24 h. The inoculum was determined for both bacterial cultures with serial dilution in sterile physiological solution (8.5 g·L⁻¹ NaCl) and plating on nutrient agar. The pH in the experiments for both cultures with media at pH 9, with and without calcium addition, was recorded automatically using a R305 (Consort, Antwerpen, Belgium) instrument fitted with separate electrodes. After 24 h, samples were taken from all experiments and the number of colony forming units per millilitre (cfu·mL⁻¹) was determined (as above).

Ca²⁺ and pH influence on *M. odoratus* growth

Semi-solid plating media were prepared containing 50 mM TRIS buffer (pH 7.5 and 8.5 respectively), 2.5 g·L⁻¹ nutrient broth, 13 g·L⁻¹ agar, and with and without the further addition of 10 mM Ca²⁺ (as CaCl₂). Similar media were prepared with a pH of 8.5 and containing varying concentrations of calcium: 0, 5, 10, 20 mM, as well as media containing 20 mM Na⁺ (as NaCl) and K⁺ (as KCl) respectively. All media were sterilised and poured into sterile petri dishes. A pre-cultivated sample of *M. odoratus* was diluted in sterile physiological solution, and plated on the respective growth media using the spread-plate technique. All plates were incubated at 28 °C and assessed daily with light microscopy (Axioskop 2 Plus, Zeiss). Only plates containing less than 2x10¹ colonies per plate were used for analysis. Microscopic images of colonies were

captured with a 1-CCD camera (Hamamatsu Photonics GmbH, Hersching, Germany) and analysed with MicroImage 4.0 software (Olympus Optical Co. (Europe)). Colony diameter was measured as indication of growth. Per experiment, 30 colonies were analysed.

Effect of nutrient addition on *M. odoratus* survival

Sterile media were prepared containing 50 mM TRIS buffer (pH 8.5) and 10 mM Ca²⁺, with and without the addition of 1 g·L⁻¹ nutrient broth. These media were inoculated with *M. odoratus* and incubated (28 °C, 100 rpm). The inoculum was determined with serial dilution and plating on nutrient agar. After 24, 48 and 72 hours respectively, samples were taken from the media, diluted and plated on nutrient agar (as above).

Chemical effect of precipitation on the environment

NaHCO₃ (10 mM) solutions were prepared with milliQ water and the pH of these solutions was fixed at 7, 8 and 9 respectively. Thereafter, calcium (10 mM CaCl₂) was added to these solutions and the pH was measured. Separately, solutions were prepared containing urea (100 mM) and calcium (0, 10, 20 and 30 mM) and commercial urease (Sigma; Type III from Jack Beans) was added. The pH was measured automatically every 60 seconds (as above).

Effect of precipitation on the precipitating organisms

A sample of isolate CPB 1 (see above) was diluted and plated on precipitation media, consisting per litre of: 3 g nutrient broth (Oxoid), 20 g urea, 2.12 g NaHCO₃ (Sigma), 10 g NH₄Cl (Sigma), and 30 mM CaCl₂·2H₂O (Sigma) (Ferris and Stehmeier, 1992; Stocks-Fischer *et al.*, 1997). Plates were incubated at 28 °C for 5 days. After 5 days of growth and precipitation, crystals were harvested from the agar, washed in sterile physiological solution repetitively, and analysed with light microscopy. Some of the crystals were also dried at critical point in a series of gradually increasing ethanol concentrations, gold-coated, and analysed with SEM using a JSM 840 instrument (JEOL LTD, Tokyo, Japan). Moreover, some of the harvested crystals were transferred to sterile Eppendorf tubes (6 crystals per tube), and washed three times in sterile physiological solution to remove the bacteria attached to the exterior of the crystals. After

these washes, the crystals were pulverised using a sterile micro-pipette coupled with vortexing. The pulverised samples were plated on growth medium (see above), while the liquid from a non-pulverised sample was plated as well as negative control. Samples were also taken for viability staining. For the latter, commercial live/dead stain (L-13152, Molecular Probes Europe) was used (Boulos *et al.*, 1999). Stained samples were incubated in the dark for 2 h and analysed with epifluorescent microscopy an Axioplan II (Zeiss, Germany) microscope.

Effect of ureolytic precipitation on growth and survival

Precipitation agar was prepared containing nutrient broth (3 g·L⁻¹) and agar (13 g·L⁻¹) and urea (100 mM), with and without calcium addition (30 mM). Pure cultures of CPB 4 and CPB 12 were diluted and plated on the media, and incubated (28 °C). Colonies were assessed and analysed daily for 7 days as discussed above. Colony diameter and crystal diameter (where applicable) were measured with digital image analysis software (as above).

RESULTS

Ca²⁺ effect on bacterial survival/proliferation at different pH

Bacterial growth on nutrient broth would normally lead to acidification. Figures 4.2a and 4.2b show the different pH responses recorded for *M. odoratus* and *D. acidovorans* starting from pH 9 in the presence and absence of 10 mM Ca²⁺, recorded during 24 h. A noticeably different effect is visible for *D. acidovorans*, where nearly no pH change is seen in the presence of Ca²⁺. Figure 4.3 shows the changes in colony forming units during the same time period at three alkaline pH levels with and without calcium present. It is apparent that both pure cultures displayed inhibited growth responses at high alkaline pH levels (pH 9), and this adverse effect became much more pronounced in the presence of calcium. Also, these effects were much more

pronounced for *D. acidovorans*. In fact complete die-off is seen for *D. acidovorans* at pH 9 in the presence of 10 mM Ca²⁺, which explains the pH results from Figure 4.3.

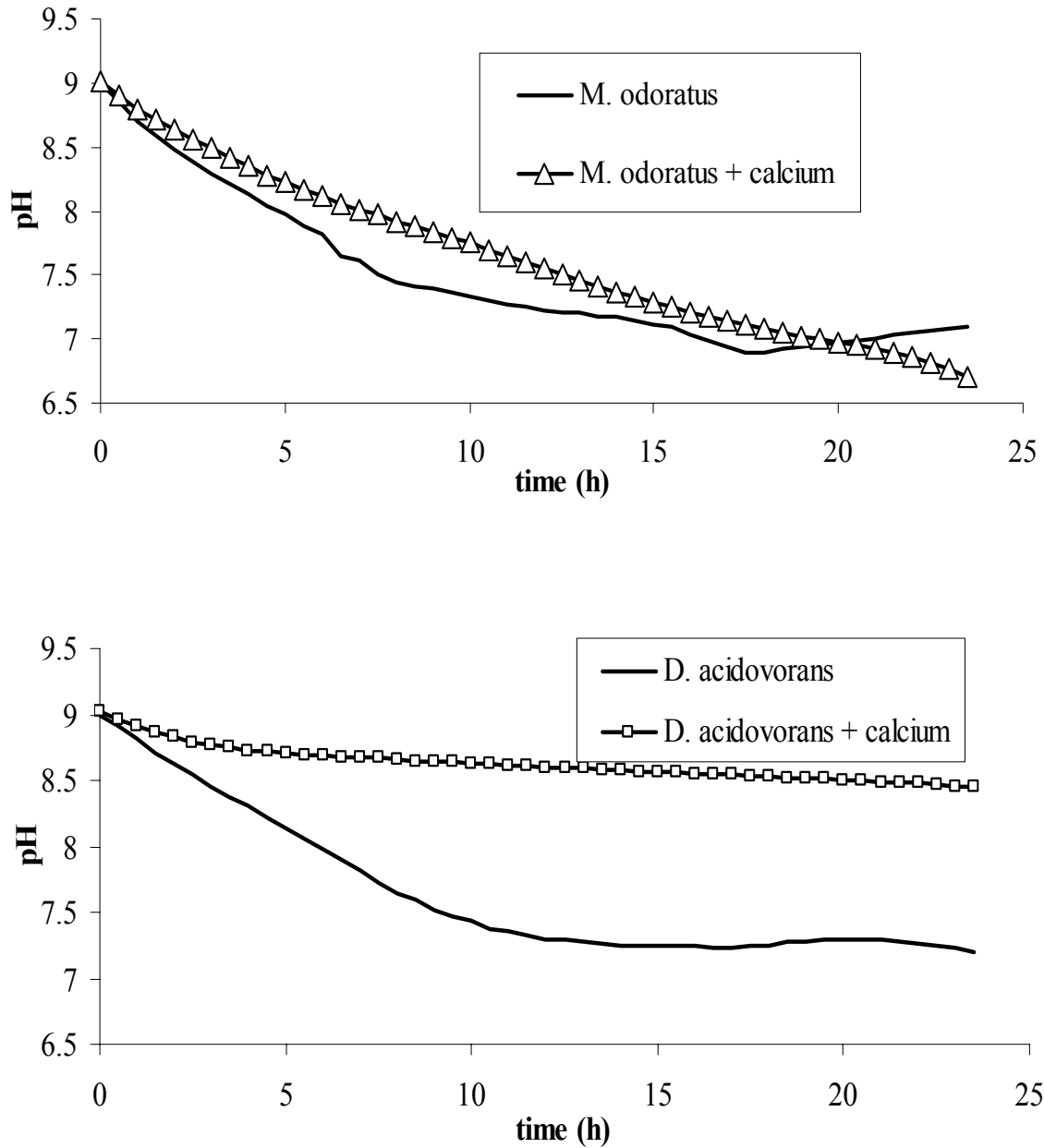


Figure 4.2. Fluctuations in pH measurements recorded during 24 h of growth of *M. odoratus* (a) and *D. acidovorans* (b) in the presence of 10 mM Ca²⁺ and starting from an initial pH of 9.

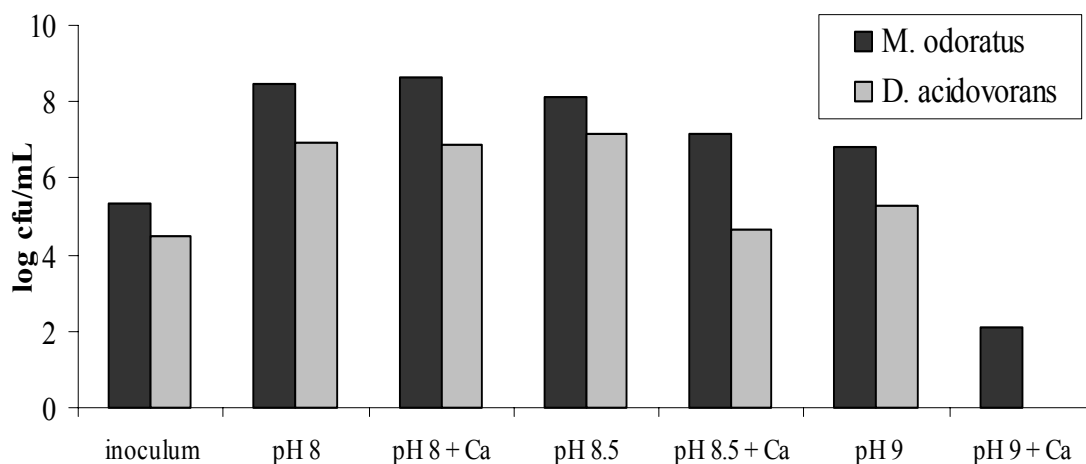


Figure 4.3. Changes in cfu.mL⁻¹ after 24h for *M. odoratus* and *D. acidovorans*

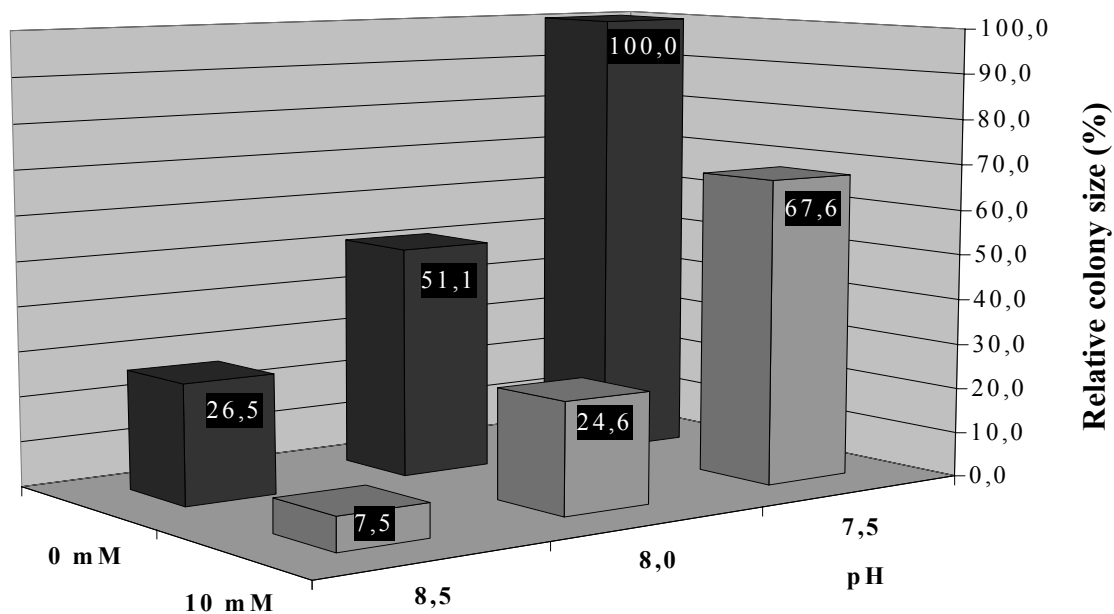


Figure 4.4. Combined effect of alkaline pH and 10 mM calcium on *M. odoratus* growth.

Ca²⁺ and pH influence on *M. odoratus* growth

The adverse effects of increasingly alkaline pH and soluble calcium on the growth of *M. odoratus* are indicated in Figure 4.4. The higher the pH was, the more pronounced the adverse

effects of Ca²⁺. The inhibitory effect of calcium on colony growth at pH 7.5 equals about 30 %, at pH 8 about 50 %, and at pH 8.5 about 70 %. Figure 4.5 shows that at pH 8.5, the inhibitory effect of calcium is directly proportional to the calcium concentration, while Figure 4.6 indicates that a similar ionic charge (20 mM) from monovalent ions (Na⁺ and K⁺) have no adverse effect on growth compared to divalent ions (10 mM Ca²⁺ and Mg²⁺ respectively), while the effect of Mg²⁺ was apparently less pronounced than that of Ca²⁺.

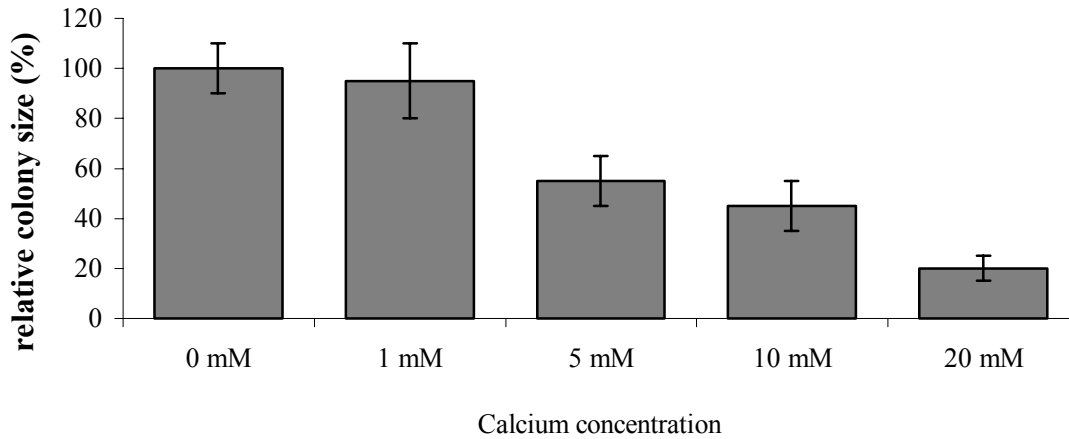


Figure 4.5. Relative effect of calcium concentration on *M. odoratus* growth at pH 8.5.

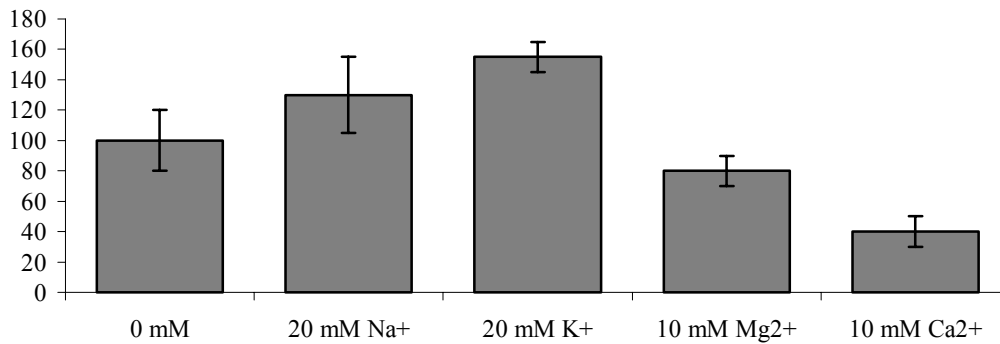


Figure 4.6. The relative effects of different cations on *M. odoratus* growth at pH 8.5.

Effect of nutrient addition on *M. odoratus* survival

Nutrient addition ensured the survival of *M. odoratus* under conditions of pH and calcium stress. The effects of nutrient presence and absence to the survival of *M. odoratus* at pH 8.5 in the presence and absence of calcium is shown in Figure 4.7. Noticeable is that *M. odoratus*

survived without nutrients in TRIS buffer (pH 8.5) when calcium is not present, but complete die-off is seen when calcium ions are added to the medium. On the other hand, when nutrient broth is added to the medium as nutrient source, *M. odoratus* survived the combined calcium and pH stress.

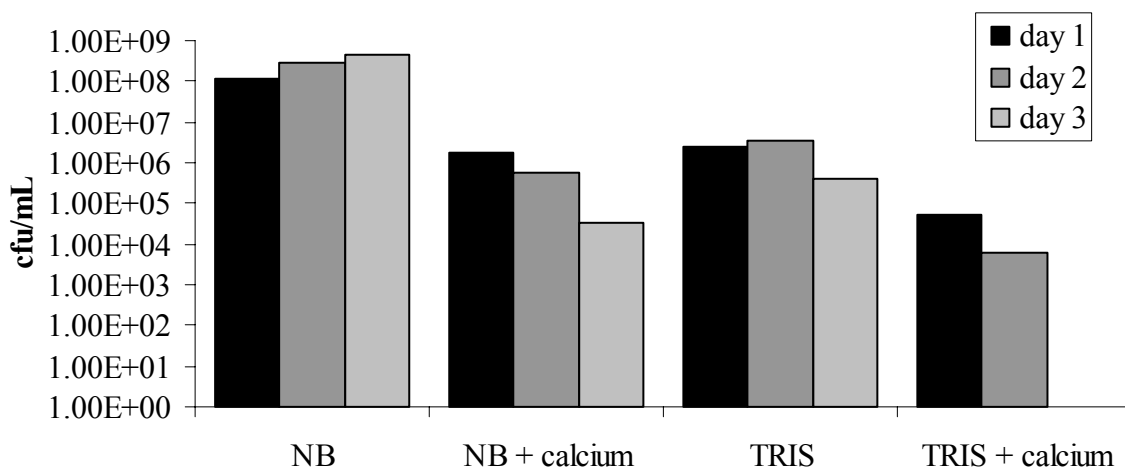


Figure 4.7. *M. odoratus* growth at pH 8.5 in the presence and absence of nutrients and presence and absence of Ca²⁺.

Chemical environmental pH changes following CaCO₃ precipitation

CaCO₃ precipitation decreases both the pH and the calcium ion concentration. To illustrate the effect of precipitation on the chemical composition of an aquatic environment, a closed system was modelled consisting of 10 mM DIC, 10 mM Ca²⁺, 25 °C and pH 8. The species was calculated as described in Equations 2.9 - 2.11 (Chapter 2). If 1 CaCO₃ precipitate, the bicarbonate buffer will balance the loss of CO₃²⁻ by producing an equal amount of CO_{2(aq)}. The system thereby acidifies, and this acidification can be calculated by substituting the newly derived CO_{2(aq)} concentration in Equation 2.11, taking into account that the total carbon concentration also changed. The other species, as well as the saturation state of the system can subsequently be calculated. Table 4.1 shows the calculated results of the precipitation of 1, 2 and 3 mM CaCO₃, and the effect thereof on the saturation state of the system.

Table 4.1. Calculated changes to a system super-saturated with respect to CaCO₃ following precipitation.

	Original	1 mM	2 mM	3 mM
Ca ²⁺	10	9	8	7
pH	8.00	7.17	6.78	6.43
IAP	4.55 x 10 ⁻⁷	4.93 x 10 ⁻⁸	1.31 x 10 ⁻⁸	3.37 x 10 ⁻⁹
Saturation	120	12.97	3.46	0.89

Urea hydrolysis results in a pH increase, but similar to above, CaCO₃ precipitation will counteract this through a pH decrease. Figure 4.8 shows pH changes occurring during urea hydrolysis in the presence of different calcium concentrations. As expected, higher calcium concentrations, equivalent to more CaCO₃ precipitation, resulted in lower final pH levels in the medium.

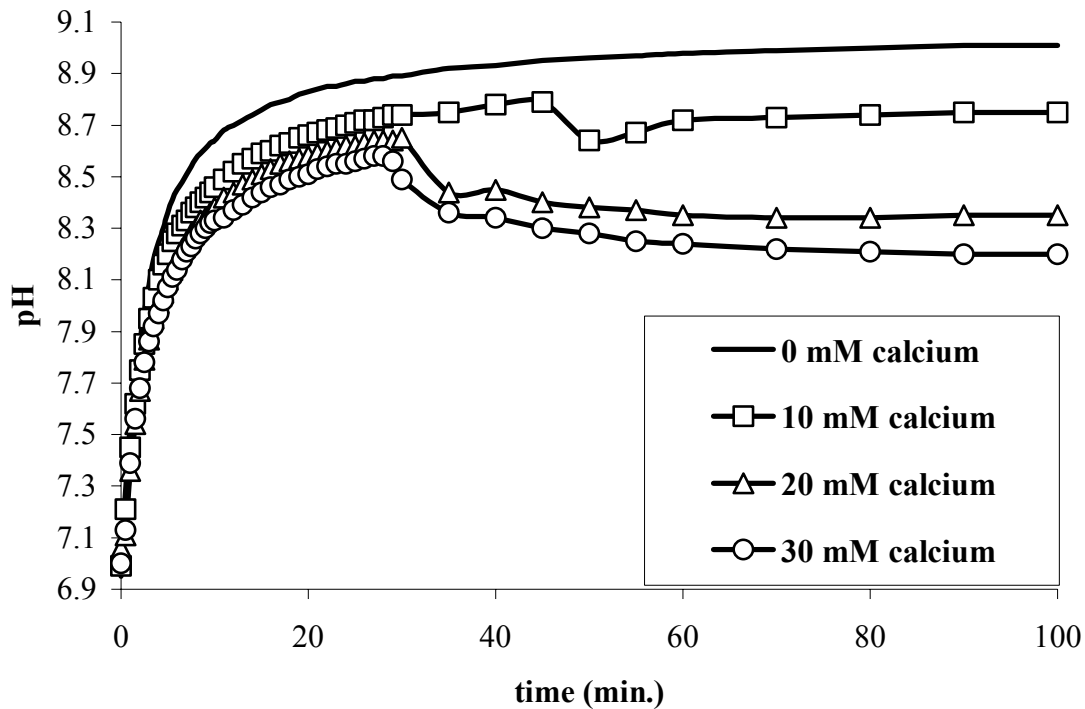


Figure 4.8. Effect of higher calcium concentrations (thus more precipitation) on the pH of a solution during the enzymatic hydrolysis of 100 mM urea.

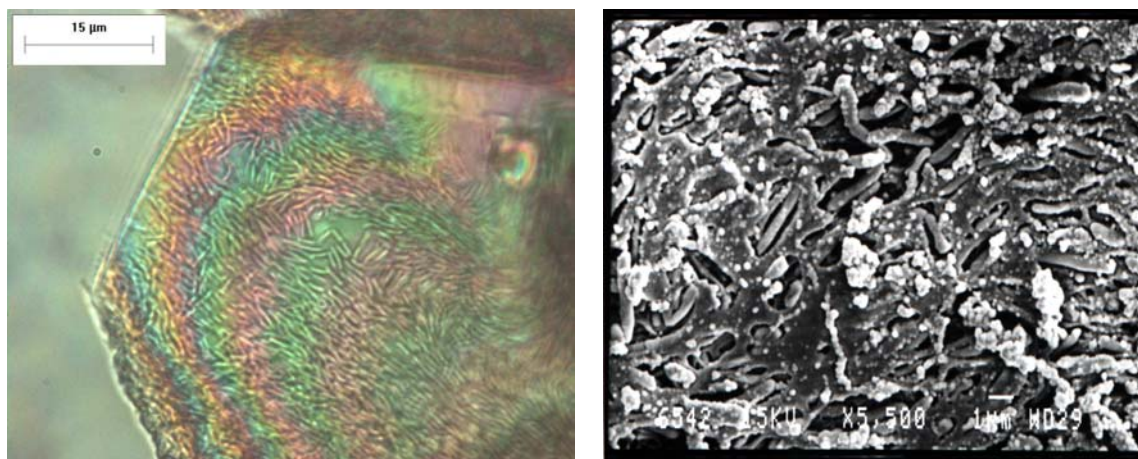


Figure 4.9. (a) Light microscopy image of the semi-transparent crystal showing bacteria-like structures apparently inside the crystal, and (b) SEM photo of the crystal surface showing imbedded bacteria in the crystal structure.

Effect of precipitation on the precipitating organisms

CaCO₃ precipitation leads to the physical capturing and eventual die-off of bacteria. Figure 4.9a shows the light microscopy image, of one of the crystals harvested from the precipitation media, and after washing in sterile physiological solutions. Morphological rod-like shapes, resembling that of the precipitating organism in both shape and dimensions, are visible inside the crystal. Figure 4.9b shows a SEM image of a similar crystal. Bacterial bodies, captured within the crystal structure, are seen. Both re-growth experiments and viability staining of pulverised crystals showed that the bacteria captured within the crystal structure were no longer viable.

Effect of ureolytic precipitation on growth and survival

Figures 4.10 and 4.11 show the effects of calcium presence on colony (and crystal) development during ureolytic microbial calcium carbonate precipitation for the two isolates used. Two distinct patterns are evident: for CPB 4, the high calcium concentration and concomitant precipitation, had a positive effect on colony growth and proliferation. For CPB 12, the effect was the opposite: though CaCO₃ precipitation did not affect colony growth, the culture was visibly adversely affected by the presence of calcium in the medium.

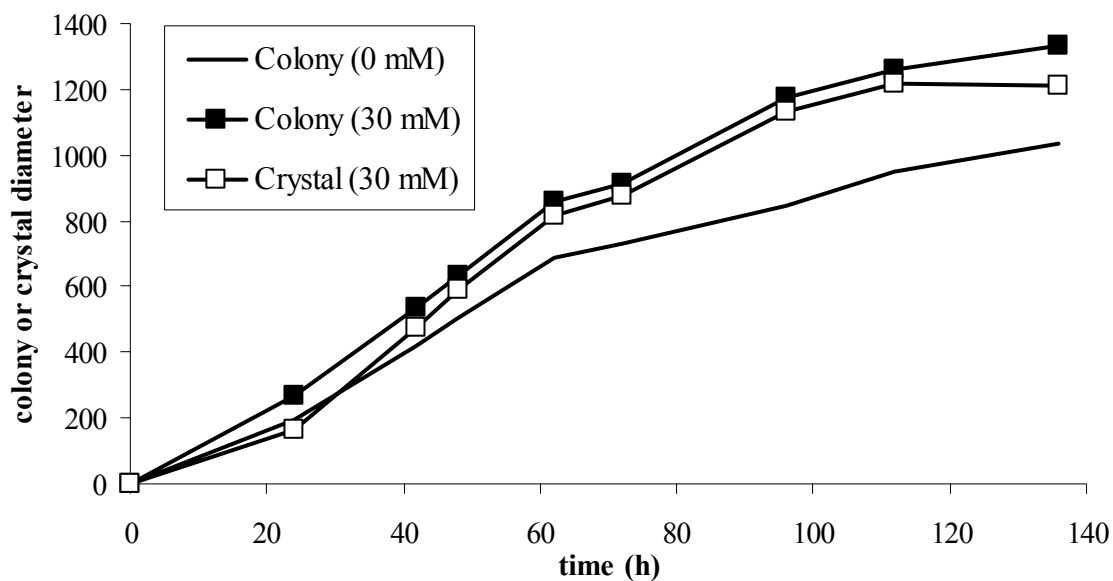


Figure 4.10. Colony (and crystal) growth of isolate CPB 4 in the presence and absence of 30 mM Ca²⁺.

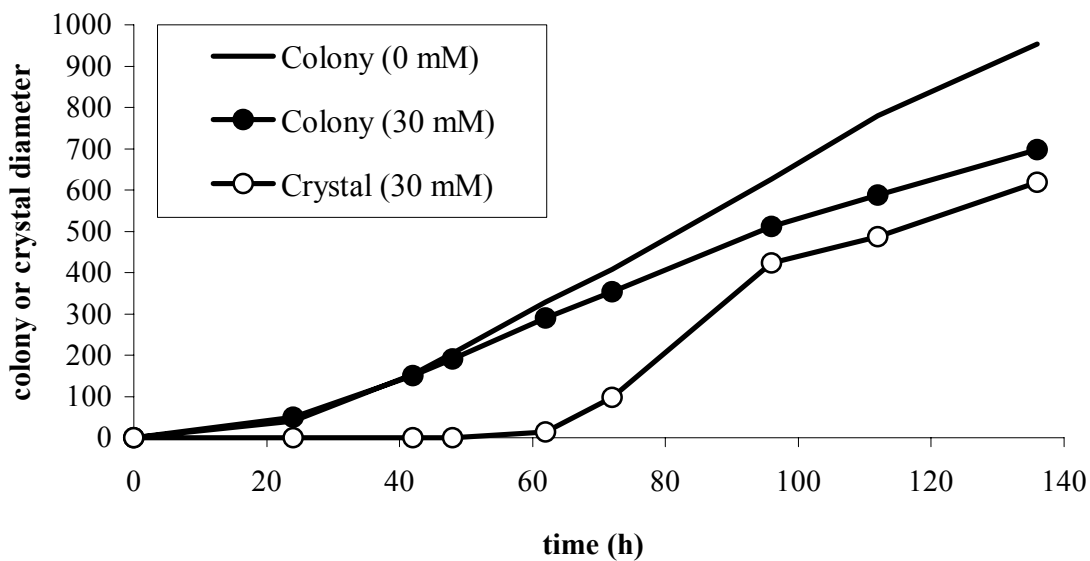


Figure 4.11. Colony (and crystal) growth of isolate CPB 12 in the presence and absence of 30 mM Ca²⁺.

DISCUSSION

The aim of this study was to illustrate with a number of straightforward experiments the effect of a typical precipitation environment (high pH and high Ca²⁺ concentration) on bacteria survival and proliferation. In the hypothesis it was suggested that:

- (i) Calcium would present a toxic effect on bacteria at alkaline pH regimes
- (ii) Survival/proliferation would require energy (for active Ca²⁺ metabolism)
- (iii) Precipitation favourably alters the above-mentioned toxic environment

Ureolytic bacteria were not ideal for the first part of the study, since growth of these organisms result as such in pH changes, complicating the interpretation of any effect. *M. odoratus* was selected as test strain for this study, since the presence of ATP dependant calcium pumps have been shown for this organism (Desrosiers *et al.* 1996; Peiffer *et al.*, 1996). *D. acidovorans* was taken as control strain. The initial idea was to differentiate between the calcium metabolising abilities of these two organisms using the specific Ca²⁺-ATPase PCR primers described by (Desrosiers *et al.* 1996). This PCR reaction was, however, not successful, and the further experiments were therefore only continued with *M. odoratus*. Analysis of colony size is a simple and effective method to assess stress conditions on bacterial growth (Booth *et al.*, 1996). Figures 4.3 – 4.6 show that calcium ions at alkaline pH regimes were indeed toxic for bacteria, and that this toxicity is proportional to the calcium concentration and to pH: higher pH levels resulted in a more pronounced effect of toxicity. Moreover, the toxicity was not merely a result of saline stress, since similar adverse responses to sodium and potassium could not be recorded. These straightforward growth tests thus provide validation for the first part of the hypothesis.

To our knowledge, experimental evidence of toxicity of calcium ions has not been reported previously. Although Anderson *et al.* (1992) did hypothesise a major role of calcium metabolism and CaCO₃ precipitation in bacterial homeostasis, their experiments failed to detect an inhibitory effect of calcium on growth of *Pseudomonas fluorescens*. But this is in fact consistent with the findings reported in this study, since Anderson *et al.* (1992) used an experimental pH of about 7. The essence of the alkaline pH, bringing about complimentary electrochemical gradients, should therefore not be underestimated. The link with metal toxicity and biological mineral precipitation reactions, as detoxification mechanisms, has previously

been established, specifically for divalent heavy metals (Loyd and Loveley, 2001; Anderson *et al.*, 1992). In fact, Loyd and Loveley (2001) described a specific example of *Ralstonia eutropha* much similar to the hypothesis stated in this study. Apparently, *R. eutropha* precipitate toxic cationic metals within an extracellular coat of insoluble metal carbonates. This precipitation reaction is a result of the generation of high concentrations of metal ions at the cell surface in a zone of high local pH, caused by the uptake of protons by metabolically active cells. Moreover, this precipitation was facilitated by active efflux systems (ionic pumps). Similarly, cyanobacteria commonly precipitate toxic heavy metals on S-layers surrounding these organisms in an apparent detoxification process (Ferris and Beveridge, 1985). Figure 4.7 showed that survival of *M. odoratus* in the presence of alkaline calcium toxicity improved significantly in the presence of nutrients (energy source). Although this is in confirmation of the second part of the hypothesis, to actually underpin a metabolic pathway of calcium through the bacteria, including the role of active ATP-dependant export, would require a much more in depth physiological study.

The third part of the hypothesis assessed the effect of precipitation on the chemical composition of the environment. Both Mers-Preiß (2000) and McConnaughey and Whelan (1997) already suggested that cyanobacterial CaCO₃ precipitation lowers environmental pH, thereby favouring several bacterial processes such as nutrient uptake and bicarbonate availability. Such pH changes were confirmed with both theoretical modelling, as well as experiments with ureolytic precipitation.

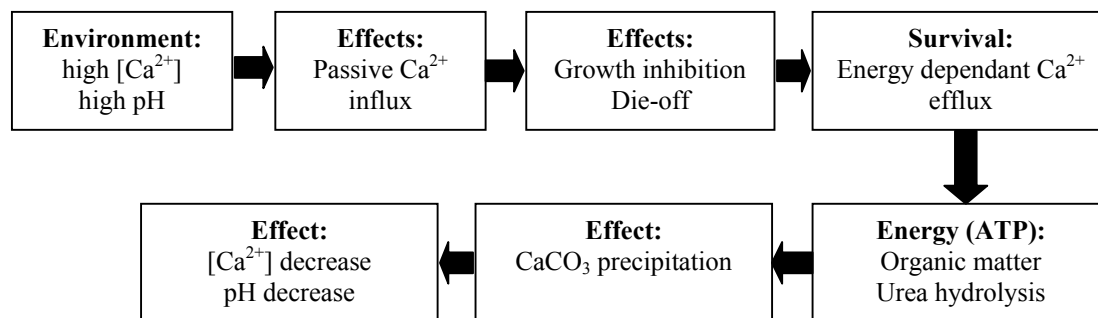


Figure 4.12. Possible precipitation-detoxification following the exposure of bacteria to an alkaline environment rich in calcium ions.

If all these results are considered together, it seems that indications exist of a detoxification-feedback system (Figure 4.12). Calcium and alkaline pH present a toxic environment to bacteria. CaCO₃ precipitation relieves this toxicity, by lowering not only the pH, but also the concentration of toxic calcium ions. Moreover, strong theoretical arguments exist which link this detoxification to active ATP-dependant calcium metabolism.

Although this detoxification-precipitation reaction holds an apparent ecological advantage for bacteria in terms of the effect thereof on environmental chemistry, the consequences of such precipitation on cellular level should also be considered. If the precipitation occurs on a sheath, capsule or S-layer, all of which can be shed by the organism, it holds no disadvantage to the bacteria (Southam, 2000). In fact, it can even provide a protective layer (Loydd and Lovley, 2001). In fact, it was reported by (Vreeland *et al.*, 2000) that spores of *Bacillus* type bacteria were able to survive for billions of years inside inorganic crystals (in this particular case halite (NaCl) crystals). Based on findings such as those, McGenity and Sellwood (1999) stressed the need for renewed studies towards understanding the role of precipitation towards the microbial ecology of the organisms involved. However, if the precipitation is on the cell wall of a viable cell, it will lead to die-off (Knorre and Krumbein, 2000). Southam (2000) argued that the die-off effect was a result of trans-membrane transport inhibition of nutrients and protons, and eventual disruption of the proton motive force of the organisms. Die-off on cellular level was also observed to occur during ureolytic precipitation in our experiments.

But although ureolytic CaCO₃ precipitation can lead to physical capturing and die-off on cellular level, Figures 4.10 and 4.11 show that on the synthetic precipitation agar, this encrustation effect never encompassed the entire bacterial colony. In fact, even though up to 95 % of the organisms in the colony was captured in the crystal structure, the youngest cells continuously survived and proliferated on the colony outer perimeter. The ecological impact of this is significant: the oldest cells are continuously 'removed' from the colony, simultaneous with an improvement of the environmental chemistry, thereby ensuring proliferation of the youngest cells. Whether this represents a form of single-cell sacrifice to ascertain colony survival under stressed conditions, remains to be elucidated.

Even more interesting results from Figures 4.10 and 4.11 were perhaps the two distinctly different growth responses shown by the two ureolytic isolates when cultivated on media with and without calcium addition. As shown also in the previous chapter, some ureolytic bacteria can utilise urea as ATP source (Burne and Chen, 2000; Mobley and Hausinger, 1989). In a medium containing 100 mM urea (as used herein), this rapidly available energy source could ensure the survival and proliferation of such an organism if exposed to alkaline calcium toxicity. The major differentiation between CPB 4 and CPB 12 in this regard, was indicated in the previous chapter, where it was shown that isolate CPB 4 increased its urease activity up to 10-fold in the presence of calcium, while that from isolate CPB 12 remained unchanged. Within the light of the other results presented above, the deduction can be made that isolate CPB 4 can utilise urea as ATP source, and does so under conditions of alkaline calcium toxicity. These results seem to present further vindication for the existence of an ATP-driven calcification mechanism in bacteria.

CONCLUSION

The complex physiological responses of microorganisms to pH and high concentrations of cations were not studied. In stead, straightforward growth experiments were used to validate the hypothesis that a combination of high calcium concentrations and alkaline pH in the environment are detrimental to bacterial growth, and that CaCO₃ precipitation alter these conditions in a favourable manner. These results present only first steps in the physiology and microbial ecology of MCP, but suggest that key factors to this phenomenon might be cation toxicity and resultant ATP-dependant detoxification reactions. [Link to Contents](#) [Link to Chapter 5](#)

ACKNOWLEDGEMENTS

The authors would like to express their gratitude for the invaluable contributions of Nico Boon, Karen Agrella and Patrick De Boever towards completion of this work.

EXPLORATORY STUDY TOWARDS Ca^{2+} REMOVAL FROM INDUSTRIAL WASTEWATER THROUGH MICROBIAL CaCO_3 PRECIPITATION

Redrafted from:

- (1) **F. Hammes, A. Seka, S. De Knijf and W. Verstraete.** 2002. A novel approach to calcium removal from industrial wastewater. *Water Research* (in press).

ABSTRACT *Calcium-rich industrial wastewater poses a significant problem to industries, especially those following the current tendency of water circuit-closure. It was investigated what the potential is for calcium removal from wastewater in an adapted type of activated sludge system, using ureolytic microbiological calcium carbonate precipitation (MCP). Batch experiments showed 1 g·L⁻¹ urea addition and a 48 h hydraulic retention time to be feasible operational parameters. These parameters were subsequently applied in a semi-continuous reactor system, where the emphasis was placed on the development of an activated calcifying sludge. Calcium removal in excess of 90 % was achieved throughout the experimental period.*

INTRODUCTION

Calcium ions are common in many natural environments such as seawater, salt lakes, saline soils and sediments, and in these environments it often precipitates as carbonate minerals e.g. calcite, aragonite and vaterite (all polymorphs of CaCO₃), and dolomite (CaMg(CO₃)₂). Previous geo-microbiological studies of calcium carbonate precipitates from natural environments suggested both the presence of bacteria, and specific interactions of these microorganisms with the precipitated minerals (Wright, 1999; Folk, 1999). The general mechanism of microbiological calcium carbonate precipitation (MCP) has been described as the ability of microorganisms to alkalise (increase of pH and dissolved inorganic carbon (DIC)) a given environment through various physiological activities (Douglas and Beveridge, 1998). The recognised metabolic pathways for MCP was summarised by Castanier *et al.* (1999) as being autotrophic photosynthesis by algae or cyanobacteria (accounting for most microbial precipitates), heterotrophic sulfate reduction by sulfate reducing bacteria, and the processes of nitrate reduction, amino-acid ammonification, and urea degradation. The general nature of these precipitation mechanisms accounts for the common occurrence of microbial calcification in diverse natural environments, and also validates the statement by Boquet *et al.* (1973) that most bacteria are capable of inducing precipitation, depending on the given environment.

Microbial calcification has been used in several biotechnological applications in the past decade, all of which focussed specifically on use of the end product i.e. mineral carbonate. In the building sector, a microbial carbonate precipitation technique has been developed for the restoration of sandstone monuments, from which at least two patents have already resulted (Le Metayer-Levrel *et al.*, 1999). In the same context, Bang *et al.* (2001) investigated this process, specifically the pathway of urea degradation, for the strengthening of concrete surfaces. An application of the urea pathway for the mineral plugging of soil pores and subsequent control of groundwater (and pollutant) flow, has also been patented (Ferris and Stehmeier, 1993) and thoroughly investigated (Fujita *et al.*, 2000; Stocks-Fischer *et al.*, 1999; Gollapudi *et al.*, 1995).

Calcium-rich wastewater primarily results from industries such as paper recycling, bone processing and citric acid production, and also from landfill leachates. In such wastewaters, the calcium concentration can range from 500 – 1500 mg/L Ca²⁺ (Habets and Knelissen, 1997; Van Langerak *et al.*, 1997). Calcium ions are usually not considered in the determination of effluent quality, but they are recognised to cause several operational problems. These include severe scaling in pipelines and reactors, due to calcium precipitation as gypsum, phosphate and/or carbonate, and malfunctioning of anaerobic reactors (Van Langerak *et al.*, 1997). Moreover, these problems increase significantly when the current global tendency of water circuit closure is applied in such industries.

This study investigated the potential application of microbial carbonate precipitation for the removal of soluble calcium from industrial wastewater. To our knowledge, this process has never been used as such, and the aim of this chapter is therefore to present results from initial experiments in this regard, as well as perspectives for future applications.

MATERIALS & METHODS

Batch experiments

Wastewater. Raw wastewater was obtained from a paper recycling facility and used on the day of collection. The average composition of the wastewater during the experimental period was: pH 6.6 (\pm 0.2); volatile fatty acids (VFA) 1291 (\pm 232) mg·L⁻¹; soluble chemical oxygen demand (COD_s) 3096 (\pm 517) mg·L⁻¹; soluble calcium 489 (\pm 39) mg·L⁻¹; ammonium-nitrogen 11 (\pm 5) mg·L⁻¹ NH₄⁺-N.

Urea concentration. Batch experiments were used consisting of 250 mL Erlenmeyer flasks with 100 mL raw wastewater and urea (Sigma) concentrations of 0, 0.1, 0.5, 1, 2, 4, 8 and 16

g·L⁻¹ respectively. These were incubated aerobically (28 °C and 100 rpm shaking) for five days, and sampled at completion of the experiment. Soluble calcium was analysed with flame atomic absorption spectrometry (FAAS) (Perkin-Elmer AAS 3110, Perkin-Elmer, Belgium), after filtration (0.22 µm Millipore) and acidification with 0.1 N HNO₃. pH and ammonium (NH₄⁺-N) were also measured (Greenberg et al., 1992).

Hydraulic retention time (HRT). Urea was added to final concentrations of 0 (control), 0.5 and 1 g·L⁻¹ in 100 mL wastewater samples in 250 mL Erlenmeyer flasks and incubated for four days (28 °C and 100 rpm shaking). Samples were taken at 0, 15, 25, 42, 68, and 88 h, and analysed as described above. All experiments were performed in triplicate.

Semi-continuous reactors

Two semi-continuous calcification reactors (Reactor1 and Reactor2), consisting of 2 L plastic Erlenmeyer flasks, were started with 1.5 L raw wastewater and an initial urea concentration of 1 g·L⁻¹, while the two control reactors (Control1 and Control2) were identical but without the addition of urea. These reactors were incubated (28 °C and 100 rpm shaking) for 48 h. After this period, the “sludge” was allowed to sediment after which 1.35 L (90 %) of the supernatant was removed manually and refreshed with raw wastewater and dosed with urea where applicable. This cycle was repeated. Both the raw wastewater and the effluents from the respective reactors were analysed for pH, COD_s, total and volatile suspended solids (TSS and VSS) (Greenberg *et al.*, 1992), and total and soluble calcium (see above). After 18 days of operation, the HRT of one control (Control1) and one calcification (Reactor1) reactor was set at 24 h, while that of the other two remained unchanged. At completion of the experimental period, sludge samples from the reactors were examined with light microscopy (Polivar, Reichert-Jung), and digital images were captured with a 1-CCD camera (Hamamatsu Photonics GmbH, Hersching, Germany).

RESULTS

Batch tests

Urea concentrations. Batch tests were used for an initial assessment of the most important operational parameters. Figure 5.1 shows results of soluble calcium removal and pH evolution at different urea concentrations after five days. Urea addition and hydrolysis was a prerequisite for soluble calcium removal. It is also apparent that more than 90 % calcium removal could be obtained with urea concentrations exceeding $1 \text{ g}\cdot\text{L}^{-1}$. Ammonium increased directly proportional to the increased urea concentration at an average ratio of $420 \text{ mg NH}_4^+ \text{-N}$ per gram urea (results not shown). pH also increased proportional to urea addition/hydrolysis at low urea concentrations but from $4 \text{ g}\cdot\text{L}^{-1}$ onwards it remained at about 9.3.

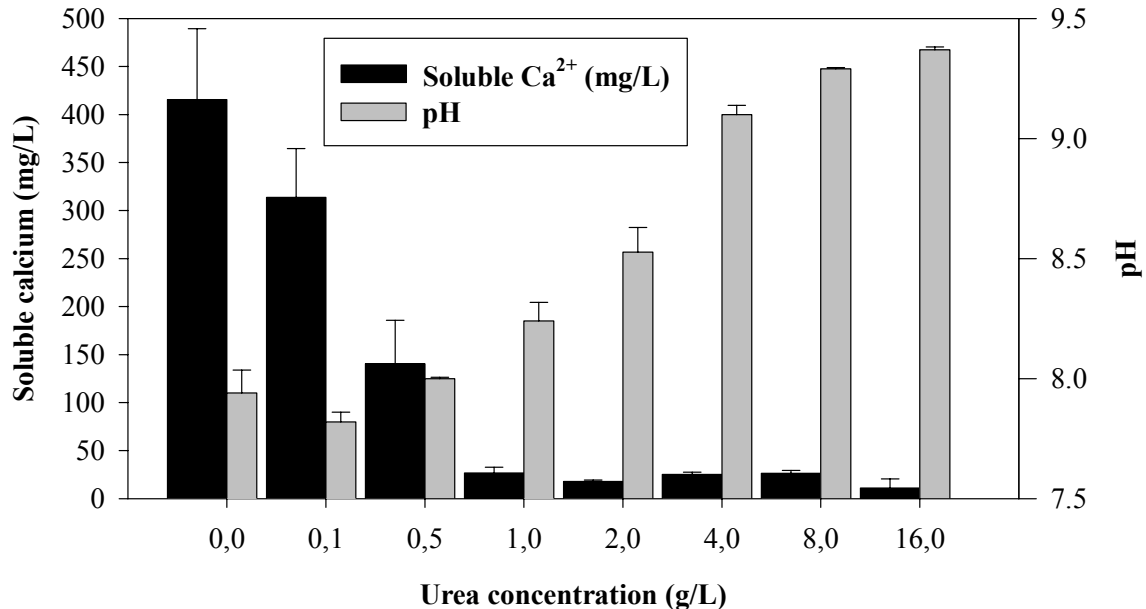


Figure 5.1. Soluble calcium ($\text{mg}\cdot\text{L}^{-1}$) and pH measurements of batch tests on raw wastewater dosed with different urea concentrations after 5 days incubation. Error bars indicate the standard deviation ($n = 3$).

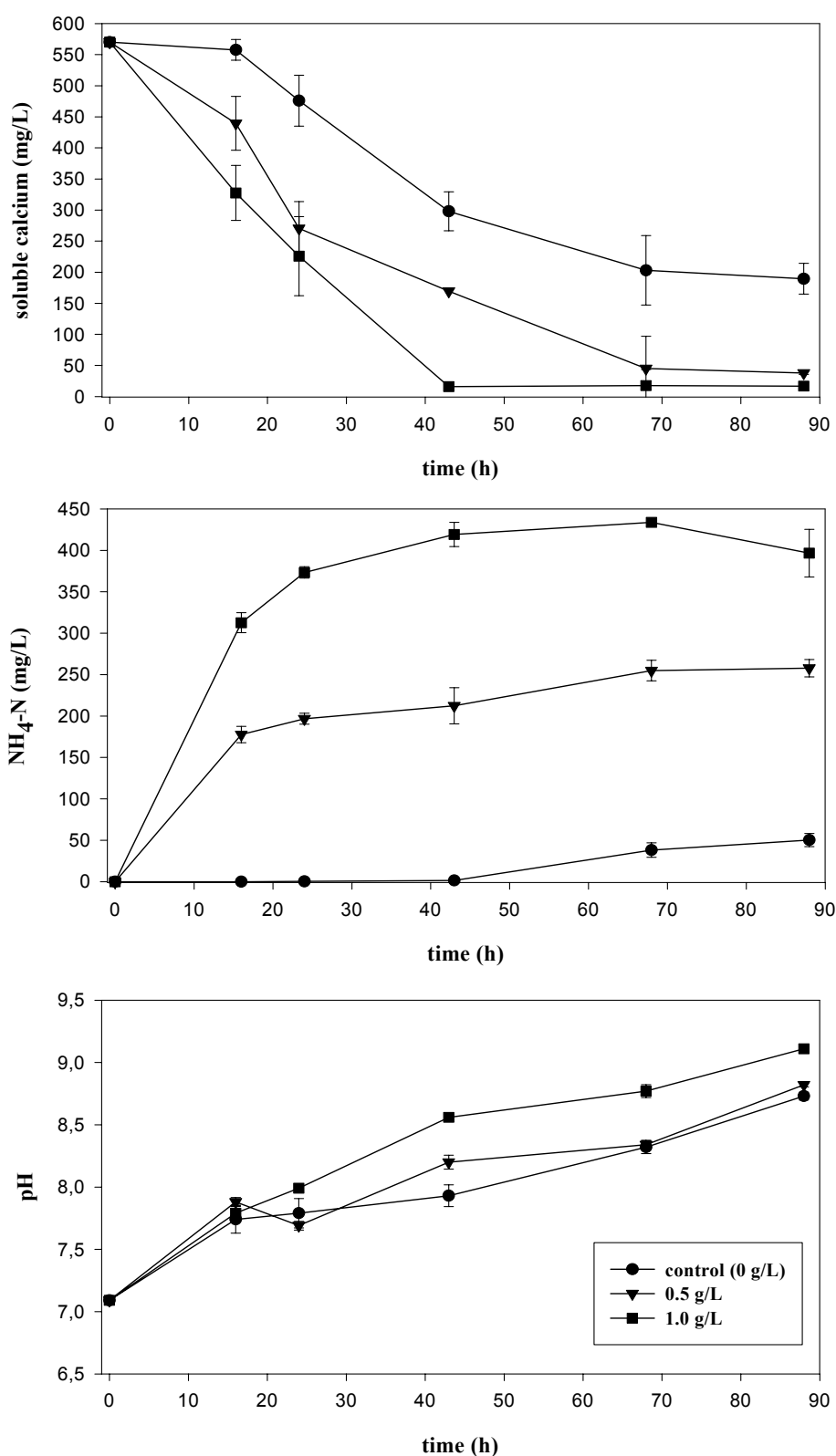


Figure 5.2a-c. Evolution of soluble calcium removal, ammonium and pH in raw wastewater at two different urea concentrations during 4 days. Error bars indicate standard deviation (n = 3).

Hydraulic retention time. Soluble calcium, ammonium and pH measurements for a batch-experiment, where the required HRT (relative to the urea concentration) was assessed, are shown in Figure 5.2a-c respectively. As above, calcium removal efficiency was related to the amount of urea hydrolysed. Soluble calcium removal at a urea concentration of $1 \text{ g}\cdot\text{L}^{-1}$ was completed ($> 95\%$ removal) first at 42 h, while at $0.5 \text{ g}\cdot\text{L}^{-1}$ it required between 70 and 90 hours for removal in excess of 90%. However, it is also apparent that given enough time, as much as 55 – 60% calcium removal can be obtained without any urea addition. Ammonium increased rapidly for both urea concentrations, and at 42 hours, the measured concentrations reflected complete urea hydrolysis. pH increased constantly over the entire experimental period, in the control sample as well as where urea was dosed.

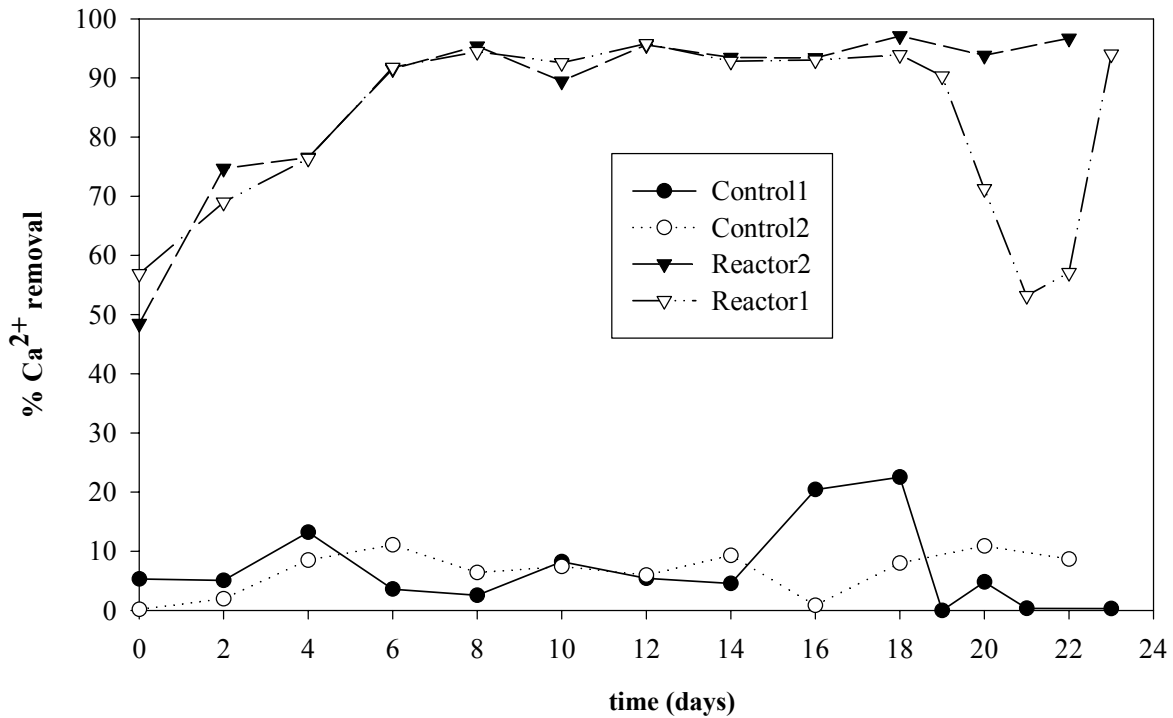


Figure 5.3. Evolution of soluble calcium removal in the semi-continuous reactors. Control1 and Control2 are duplicate control reactors. Reactor1 and Reactor2 represent duplicate treatments with urea. In the period 0 – 18 d, the hydraulic residence time was 48 h in all reactors. From day 18 it was lowered to 24 h for Reactor1 and Control1.

Semi-continuous reactors

Following a six-day start-up period, calcium removal in the reactors with urea addition constantly exceeded 90 %, whilst in the control reactors it remained at about 10 % (Figure 5.3). ‘Removal’ in this case refers to the immobilisation of soluble calcium ions, thus including both calcium remaining behind in the reactors (as sludge), as well as fine insoluble calcium carbonate suspended in the effluent. Though it was not specifically examined in this study, this “start-up period” was considered to be due to the development of a calcifying sludge, with increased urease activity and a build-up of crystal nucleation sites. After shortening the hydraulic retention time (from 48 h to 24 h) in one calcification reactor (Reactor1) on day 18, calcium removal efficiency dropped temporarily, but regained in time the level of 90 %.

Table 5.1. Average values and standard deviation of all parameters for the influent and the effluents from four semi-continuous reactors as measured from 6 days onwards after start-up.

	Influent	Control 1	Reactor 1	Control 2	Reactor 2
pH	6.6 ± 0.3	7.4 ± 0.3	7.8 ± 0.3	7.4 ± 0.2	7.9 ± 0.4
Ca²⁺ (mg·L⁻¹)^a	482.7 ± 36	452.0 ± 33	147.0 ± 63	445.4 ± 48	105.2 ± 66
Ca²⁺ (mg·L⁻¹)^b	471.1 ± 22	453.7 ± 69	31.8 ± 7	440.2 ± 72	28.7 ± 12
CODs (mg·L⁻¹)	3075 ± 522	1319 ± 465	1653 ± 465	1236 ± 340	1267 ± 127
NH₄-N (mg·L⁻¹)	12.0 ± 5	2.1 ± 3	418.5 ± 19	2.5 ± 3	409 ± 32

a Total calcium

b Soluble calcium

The average results following the six-day start-up period of all measurements are given in Table 1. For the influent as well as for the control reactors’ effluents, no detectable difference was found between total calcium and soluble calcium. For the calcification reactors, it is evident that most of the calcium (about 80 %) precipitated inside the reactors, but also that a significant percentage of insoluble calcium (about 10 – 15 %) remained suspended in the effluent. This was confirmed by measurements of TSS and VSS,

expressed as percentage (%) VSS of TSS (Figure 5.4). While the VSS remained more or less constant in both the calcification and control reactors (between 300 – 500 $\text{mg}\cdot\text{L}^{-1}$), the TSS increased in the calcification reactors up to 900 $\text{mg}\cdot\text{L}^{-1}$.

For all the semi-continuous reactors, COD removal was around 60 % (Table 5.1). Ammonium levels were on average slightly lower than expected (1 g urea equals 468 mg $\text{NH}_4^+ -\text{N}$), which could be ascribed to a combination of volatilisation and microbial uptake processes.

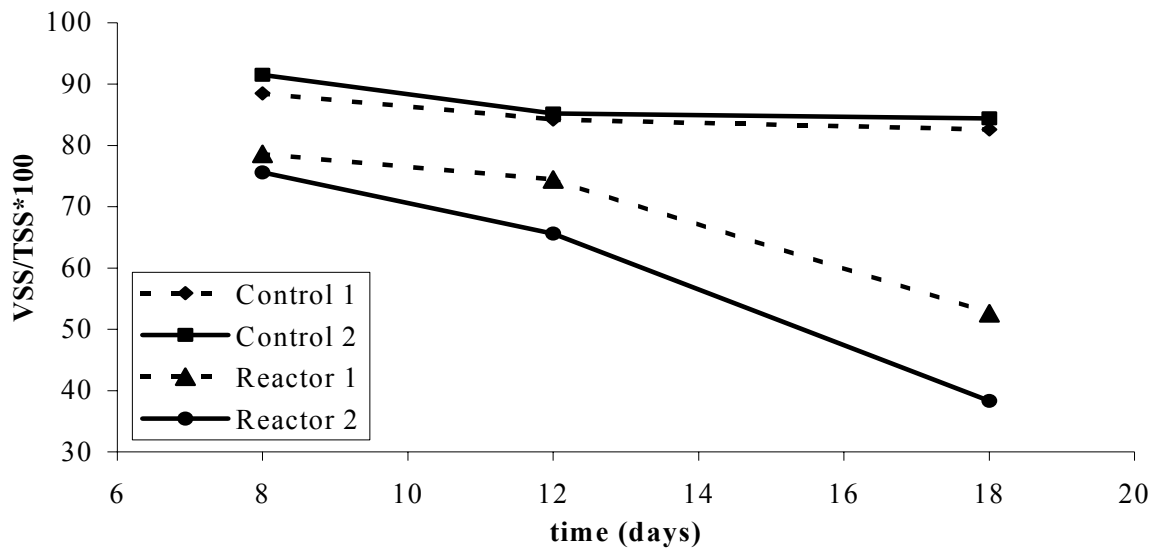


Figure 5.4. Percentage VSS/TSS measured in the effluents from two control reactors and two calcification reactors.

Figure 5.5a and 5.5b show light microscopic pictures of the resultant sludge from both the control (Control1) and the calcification (Reactor1) reactors. The control sludge comprised large flocs as a result of microbial attachment and development on the fibres already present in the water. The calcifying sludge comprised of heavy, small, dense calcareous flocs. Further microscopic studies showed that both the sludge types (control and calcifying) were characterised by large amounts of free-swimming bacteria, and also confirmed the crystalline nature of the calcifying sludge (green fluorescence under UV-light) (results not shown).

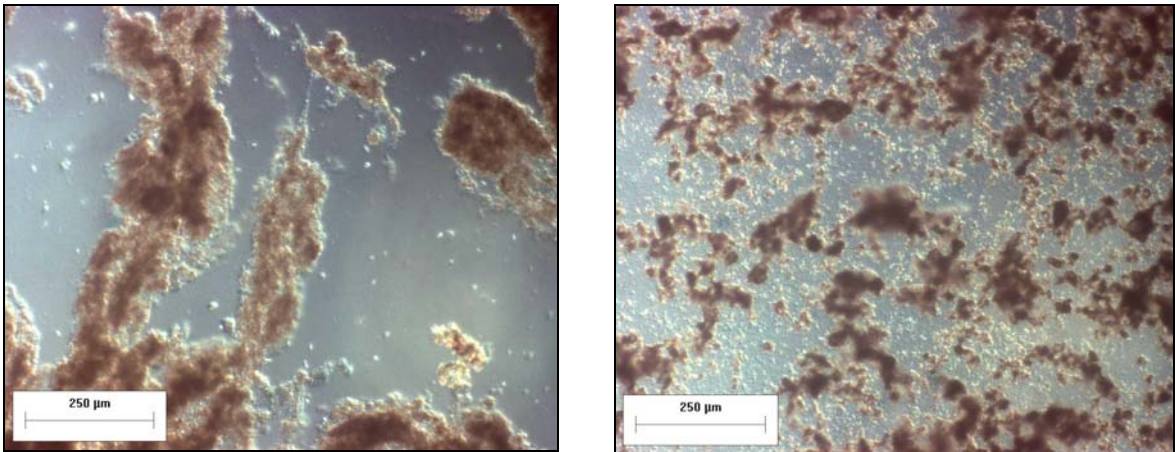


Figure 5.5. Microscope images of sludge from a control reactor (a) and from a calcification reactor (b), showing the latter to develop small, dense calcareous flocs.

DISCUSSION

A biological catalysed precipitation process, based on urea hydrolysis, was investigated as a potential alternative to chemical carbonate precipitation for the removal of calcium from industrial wastewater. To our knowledge, the only calcium removing technology, which is related to a biological process, is a fluidised sand bed reactor (FSBR) concept proposed by Van Langerak *et al.* (1997). This system reportedly recycles a part of up-flow anaerobic sludge bed (UASB) reactor effluent, mixes it with the influent in a FSBR placed before the UASB reactor, and thus uses the alkalinity of the recycled stream, generated by microbial processes, to precipitate calcium as CaCO₃. Urea hydrolysis is a straightforward process, and since it is based on the working of the urease enzyme, which is common in many organisms, it has the potential to be integrated in an existing biological wastewater treatment system (Mobley and Hausinger, 1989). Moreover, urea is a relatively inexpensive chemical and provides upon hydrolysis simultaneously a pH increase and DIC

increase, both of which are essential components of precipitation (Castanier *et al.*, 1999; Douglas and Beveridge, 1998). The high starting urea concentrations (i.e. 16 g·L⁻¹) in the first batch experiment were based on previous reported applications of microbial carbonate precipitation. For example, both Stocks-Fischer *et al.* (1999) and Ferris and Stehmeier (1993) reported the use of 20 g·L⁻¹ urea for the mineral plugging of soil columns, while Bang *et al.* (2001) used 10 g·L⁻¹ urea in microbial crystallisation experiments on concrete surfaces. However, these experiments were performed on soils and concrete with specific focus on the end product (i.e. the production of mineral CaCO₃) and also employed high calcium concentrations of 25 – 50 mM. In wastewater, the required amount of precipitation is governed by the soluble calcium which is to be removed. Two further important effluent parameters to be considered are the maintenance of a near-neutral pH, and low nitrogen (ammonium resulting from urea hydrolysis) concentrations. Especially the latter is strictly controlled by legislation (< 50 mg·L⁻¹) and increased nitrogen concentrations thus automatically imply increased costs. Therefore it was essential to establish a combination of the most efficient as well as lowest possible urea concentration.

The raw wastewater used in these experiments contained about 490 ± 40 mg·L⁻¹ Ca²⁺, which corresponds roughly with 12 mM Ca²⁺. One mole of calcium reacts with one mole of carbonate to form calcium carbonate (Equation 5.1). Based solely on the DIC requirement, it could be argued that a minimum of 12 mM urea (= 0.72 g·L⁻¹) is required to precipitate 12 mM calcium, since one mole hydrolysed urea produces one mole DIC (as H₂CO₃) and two moles of ammonium (Equation 5.2).



In fact, Figure 5.1 and 5.2c suggest the most efficient urea concentration under the tested conditions to be between 0.5 and 1 g·L⁻¹ urea, which concurs with the theoretical required amount. While ammonium levels remained in the expected range (theoretically 1 g urea gives 468 mg NH₄⁺-N) and increased proportionate to increased urea concentrations, the

pH did not increase above about 9.3 from urea concentrations of $4 \text{ g}\cdot\text{L}^{-1}$ and onwards, as a result of the $\text{NH}_3(\text{g})\text{-H}_2\text{O}$ buffer equilibrium ($\text{pK}_a = 9.26$).

The HRT is dependant on the rate of urea hydrolysis and the rate of crystallization. The latter is a combination of complex factors including saturation of CaCO_3 in the wastewater, and the availability of crystal nucleation sites (Nilsson and Sternbeck, 1999; Stumm and Morgan, 1981). About 42 hours were sufficient for complete urea hydrolysis, which, in the case of the $1 \text{ g}\cdot\text{L}^{-1}$ urea addition, was also sufficient time for calcium immobilisation (Figure 5.2). However, integration into a wastewater treatment system would normally require an HRT of maximum 12 hours, which goes to show that the development of a highly active ureolytic sludge is at least one major pre-requisite for efficient reactor operation. Based on the results of both batch experiments, it was opted to continue with a working urea concentration of $1 \text{ g}\cdot\text{L}^{-1}$ and a hydraulic retention time of 48 h in the semi-continuous reactors. Both Figure 5.1 and Figure 5.2 suggest that at $1 \text{ g}\cdot\text{L}^{-1}$ urea, a final pH of about 8.5 could be expected.

Though not all the required parameters for speciation computations were measured (e.g. alkalinity), it was undoubtedly shown that urea addition was required for calcium removal from the wastewater. This is deduced from the fact that the COD/VFA removal, together with subsequent DIC increase and measured pH values, were similar in the control and calcification reactors. However, the DIC resulting from urea hydrolysis seems little (about $16.7 \text{ mM CO}_3^{2-}$) in comparison with that from COD/VFA degradation (about 56 mM CO_2), prompting the suggestion that pH shifts are the key to the ureolytic precipitation process.

An effluent pH of lower than 8 was continually detected for both calcification reactors, which is certainly acceptable with regards to the requirements of downstream biological treatment processes. pH is often described as the “master variable” in aquatic chemistry (Stumm and Morgan, 1981). It was previously established that the main attribute of urea hydrolysis towards CaCO_3 precipitation is the resultant pH increase (from ammonium), with DIC only being an added advantage (Equation 5.3) (Castanier *et al.*, 1999; Stocks-Fischer *et al.*, 1999; Ferris and Stehmeier 1993).



Whereas urea hydrolysis results in a pH increase, CaCO₃ precipitation leads to acidification (McConnaughey & Whelan, 1997). Therefore, the bulk solution pH, measured at 24 or 48 h intervals, might not necessarily reflect the fluxes occurring in-between (Table 5.1), and are insufficient for accurately judging the effect of urea hydrolysis on the overall system chemistry.

Effective calcium removal from wastewater was achieved with the addition (and subsequent hydrolysis) of urea. But the exact mechanism of the ureolytic precipitation process was, however, not fully elucidated. This would essentially require more thorough analysis of all wastewater parameters, coupled to modelling, and as was shown, continuous pH measurements. With regards to possible future applications of such a process, the current drawbacks are the required urea concentration, the long hydraulic retention time, and the increase in TSS in the calcification reactors. The results of 0.5 g·L⁻¹ urea (Figure 5.1 and Figure 5.2a) suggest definite optimisation possibilities, while it should also be taken into account that the resulting nitrogen in the form of ammonium is easily removable through standard nitrification/denitrification processes. In this regard, the calcification process should thus be seen as a pre-treatment process, which should be followed by conventional wastewater treatment. An interesting hydraulic retention time would be similar to that of conventional wastewater treatment i.e. 7 – 12 hours. The problem with VSS/TSS could either be solved through the inclusion of sand grains in the reactor as crystal nucleation sites, or a post-filtration step (Battistoni *et al.*, 2001). These latter authors used a crystallisation reactor for the removal of phosphate from real wastewater through chemical struvite (NH₄MgPO₄) precipitation. Co-precipitation of components other than phosphate, such as volatile fatty acids (VFA) and heavy metals, under carbonate precipitation conditions such as those described above, would add further significance to this process.

CONCLUSION

The potential of Ca^{2+} removal from wastewater using, ureolytic MCP, has been demonstrated in this chapter. The positive results obtained herein warrant further investigation into this process, specifically focussing on the engineering aspects and the precise function of the bacteria in the precipitation process.

ACKNOWLEDGEMENTS

The author would like to express his utmost gratitude to the contribution of Stefaan de Knijf towards the completion of this work, and Greet Vandevelde for the numerous calcium measurements.

[Link to Contents](#) [Link to Chapter 6](#)

BIO-CATALYTIC CALCIUM REMOVAL FROM INDUSTRIAL WASTEWATER: TOWARDS INDUSTRIAL APPLICATION

Redrafted from:

- (1) **F. Hammes, A. Seka, K. Van Hege, T. Van De Wiele, J. Vanderdeelen, S.D. Siciliano and W. Verstraete.** Calcium removal from industrial wastewater by bio-catalytic CaCO_3 precipitation. *Submitted* to the Journal of Chemical Technology and Biotechnology (June 2002).

ABSTRACT *A laboratory-scale reactor was developed, which utilises microbial urea hydrolysis for the precipitation-removal of calcium ions from industrial effluents. Two such reactors, both with a hydraulic retention time of 8 h, were fed with 1.8 L of anaerobic effluent (containing about 11 mM Ca^{2+}) from a paper recycling plant. Both reactors were inoculated with pre-cultivated calcareous sludge and the treatment reactor was additionally dosed with urea to a final concentration of 8.3 mM. Even though the anaerobic wastewater was saturated as such with respect to CaCO_3 , urea addition and hydrolysis were shown to be prerequisites for CaCO_3 precipitation. Almost all (85 – 90 %) of the soluble calcium was precipitated as calcite, and removed through sedimentation in the treatment reactor. This bio-catalytic process presents an uncomplicated and efficient method for the removal of calcium from industrial wastewater.*

INTRODUCTION

Paper recycling and bone processing (e.g. gelatine production) are the main industries dealing with calcium-rich wastewater. The European paper/cardboard industry have an estimated annual production of 70 million tons paper products, which requires about 20 m³ water per ton for production (thus up to 1.4 billion m³ water per year), while producing effluents containing 10 – 40 mM Ca²⁺ (Habets and Knelissen, 1997; Van Langerak *et al.*, 1997). Such high calcium concentrations are problematic, because they lead to clogging of pipelines, boilers and heat exchangers through scaling (as carbonate, sulphate or phosphate precipitates), or malfunctioning of aerobic and anaerobic reactors (Morizot *et al.*, 1999; Van Langerak *et al.*, 1998). Apart from mechanistic damage to aerobic and anaerobic wastewater reactors, mineral precipitation could also hinder the biological processes. In aerobic reactors, the adverse effects can for instance be the formation of pinpoint sludge flocs. Such small, fast-settling flocs can often result in incomplete removal of suspended solids during secondary clarification. In anaerobic reactors, precipitation on the granules can hinder nutrient transport, leading to die-off or reduced functioning (Yu *et al.*, 2001). These problems are significantly intensified by the current (and much needed) tendency towards circuit closure in the industry. As a remedy to this problem, the industry typically uses current state-of-the-science chemical crystallisation reactors which increase pH via the addition of a base e.g. Ca(OH)₂ or NaOH, and thereby precipitate CaCO₃ in the presence of crystal nucleation sites e.g. sand grains. These reactors are efficient but often require complex monitoring and control, and as a drawback, can give rise to highly alkaline effluents.

Biominalisation and biosorption are emerging as alternative mechanisms for the removal of inorganic contaminants from aqueous environments. These processes often utilise microorganisms that have key roles in natural bio-geochemical cycling, which allow both high selectivity and operational flexibility (Lloyd and Lovley, 2001). Microorganisms have long been known to catalyse the precipitation of CaCO₃ in natural environments such as oceans, soils and saline lakes, in a process referred to as microbial carbonate precipitation (MCP) (Castanier *et al.*, 1999; Douglas and Beveridge, 1998). The generally accepted

mechanism of MCP is the increase of pH and dissolved inorganic carbon (DIC) of a given environment through normal microbial physiological activities (Douglas and Beveridge, 1998). This reaction can be used in industrial processes for the immobilisation of soluble Ca^{2+} . For example, Van Langerak *et al.* (1997) proposed a fluidised sand bed calcification reactor, which utilised the alkalinity generated by microorganisms in a standard up-flow anaerobic sludge bed (UASB) reactor, for the removal of Ca^{2+} from industrial wastewater. Several other microbial precipitation induced pathways and precipitation mechanisms have been recognised (Castanier *et al.*, 1999). One of the most straightforward examples is microbial urea degradation. In this reaction, urea is hydrolysed via the urease enzyme (urea amidohydrolase; EC 3.5.1.5) to ammonium and carbon dioxide (Bachmeier *et al.*, 2002; Stocks-Fischer *et al.*, 1999). These products can subsequently react to form ammonia and carbonate ions, which, in the presence of soluble calcium ions, can react and precipitate as CaCO_3 . Urease enzymes are common to a wide variety of plants, fungi and bacteria (Bachmeier *et al.*, 2002; Burne and Chen, 2000). This feature allows for the integration and application of urease-based biotechnologies in almost any environment containing natural mixed-microbial populations.

In the previous chapter we have introduced the use of ureolytic MCP as a potential technology for calcium removal from raw industrial wastewater. In this study we describe some of the operational and engineering aspects of a bio-catalytic calcification (BCC) reactor process, based on ureolytic MCP combined with alkalinity generated in a UASB reactor, within the framework of an existing wastewater treatment (WWT) system. From a practical and economic perspective, the primary points of interest were (1) an uncomplicated process design, (2) the use of minimal urea concentrations, and (3) a feasible hydraulic retention time (HRT). The overall approach described herein has, to the best of our knowledge, as yet not been investigated before for industrial purposes.

MATERIALS & METHODS

Start-up sludge production

Anaerobic effluent was obtained weekly from a paper recycling facility (VPK, Oudegem, Belgium) and stored at 5 °C in sealed plastic vessels before use. 1 L Erlenmeyer flasks were filled with wastewater (described above), and supplemented with urea (Sigma, analytical grade) to final concentrations of 16.6 mM (= 1 g·L⁻¹). These were then shaken (100 rpm) at 30 °C for 24 hours. Thereafter, solids were allowed to sediment for 30 minutes, after which the supernatant was removed and analysed for pH and NH₄⁺-N. The “sludge” was retained in the flasks and raw wastewater was again added to a final volume of 1 L. This cycle was repeated for several days until a sufficient sludge volume was obtained, and nitrogen and pH measurements showed complete urea hydrolysis within 24 h. The produced sludge was analysed for dry matter (DM) content, ash content and total COD content.

Experimental set-up

The reactors consisted of two Erlenmeyer flasks (2.5 L), coupled to identical influent pumps (LMI, Milton Roy, USA), a common effluent pump (Watson-Marlow) and urea pump (Precidor, Infors, Basel), while magnetic stirring (Labinco, 100 rpm) was used to achieve sufficient mixing inside the reactors. All of this was controlled by three separate time switches. Both reactors were initially inoculated with 100 mL pre-cultivated sludge (see above), while a sludge volume of 200 mL was maintained in the reactors throughout the experimental period. Both reactors were fed with 1.8 L of anaerobic effluent. The BCC reactor was simultaneously fed with 10 mL of concentrated urea to a final reactor concentration of 8.3 mM urea, while the control reactor was not supplemented with urea. Both reactors were operated as sequential batch reactors (SBR) with a HRT of 8 h. One reactor cycle comprised: (1) addition of 1.8 L raw wastewater; (2) addition of urea (not in the control); (3) 6 hours mixing; (4) 2 hours sedimentation; (5) removal of 1.8 L supernatant.

Water analysis

Effluents from the calcification and control reactors were analysed regularly for pH, temperature, Ca^{2+} (total and soluble), Mg^{2+} (total and soluble), PO_4^{2-} , alkalinity, conductivity, turbidity, COD (total and soluble), total/volatile suspended solids (TSS/VSS) and ammonium-nitrogen (Greenberg *et al.*, 1992). Precipitation indices combine several water parameters such as temperature, pH, hardness, alkalinity, and are used to indicate the tendency of calcium carbonate to precipitate or dissociate in water (You *et al.*, 2001). Two commonly used indices for carbonate precipitation are the Langelier saturation index (LSI), and the Ryznar stability index (RSI). From the obtained data, the Langelier saturation index (LSI), and the Ryznar stability index (RSI), were determined as described previously (You *et al.*, 2001).

$$\text{LSI} = \text{pH} - \text{pH}_s$$

$$\text{RSI} = 2(\text{pH}_s) - \text{pH}$$

Where:

- pH is the measured water pH
- pH_s is the pH at saturation in calcite or calcium carbonate and is defined as:

$$\text{pH}_s = (9.3 + A + B) - (C + D)$$

and:

- $A = (\log_{10} [\text{total dissolved solids (TDS)}] - 1) / 10$
- $B = -13.12 \times \log_{10} (^{\circ}\text{C} + 273) + 34.55$
- $C = \log_{10} [\text{Ca}^{2+} \text{ as CaCO}_3] - 0.4$
- $D = \log_{10} [\text{alkalinity as CaCO}_3]$

The reactor pH was measured and logged every 300 seconds using a R305 (Consort, Antwerpen, Belgium) instrument.

Sludge analysis

Sludge samples were taken weekly from both reactors and analysed for total COD, dry matter, ash content and X-ray diffraction (XRD) analysis. For the latter, dried sludge was examined with X-ray diffraction (XRD powder diagrams) using a Phillips PW 1140 diffractometer equipped with Ni filter and a Cu $K\alpha$ radiation source, and identification was done according to

JCPDS (Joint Committee on Powder Diffraction Standards) and ASTM (American Society for Testing Materials) criteria. The sludge was also investigated with light microscopy as well as fluorescent microscopy using an Axioplan II (Zeiss) microscope. Digital micro-images were captured with a 1-CCD camera (Hamamatsu Photonics GmbH, Hersching, Germany) and analysed for particle size distribution with MicroImage 4.0 software (Olympus Optical Co. (Europe)).

Batch experiments

Batch experiments consisted of 1 L distilled water containing 31.7 mM NaHCO₃, 11.2 mM CaCl₂, a pH of 7.35, and the addition of 8.3 mM urea. The latter was used together with different amounts (222, 277 and 332 units) of commercial urease (Sigma; Type III from Jack Beans). In a further experiment, different concentrations of pre-cultivated sludge (0, 0.25, 0.5, 1.0 g·L⁻¹, based on DM) were added to the same medium together with 277 units urease. The sludge for these experiments was washed repetitively in sterile distilled water and subsequently autoclaved to inactivate biological activity.

RESULTS

Reactor performance

Urea addition and hydrolysis in the BCC reactor was a pre-requisite for calcium removal. Preliminary experiments demonstrated that inoculation of the reactors with a pre-cultivated calcification sludge is a pre-requisite for rapid onset of reactor efficiency (data not shown). The purpose of pre-cultivation was to select and stimulate autochthonous ureolytic organisms, and to develop natural crystal nucleation sites. Both these components are deemed essential to the overall efficiency of the precipitation process. Soluble calcium removal exceeded 85 %

throughout the experimental period in the BCC reactor (with urea), but only 13 % on average in the control reactor (without urea addition) (Figure 6.2; Table 6.1). Table 6.1 provides an overview of all parameters from the influent, control-effluent and BCC-effluent, as measured during 25 successive reactor cycles (equalling 8 days and 45 litres per reactor).

Table 6.1. Average values and standard deviation ($n = 25$) of all reactor parameters measured during the experimental period.

Parameter	Unit	Influent	Control Effluent	BCC Effluent
Temperature	°C	19.6 (± 1.6)	22.1 (± 1.03)	22.1 (± 1)
PH	-	7.37 (± 0.08)	7.84 (± 0.06)	7.54 (± 0.1)
Ca ²⁺ total	mg·L ⁻¹	463 (± 28)	426 (± 43)	97.8 (± 33.8)
Ca ²⁺ soluble	mg·L ⁻¹	448 (± 33)	390 (± 59)	54.7 (± 16.7)
Mg ²⁺ total	mg·L ⁻¹	32.2 (± 2)	30,8 (± 1.4)	28.7 (± 3.7)
Mg ²⁺ soluble	mg·L ⁻¹	30.0 (± 2.6)	30.1 (± 1.4)	26.6 (± 1.1)
PO ₄ ²⁻	mg·L ⁻¹	10 (± 3.2)	7.1 (± 2.7)	3.0 (± 1.8)
Hardness	*	1250 (± 79)	1082 (± 148)	238 (± 41)
Alkalinity	mg·L ⁻¹	1900 (± 48)	1799 (± 62)	1656 (± 98)
Conductivity	μS·cm ⁻¹	3592 (± 133)	3641 (± 133)	4058 (± 91)
COD total	mg·L ⁻¹	632 (± 97)	537 (± 75)	581 (± 84)
COD soluble	mg·L ⁻¹	491 (± 62)	442 (± 53)	480 (± 31)
TSS	mg·L ⁻¹	112.1 (± 6.3)	97 (± 18.9)	103 (± 27)
VSS	mg·L ⁻¹	69.7 (± 4.7)	59.4 (± 6.5)	60.3 (± 9.2)
Turbidity	NTU	107.4 (± 15.6)	98.2 (± 13)	105 (± 9.7)

* Hardness = $2.497[\text{Ca}^{2+}] + 4.118[\text{Mg}^{2+}]$ (Greenberg *et al.*, 1992)

In the BCC effluent remained about 2.5 mM total calcium, of which 1.5 mM was soluble. This implies that more than 80 % of the soluble calcium were not only immobilised as CaCO₃, but that it was also retained inside the reactor as sludge through straightforward sedimentation. This is furthermore confirmed by the fact that both the turbidity values and the TSS/VSS values from the BCC reactor differed very little from that of the influent (Table 6.1).

Table 6.1 also shows that apart from calcium removal, the reactors had little effect on the overall composition of the wastewater. Phosphate decreased slightly, probably due to co-precipitation as calcium phosphate or struvite, while nitrogen increased significantly in the BCC reactor as a result of the urea hydrolysis. Theoretically $500 \text{ mg}\cdot\text{L}^{-1}$ hydrolysed urea yields $230 \text{ mg}\cdot\text{L}^{-1} \text{NH}_4^+ \text{-N}$. The obtained value for the BCC reactor ($215 \text{ mg}\cdot\text{L}^{-1} \text{NH}_4^+ \text{-N}$) was within this range, indicating that the majority of the urea was indeed hydrolysed. The control reactor displayed slight nitrogen removal (compared to the influent), either due to microbial uptake or struvite precipitation, which could explain the discrepancy between the obtained and expected result in the BCC reactor.

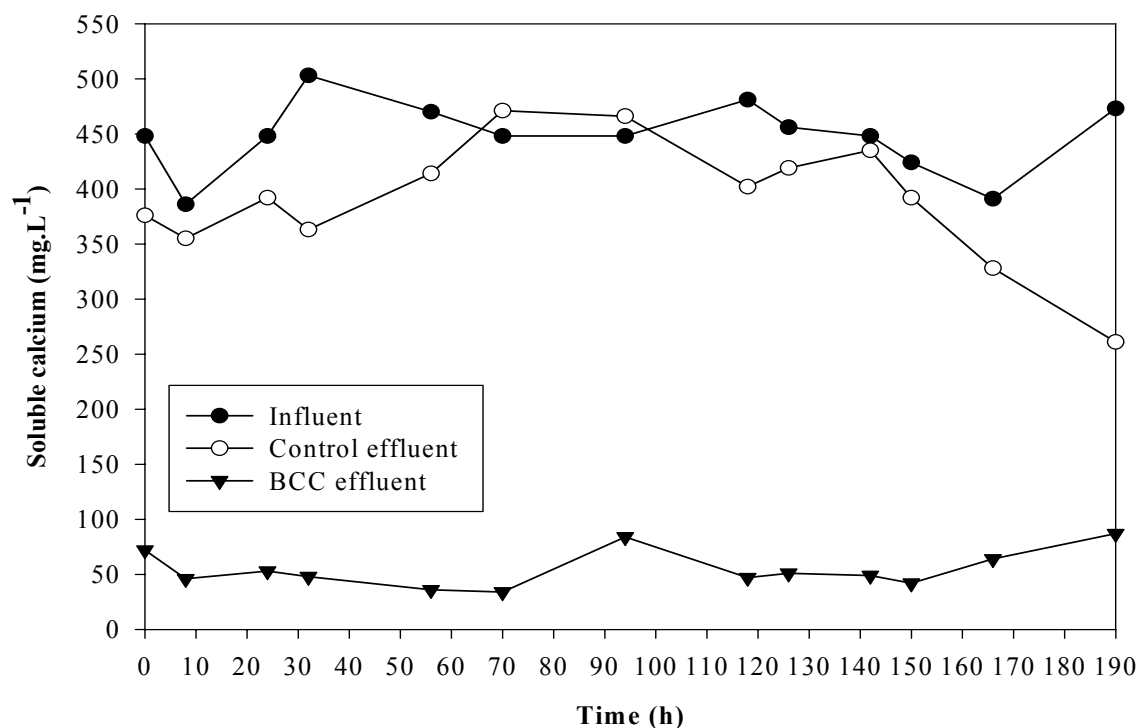


Figure 6.2. Soluble calcium in the influent, control-effluent, and BCC reactor effluent during the experimental period (one reactor cycle equals 8 hours)

Sludge analysis

Microscopic examination of the BCC-sludge revealed small, dense calcareous “flocs” (Figure 6.3(a)), clearly different from the control reactor sludge (Figure 6.3(b)), with expected fluorescence of CaCO_3 under UV light (results not shown). Figure 6.4 shows a comparison of particle size distribution of the BCC sludge at the beginning, middle, and completion of the experimental period. The evolution of the calcareous flocs is evident: an increased average crystal-floc size and more large crystals over the time period. This indicates an increase in the total available crystal nucleation surfaces in the reactor in time.

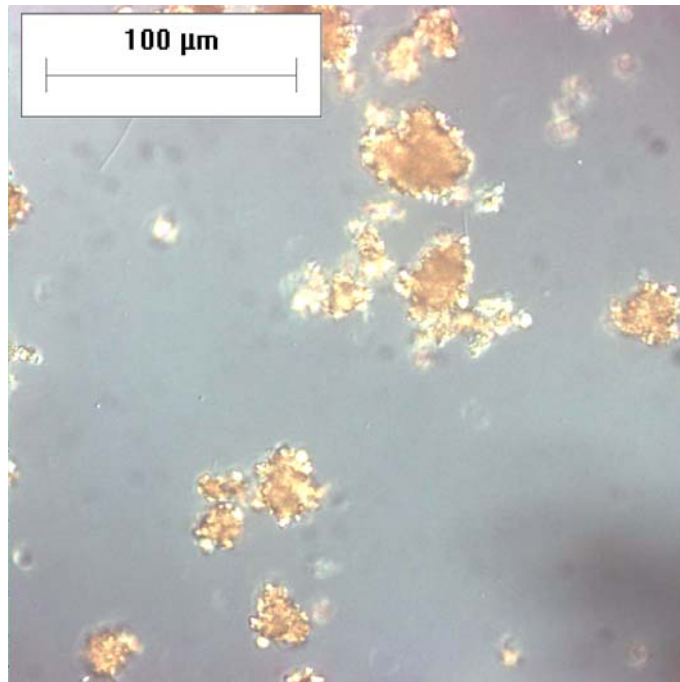


Figure 6.3. Microscope image of the calcareous sludge from the BCC reactor at completion of the experiment, showing small dense particles, mostly crystalline in nature.

Calcium removal was reflected in the sludge analysis, revealing a significant difference between the control sludge and BCC sludge. At completion of the experiments, the control sludge comprised $8.9 \text{ g}\cdot\text{L}^{-1}$ COD, $50.5 \text{ g}\cdot\text{L}^{-1}$ dry matter and $43.1 \text{ g}\cdot\text{L}^{-1}$ ash, with a VSS/TSS ration of

13.25 %, while the BCC sludge comprised respectively 12.9 g·L⁻¹ COD, 491.5 g·L⁻¹ dry matter and 473.5 g·L⁻¹ ash, with a VSS/TSS ratio of 3.175. Semi-quantitative XRD analysis identified the inorganic component of both sludge samples as calcite. The XRD results confirmed the inorganic nature of the sludge, while the large increase in the ash-content together with the VSS/TSS ratio in the BCC reactors substantiates the suggested increase in total available crystal nucleation sites in the BCC sludge. The crystalline characteristics of the sludge allowed for extremely rapid sedimentation in the reactors (results not shown).

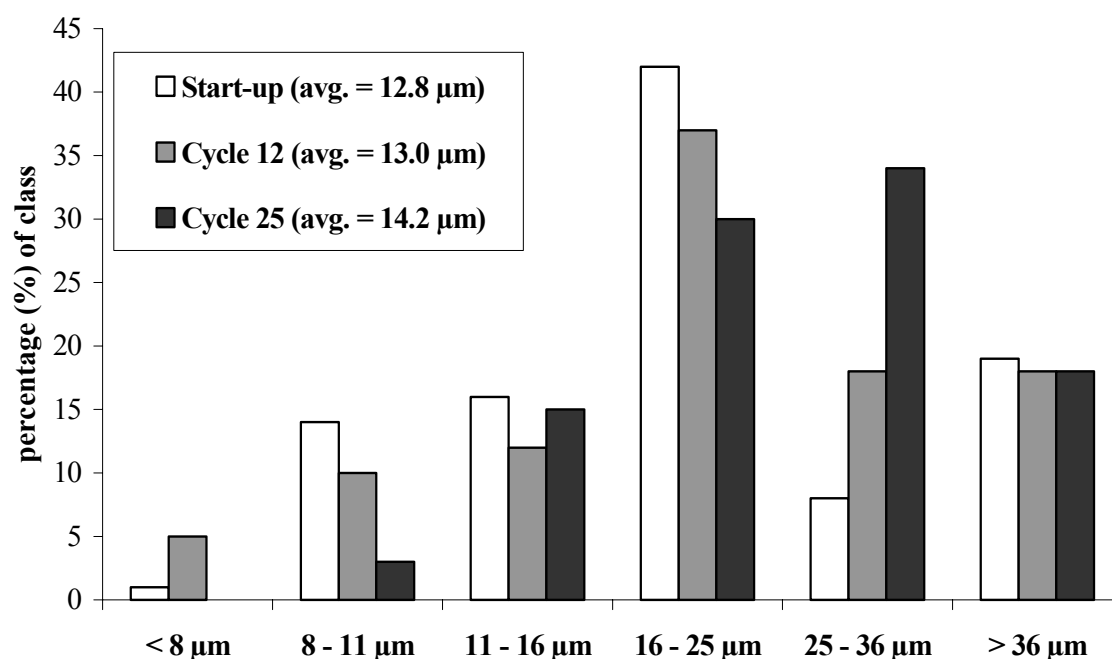


Figure 6.4. Particle size distribution of the BCC sludge before, during, and at completion of the experimental period (as classed by average floc diameter)

Precipitation indices

The BCC-process decreased the overall tendency of the wastewater to precipitate CaCO₃. Nonetheless, both the Langelier saturation index (LSI) and Ryznar stability index (RSI) still indicated a tendency for precipitation to occur (Figure 6.5). The neutral point of the LSI is 0,

with values above indicating a tendency for precipitation. The neutral point of the RSI is 6.0, with values below indicating a tendency for precipitation. The average LSI and RSI values for the influent were 1.66 and 4.05 respectively, and for the BCC effluent 1.06 and 5.42 respectively. The remaining tendency for precipitation in the wastewater following BCC treatment is primarily because of the high alkalinity remaining in the effluent (about $1600 \text{ mg}\cdot\text{L}^{-1} \text{ CaCO}_3$). However, actual data from the existing WWT system at the industry indicates that alkalinity decreases further during the aerobic treatment step to about $800 \text{ mg}\cdot\text{L}^{-1}$. Re-calculating the two indices for the BCC-effluent using the latter value shows further improvement of the values to 0.75 and 6.05 for respectively the LSI and RSI. Therefore, during an assessment of eventual circuit closure, parameters from the entire wastewater treatment process, as well as the parameters of recycle volume and number of cycles, should be taken into consideration.

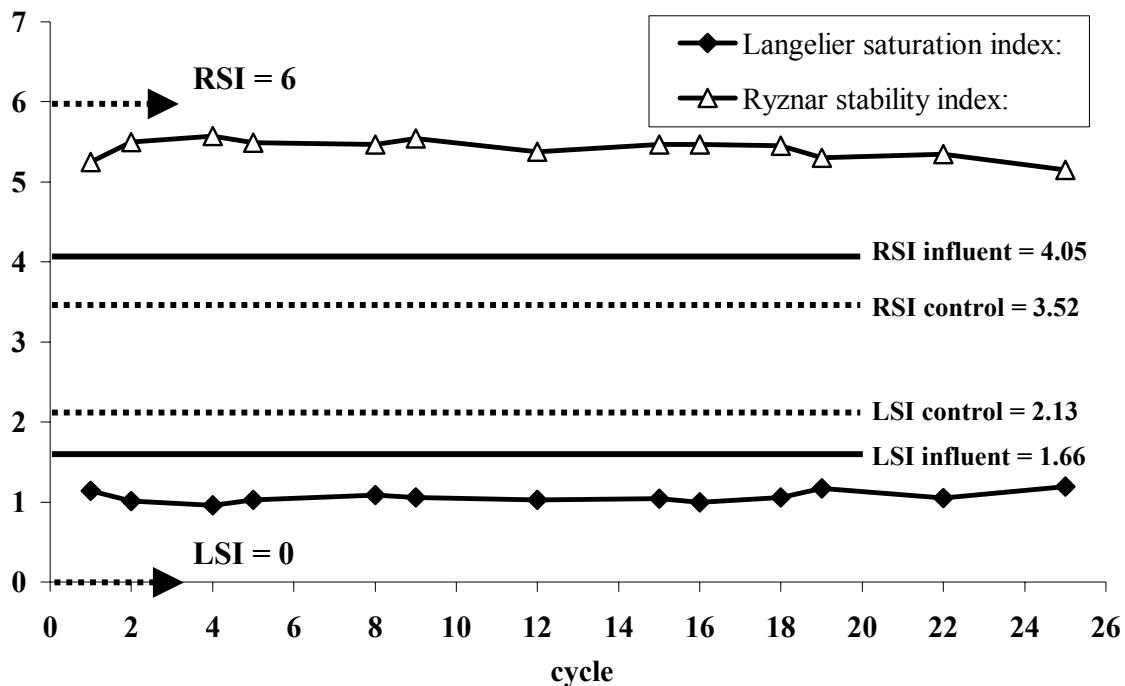


Figure 6.5. The Langelier saturation index values (LSI), and Ryznar stability index values (RSI) for the BCC reactor during the experimental period. The average LSI and RSI values for the influent and control reactor effluent are also indicated.

pH evolution and batch experiments

A remarkably distinctive repetitive pattern was observed in automatic sequential pH measurements in the BCC-reactor (Figure 6.6a). This pattern is elucidated in Figure 6.6b, where three sequential reactor cycles are shown together with a typical control cycle. While the control reactor only displayed a slight but continuous pH increase, the BCC reactor showed two further pH fluxes of significant importance to the process: a rapid pH increase, and a rapid pH decrease, giving the characteristic heartbeat-like pH pattern of this process. Moreover, two different levels of evolution-in-time of the BCC-reactor pH were observed (Figures 6.6a and 6.6b). Firstly, a decrease in the required time period for the first upper pH peak (horizontal evolution), and secondly, a decrease in the intensity of the upper peak (vertical evolution). Both these evolutions could be ascribed to the development of the ureolytic calcareous sludge: (1) higher ureolytic activity would account for the decrease in time required to reach the first peak, and (2) an increase in sludge volume (nucleation sites) would result in more rapid crystallisation, thus less peak intensity.

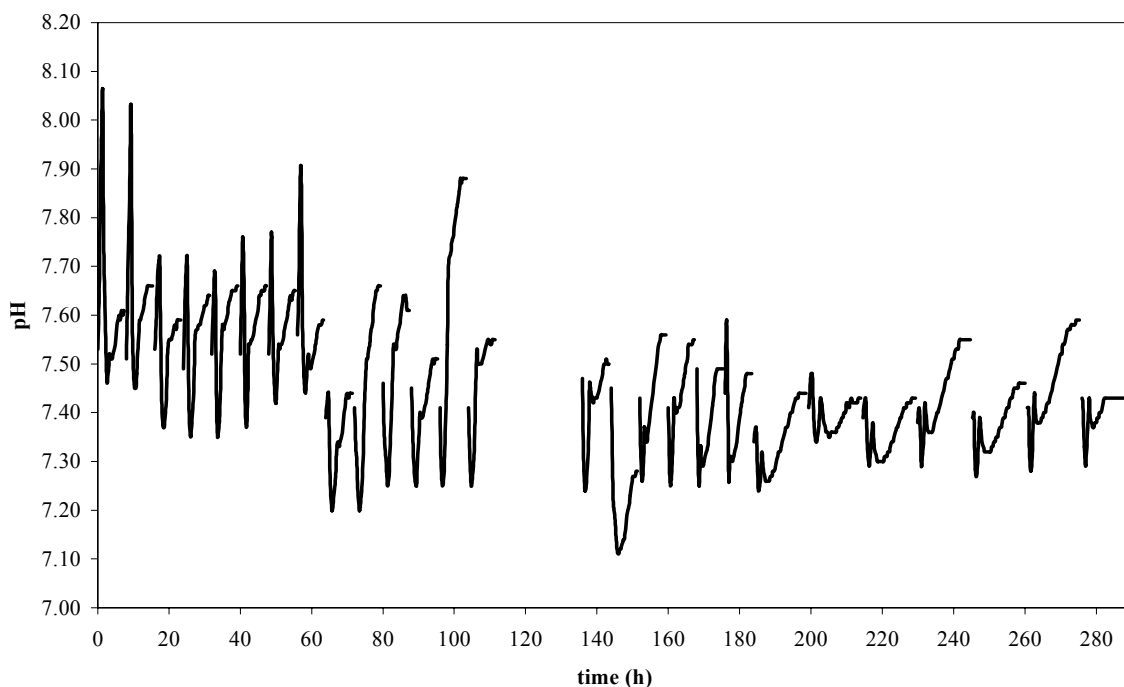


Figure 6.6a. Continuous pH measurements from sequential BCC reactor cycles (one cycle equals 8 hours), showing not only repetitive patterns, but also time dependant evolution.

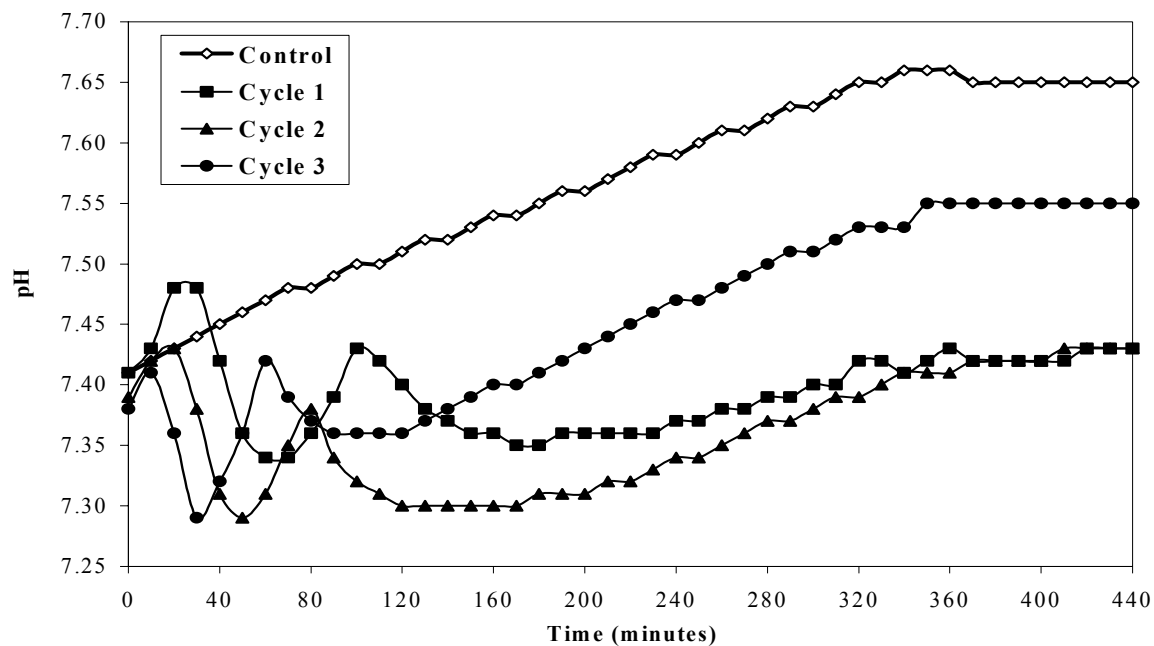


Figure 6.6b. The pH evolution as seen in three sequential BCC reactor cycles and one typical control cycle

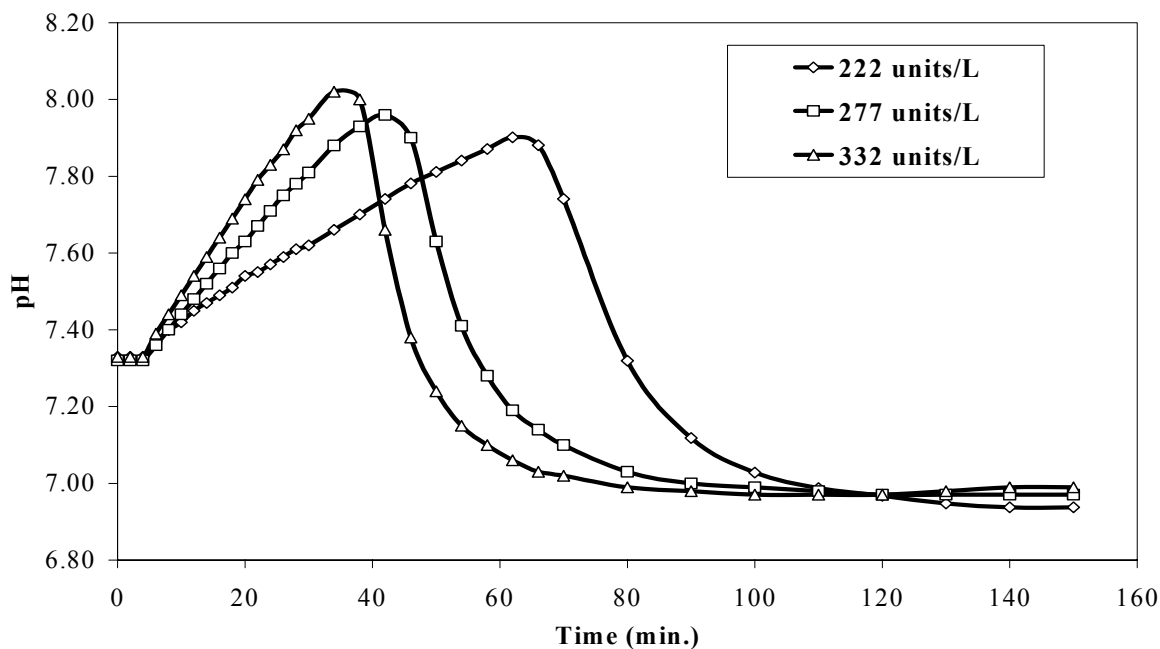


Figure 6.7a. Batch experiments simulating reactor conditions using urea with three different concentrations of urease enzyme.

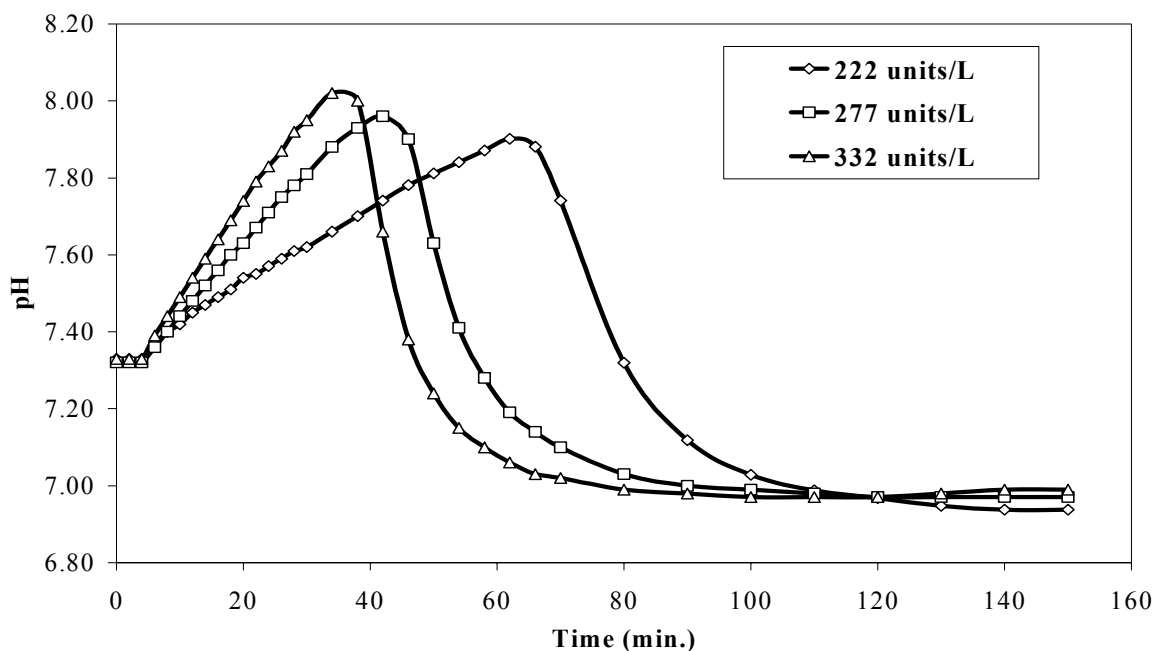


Figure 6.7a. Batch experiments simulating reactor conditions using urea with three different concentrations of urease enzyme.

DISCUSSION

Placement of the bio-catalytic calcification (BCC) reactor

The placement of the calcification reactors was deemed essential to the performance thereof. Figure 6.1 displays a simplified scheme of the most important features of the wastewater treatment plant at the paper industry from which the wastewater for these experiments were taken, as well as the theoretical placement of the BCC reactor within this process. The result is that anaerobic effluent was used, which implied wastewater with a high alkalinity, near-neutral pH, and a relatively high COD content (Table 6.1).

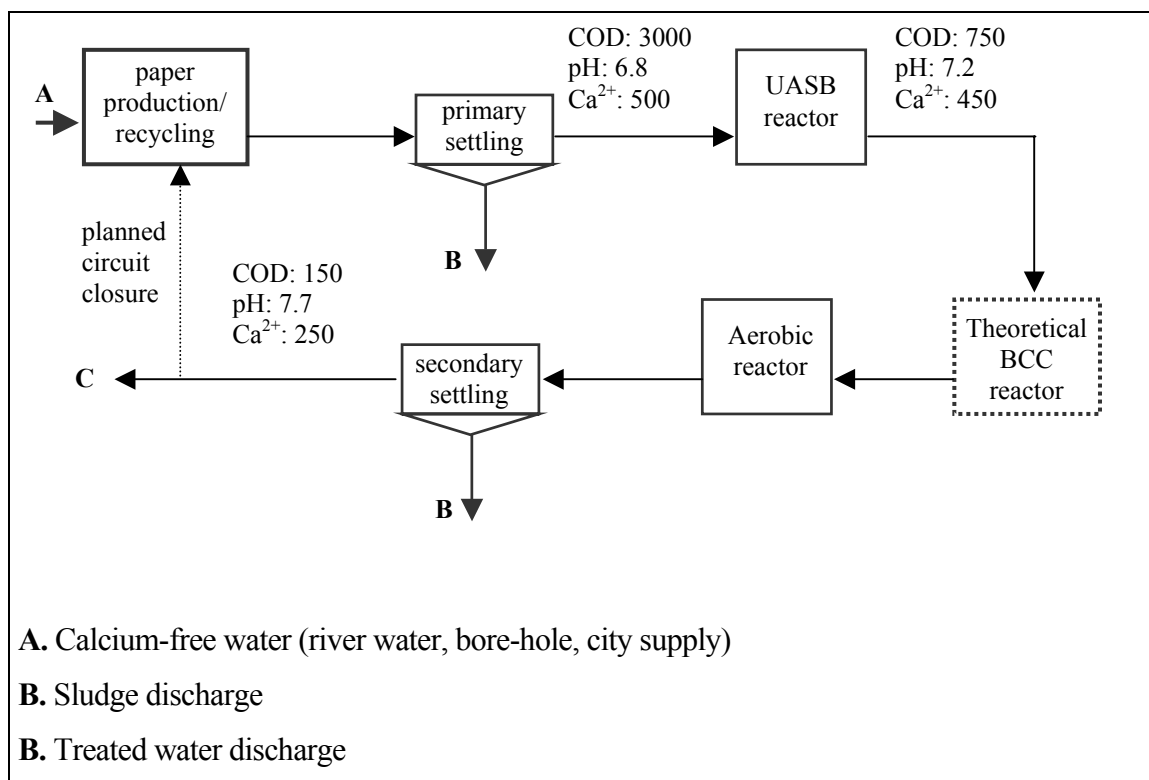


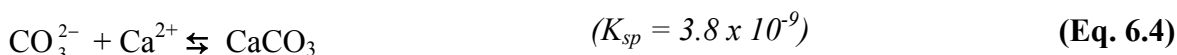
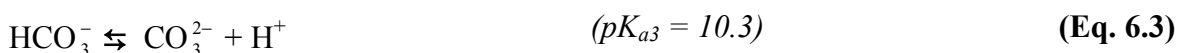
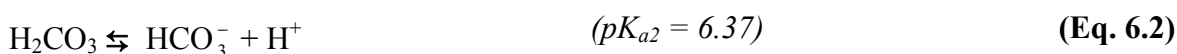
Figure 6.1. Scheme of the suggested placement of the BCC reactor within the overall wastewater treatment system of the industry. COD and Ca^{2+} values in $\text{mg}\cdot\text{L}^{-1}$.

The aim of this study was to examine the technical and economic feasibility of ureolytic CaCO_3 precipitation for a calcium removal technology from industrial wastewater, and to shed more light on some of the important operational parameters of this process. CaCO_3 used during the manufacturing of paper-products is the initial source of eventual Ca^{2+} in the effluent (Figure 6.1). The basic configuration of the WWT system of this particular industry is more or less standard for the paper industry (Habets and Knelissen, 1997; Van Langerak *et al.*, 1997). Anaerobic digestion with UASB technology is used for removal of bulk COD from the wastewater. This simultaneously results in an increase of wastewater alkalinity as a result of microbial CO_2 production (Van Langerak *et al.*, 1997), and also a pH increase. In this particular case, the pH in the UASB reactor is controlled with acid addition to avoid excessive scaling inside the reactor. The aerobic reactor is used as a “polishing step” to decrease the residual COD to legislatively acceptable levels. Annual data obtained from the industry indicates that during the aerobic treatment step, about 50 % Ca^{2+} is removed through precipitation. The latter is a

result of a pH increase in the wastewater, due to CO₂ stripping caused by aeration (Suzuki *et al.*, 2002; Saywer *et al.* 1994). The advantage of this precipitation is that the WWT system develops and maintains a rapid and compact settling sludge. However, the main disadvantage is that severe scaling occurs inside the aerobic reactor and secondary clarifier, resulting in mechanical under-performance, and a regular need for cleaning.

The theoretical placement of the BCC reactor within this WWT system was essential (Figure 6.1). In the previous chapter, raw wastewater taken from directly after the primary settling tank was used. For this study, anaerobic effluent was specifically chosen, as it already contains high alkalinity as such, which could aid the precipitation process (Van Langerak *et al.*, 1997). Simultaneously, the high bicarbonate content would add to the buffering characteristics of the wastewater, thus avoiding unnecessary large pH shifts. On the other hand, the BCC reactor had to be placed prior to an aerobic treatment step, as to at least allow for the possibility of nitrification/denitrification removal of the added nitrogen.

The chemical composition of the anaerobic effluent used in these experiments can be divided in the following primary components (Table 6.1): Ca²⁺ (11.2 mM), DIC (30.8 mM), organic matter (COD = 600 mg/L) and a pH of 7.37. The chemistry of wastewater is therefore primarily governed by the DIC buffer equilibrium reactions (Equation 6.1 – 6.3), as well as the CaCO₃ precipitation reaction (Equation 6.4).



CaCO₃ forms when the solubility product exceeds the solubility constant, in other words, roughly based on the available amount of Ca²⁺ and CO₃²⁻ ions. Using MINEQL chemical

speciation software (<http://www.mineql.com>), the DIC speciation at pH 7.37 was calculated to be: $H_2CO_3 = 2.71 \text{ mM}$; $HCO_3^- = 29 \text{ mM}$; $CO_3^{2-} = 0.03 \text{ mM}$. From this it follows:

$$[CO_3^{2-}] \times [Ca^{2+}] = 0.00003 \times 0.0112 = 3.36 \times 10^{-7} \quad (\text{Eq. 6.5})$$

$$([CO_3^{2-}] \times [Ca^{2+}])/K_s = (3.36 \times 10^{-7})/(3.8 \times 10^{-9}) = 88.4 \quad (\text{Eq. 6.6})$$

Thus, considering the K_s value (Equation 4), the calculations above implies that even though the pH is nearly neutral, $CaCO_3$ saturation in the untreated wastewater still exceed the solubility constant nearly 90 times.



During the BCC treatment, added urea is cleaved intracellularly by urease to produce one mole ammonia and one mole carbamate (Equation 6.7). The latter spontaneously hydrolyse to form a further mole of ammonia and carbonic acid (Equation 6.8). The carbonic acid could equilibrate in water according to Equation 6.2, while the ammonia ions will hydrolyse to yield two moles ammonium and two hydroxide ions (Equation 6.9) (Burne and Chen, 2000). If only the addition of DIC (8.3 mM) from urea is considered (Equation 6.8), the over-saturation would already increase to about 110 times. However, as primary effect, the pH of the system would also increase (Equation 6.9). This expected (theoretical) pH of the system can roughly be calculated as a combination of the primary buffers of the system (considering 99 % NH_3 hydrolysis).

$$pH_1 = pK_{a3} + \log \left[\frac{[CO_3^{2-}]}{[HCO_3^-]} \right] = 9.34 \quad (\text{Eq. 6.11})$$

$$pH_2 = pK_{z1} + \log \left[\frac{[NH_3]}{[NH_4^+]} \right] = 7.27 \quad (\text{Eq. 6.12})$$

A combination of these two give a resulting value of pH 8.57, which is interpreted as the maximum possible pH of the system. Considering this pH value, DIC speciation of 0.26 mM H_2CO_3 , 38.2 mM HCO_3^- and 0.63 mM CO_3^{2-} is obtained with speciation software.

$$[\text{CO}_3^{2-}] \times [\text{Ca}^{2+}] = 0.000625 \times 0.0112 = 7.0 \times 10^{-6} \quad \text{(Eq. 6.13)}$$

$$([\text{CO}_3^{2-}] \times [\text{Ca}^{2+}]) / K_s = (7.0 \times 10^{-6}) / (3.8 \times 10^{-9}) = 1842 \quad \text{(Eq. 6.14)}$$

Though chemical speciation lends itself to different interpretations, especially when complex solutions such as wastewater are considered, the overwhelming positive effect of urea hydrolysis on CaCO_3 saturation in the system is evident (Equations 6.13 and 6.14). In fact, Equation 6.10 provides a much more straightforward interpretation: if all the added urea is completely hydrolysed, it could maximally account for 8.3 mM CO_3^{2-} available for precipitation as CaCO_3 . The effect of urea hydrolysis on the pH was illustrated above (Equation 6.11 and 6.12). Concomitantly, CaCO_3 precipitation would have the opposite effect, resulting in a pH decrease relative to the amount which was precipitated. The overall sequence of events would therefore be: (1) urea hydrolysis, (2) pH increase, (3) sufficient over-saturation, (4) crystallisation, and (5) pH decrease. Thereby resulting in a wave-like pH curve. Moreover, in a best-case scenario, in which it is taken that all CO_3^{2-} which is formed is directly precipitated as CaCO_3 , only the original $\text{HCO}_3^-/\text{H}_2\text{CO}_3$ equilibrium and the $\text{NH}_3/\text{NH}_4^+$ equilibrium govern the system pH (as all produced CO_3^{2-} is directly removed). This would imply complete precipitation without any noticeable pH increase.

It is interesting to see the extent to which the experimental results corroborate with the theoretical predicted data. Firstly, only an average of 13 % Ca^{2+} precipitation was witnessed for the control reactor with no urea addition, even though the wastewater was as such over-saturated more than 80 times with CaCO_3 . Moreover, this over-saturation would have increased even more with the continuous pH increase witnessed for this reactor during one cycle (Figure 6.6a and 6.6b). In fact, using the average final pH of 7.85 from this reactor (Table 6.1), an over-saturation of 273 times is calculated (Equations 6.5 and 6.6). This result confirmed those from the previous chapter, which demonstrated that CaCO_3 precipitation was dependant on addition

and hydrolysis of urea. It is known that carbonates can often remain in solution for up to 40 times exceeding their solubility constants (Stumm and Morgan, 1981), Ca^{2+} complexation with organic matter would also have contributed to the relative small amount of CaCO_3 that precipitates as such from the water. In fact, Van Haandel and Lettinga (1994) reported that for anaerobic wastewater effluents, the normal K_s values do not apply. These authors indicated that case-specific experimental data should be obtained, but that this value can easily be as low as 2.0×10^{-7} . In the BCC reactor, 85 % Ca^{2+} was precipitated on average, equalling 9.52 mM (Table 6.1). As shown above, over-saturation in the wastewater prior to urea addition could account for 13 % (1.46 mM) of this, leaving 8.06 mM Ca^{2+} precipitation as a result of urea addition and hydrolysis. This, of course, concurs with the added amount of urea (8.3 mM).

Due to the nature of the urea hydrolysis products and the calcium carbonate precipitation process, pH evolution is an important parameter for understanding, monitoring and eventual control of this system. Experimental pH data from the BCC reactor followed the predicted pH pattern. Firstly, a rapid pH increase, presumably due to urea hydrolysis (Stocks-Fischer *et al.*, 1999), and secondly, rapid pH decrease, presumably due to calcium carbonate precipitation was observed (Figure 6.6a and 6.6b). Although the expected curve trend is seen, the predicted maximum pH value was never detected. This is ascribed firstly to the buffering effect of the bicarbonate in the water, as well as continuous acidification as a result of CaCO_3 precipitation. Combined to this was a vertical and horizontal evolution of the pH curve, which was ascribed to development of high ureolytic activity and effective crystal nucleation sites. These deductions were further buttressed by the respective batch tests (Figures 6.7a and 6.7b).

Preliminary economic analysis of the process

The required urea addition constitutes the major operational cost of the process. Based on current market prices, an addition of $0.5 \text{ g}\cdot\text{L}^{-1}$ urea to wastewater is equal to 0.075 Euro per m^3 treated water. The added nitrogen load (resulting from urea degradation) would impose additional operational costs upon further nitrification and concomitant denitrification. In this study, practically no COD was removed in the crystallisation reactor, which left a soluble COD of about $480 \text{ mg}\cdot\text{L}^{-1}$, while the BCC reactor effluent contains on average 215

$\text{mg}\cdot\text{L}^{-1} \text{NH}_4^+\text{-N}$ (Table 6.1). Nitrogen removal through classic nitrification/denitrification requires theoretically a minimum ratio of 3.4 g COD per gram nitrogen. Thus, $480 \text{ mg}\cdot\text{L}^{-1}$ COD potentially suffices to remove $140 \text{ mg}\cdot\text{L}^{-1} \text{NH}_4^+\text{-N}$, which, when considering current European legislation of $50 \text{ mg}\cdot\text{L}^{-1}$ nitrogen, is already 90 % of the required removal. However, difficulties might arise due to the recalcitrance of paper wastewater COD, and therefore further research should primarily aim at reducing the current nitrogen load. Due to the simplicity of process design and the adaptability of this system within a standard WWT system, capital costs would be low compared to other systems. Moreover, current calcification operational cost such as purchasing and transport of proper crystal nucleation sites (silver sand), would be eliminated entirely.

CONCLUSION

In conclusion, based on the experimental data it is argued that the BCC reactor operated at maximum theoretical efficiency: all the urea was hydrolysed by the biocatalyst, and that all the produced CO_2 reacted to form CO_3^{2-} , which then precipitated as CaCO_3 , all without any significant pH variations. In this, the calculations also emphasised the primary advantage that bio-catalytic urea hydrolysis adds to the precipitation event i.e. simultaneous production of DIC and a pH increase in the same space and time. However, the exact mechanism responsible, be it seemingly the formation of chemical micro-niches by the urea hydrolysis reaction, the function of crystal nucleation sites, or cell surface mediated precipitation as was previously suggested by Stocks-Fischer *et al.* (1999), has neither been the objective of, nor a conclusive deduction from, these experiments.

[Link to Contents](#) [Link to Chapter 7](#)

ACKNOWLEDGEMENTS

The authors appreciate the technical assistance of Greet Vandavelde and Els Jolie, financial support from VPK (Oudegem, Belgium) and Avecom NV (Belgium), and critical comments on the manuscript from Nico Boon and Sylvie Seurinck.

CHARACTERISATION OF THE MICROBIAL COMMUNITY AND PRECIPITATION MECHANISM IN A BCC REACTOR

Redrafted from:

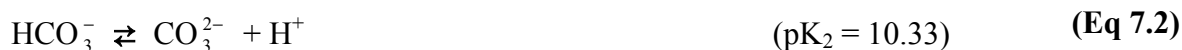
- (1) F. Hammes, N. Boon, G. Clement, J. de Villiers, S.D. Siciliano and W. Verstraete. Molecular, biochemical and ecological characterisation of a bio-catalytic calcification reactor. Submitted to the Journal of Applied Microbiology and Biotechnology (November, 2002)

ABSTRACT *This chapter characterises BCC reactor evolution from initialisation to optimisation over a six-week period. Three key parameters were studied: (1) microbial evolution, (2) the (bio)chemical precipitation pathway, and (3) crystal nucleation site development. Four to five weeks were required for the establishment of optimal reactor performance, which coincided with an increase in urease activity from initially $7 \text{ mg urea.L}^{-1}_{\text{reactor}}\text{h}^{-1}$ to about $100 \text{ mg urea.L}^{-1}_{\text{reactor}}\text{h}^{-1}$. Urease activity in the optimal period was directly proportional to Ca^{2+} removal, but urease gene diversity was seemingly limited to a single gene. Denaturing gradient gel electrophoresis of 16S rRNA genes revealed a dynamic evolution in the microbial community structure of the calcareous sludge, eventually dominated by a few species including Porphyromonas sp., Arcobacter sp. and Bacteroides sp. Epi-fluorescence and scanning electron microscopy showed that the calcareous sludge was colonised with living bacteria, as well as the fossilised remains of organisms. It appears that the precipitation event is localised in a micro-environment, due to colonisation of the crystal nucleation sites (calcareous sludge) by the precipitating organisms.*

INTRODUCTION

Biological mineral precipitation presents interesting alternative means for the treatment of industrial wastewaters as well as groundwater contaminated with excessive amounts of “unusual” pollutants such as heavy metals, radionuclides, phosphate, and salts (Lloyd and Lovley, 2001). For example, both Fujita *et al.* (2000) and Warren *et al.* (2001) confirmed the potential of ureolytic co-precipitation for the *in situ* treatment of contaminants such as $^{90}\text{Sr}^{2+}$, UO_2^{2+} and Co^{2+} in groundwater, while Lloyd and Lovley (2001) reported on the applicability of *Ralstonia eutropha* for the removal/recovery of mercury and other divalent heavy metals (as metal-carbonates) from wastewater. The European paper recycling industry annually requires up to 1.4 billion cubic meters water, while producing effluents containing 10 – 40 mM Ca^{2+} . Bio-catalytic calcification (BCC) reactors have been developed specifically for the removal of soluble calcium from industrial wastewater, in the form of calcite (Refer to Chapters 5 and 6). Such reactors are based on ureolytic microbial calcium carbonate precipitation (MCP), but, as with the natural process, preciously little is known about the microbial ecology governing the precipitation event.

CaCO_3 precipitation requires sufficient calcium ions (Ca^{2+}) and carbonate ions (CO_3^{2-}) so that the ion activity product (IAP) exceeds the solubility constant (K_s) (Equation 7.1), as well as preferably the presence of crystal nucleation sites (Stumm and Morgan, 1981). The concentration of carbonate ions is furthermore related to the concentration of dissolved inorganic carbon (DIC) and the pH of a given aquatic system (Equation 7.2).



Microorganisms can influence these four precipitation parameters. Intracellular calcium metabolism as well as the binding of cations to electron negative cell membranes and extracellular polymeric substances (EPS) could all contribute to elevated localised

concentrations of Ca^{2+} (McConnaughey and Whelan, 1997; Schultze-Lam *et al.*, 1996), with the latter two factors rendering bacterial cell walls as ideal crystal nucleation sites (Schultze-Lam *et al.*, 1996). More importantly, microorganisms can change the DIC and pH of a given environment through metabolic processes, thus catalysing precipitation (Douglas and Beveridge, 1998). One such process is urea hydrolysis. In this reaction, urea is cleaved intracellularly to yield carbonic acid and ammonia. These products spontaneously equilibrate at physiological pH, yielding bicarbonate, ammonium and hydroxide ions, thus giving rise to a pH increase as well as a simultaneous DIC increase (Equations 7.3 – 7.5) (Burne and Chen, 2000; Mobley and Hausinger, 1989). The urease enzyme (urea amidohydrolase; EC 3.5.1.5) is commonly found in various aerobic and anaerobic microbial species (Reed, 2001; Burne and Chen, 2000; Mobley and Hausinger, 1989).



The objectives were firstly to characterise the biological catalyst of a BCC reactor in terms of the population and urease enzyme development in time, and secondly to underpin the exact mechanism of precipitation, and the role of the microorganisms therein.

MATERIALS & METHODS

Reactor set-up, operation and water analysis

The wastewater used during experimentation was anaerobic effluent from a full-scale up-flow anaerobic sludge bed (UASB) reactor at a paper-recycling industry (VPK, Oudegem, Belgium). Water was collected weekly and stored in sealed plastic containers at 5 °C until required. Two duplicate sequential batch reactors (from here on referred to as bio-catalytic calcification (BCC) reactors) consisting of 3 L Erlenmeyer flasks, were operated in parallel. Both reactors were inoculated with 0.25 L activated sludge, taken from the aerobic wastewater treatment system at the industry, and this sludge volume was maintained in the reactors throughout the experimental period. For the first week the reactors were fed 1 g·L⁻¹ urea (mixed liquor initial concentration), and operated with a hydraulic residence time (HRT) of 24 h. For the second week, the urea concentration was decreased to 0.5 g·L⁻¹, while the HRT of 24 h was maintained. Thereafter, the HRT was decreased to 8 h, allowing for 3 reactor cycles per day. A standard reactor cycle consisted of 15 minutes feeding, during which 2.25 L influent (wastewater) was fed to both reactors with a double-headed pump (LMI, Milton Roy, USA), and concentrated urea (75 g·L⁻¹) (Riedel-de Haën) was fed with a separate double-headed pump (Watson Marlow 313S) to the chosen fed-batch concentration. The reactors were then mixed for 6 h using magnetic stirring (Labinco, 100 rpm), followed by a 1.5 h settling period, and eventual water discharge, using a double-headed effluent pump (LMI, Milton Roy, USA). The entire cycle was controlled with three separate electronic time switches. A sludge residence time (SRT) of approximately 14 days was used. The influent, as well as the effluents from both reactors were analysed regularly for pH, temperature, Ca²⁺ (total and soluble), Mg²⁺ (total and soluble), total phosphate, alkalinity, total COD, Kjeldahl and ammonium-nitrogen (Greenberg *et al.*, 1992). The evolution of the urease activity in the reactors was followed by measuring the amount of total ammonium-nitrogen (TAN) exactly 2 hours after start-up. Mixed liquor suspended solids (MLSS) samples were taken, filtered (0.45 µm Whatman filters), and the total ammonium-nitrogen was determined

spectrophotometrically (425 nm) according to the Nessler method (Greenberg *et al.*, 1992). Effective reactor urease activity was expressed as $\text{mg urea} \cdot \text{L}^{-1}_{\text{reactor}} \cdot \text{h}^{-1}$.

Single reactor cycle analysis

During a period of optimal calcium removal, the evolution of pH, Ca^{2+} , and TAN was followed within a single cycle in the reactors. Mixed liquid samples were taken approximately every 30 – 60 minutes, filtered immediately (0.45 μm Whatman filters), and analysed for TAN as described above. Simultaneously, some of the filtered sample was diluted (milliQ water), acidified (1 N HNO_3) and analysed for Ca^{2+} with flame atomic absorption spectrometry (Perkin Elmer Flame AAS, Überlingen, Germany). pH evolution was detected and recorded automatically every 5 minutes using a R305 instrument (Consort, Belgium) equipped with two separate electrodes. The above experiment was repeated with the same set-up and sludge, but without the addition of any urea to the reactors, to serve as negative control for the reaction.

DNA extraction of activated sludge samples

Sludge samples of 10 mL were taken approximately every 7 days from both reactors and stored at $-80\text{ }^\circ\text{C}$. An extraction protocol was adapted from Griffiths *et al.* (2000) and Kowalchuk *et al.* (1998). Briefly, in a 2 ml Eppendorf tube 0.5 g RNase-free 0.1-mm diam. Zirconia/silica beads, 0.5 ml calcareous sludge, 0.5 ml CTAB buffer (Hexadecyltrimethylammonium bromide 5 % wt/vol., 0.35 M NaCl, 120 mM potassium phosphate buffer (pH 8.0)) and 0.5 ml of phenol–chloroform–isoamyl alcohol mixture (25:24:1) were homogenized ($3 \times 30\text{ s}$ at 5000 rpm) in a Beadbeater (B. Braun Biotech International, Melsungen, Germany) with 10 s between shakings. Following centrifuging (5 min, $3000 \times g$), 300 μl of the supernatant was transferred to RNase free Eppendorf tubes. Another 0.5 ml of CTAB buffer was added to the remaining sludge suspension and the extraction procedure was repeated, giving a final volume of 600 μl . The phenol was removed by mixing with an equal volume of chloroform-isoamyl alcohol (24:1) and centrifuging ($3000 \times g$, 10 sec.). The aqueous phase was transferred to a new Eppendorf tube and nucleic acids were precipitated with 2 volumes of 30 % (wt/vol) polyethylene

glycol 6000- 1.6 M NaCl for 2 h at room temperature. Subsequently the Eppendorf tube was centrifuged ($18000 \times g$, 4 °C, 10 min.). Finally, the nucleic acid pellet was washed in ice-cold 70 % (vol./vol.) ethanol and dried under vacuum for 10 minutes prior to re-suspension in 100 µl RNase free water.

Polymerase chain reaction (PCR) and denaturing gradient gel electrophoresis (DGGE) of the 16S rRNA genes

The PCR mastermix contained 500 nM of each primer, 200 µM of each deoxynucleoside triphosphate, 1.5 mM MgCl₂, 10 µl of Thermophilic DNA Polymerase 10X Reaction Buffer (MgCl₂-free), 2.5 U of Taq DNA Polymerase (Promega, Madison, WI, USA), 400 ng/µl of bovine serum albumin (Boehringer), and Dnase and Rnase free filter-sterile water (Sigma-Aldrich Chemie, Steinheim, Germany) to a final volume of 100 µl (Boon *et al.*, 2000). One µl of DNA template was added to 24 µl of mastermix.

The 16S rRNA gene fragments of the isolates were amplified by PCR using the forward primer P338F (5'-ACT-CCT-ACG-GGA-GGC-AGC-AG-3') and the reverse primer P518r (5'-ATT-ACC-GCG-GCT-GCT-GG-3'). A GC-clamp of 40 bp (Muyzer *et al.*, 1993) was added to the forward primer to make DGGE analysis possible. The PCR program consisted of 10 min at 95 °C; 30 cycles of 1 min. at 94 °C, 1 min. at 53 °C, 2 min. at 72 °C; and a final elongation for 10 min. at 72 °C.

DGGE was performed with the Bio-Rad D Gene System (Hercules, CA, USA). PCR samples were loaded onto 7 % (wt/vol) polyacrylamide gels in 1xTAE (20 mM Tris, 10 mM acetate, 0.5 mM EDTA pH 7.4). The polyacrylamide gels were made with a denaturing gradient ranging from 50 to 65 %, using 7 M urea and 40 % formamide as 100 % denaturant (Boon *et al.*, 2002). The electrophoresis was run for 16 hours at 60 °C and 40 V. The gels were stained with SYBR GreenI nucleic acid gel stain (1:10,000 dilution; FMC BioProducts, Rockland, ME, USA) and photographed (Boon *et al.*, 2000).

PCR-DGGE of the *ureC* gene

The PCR-mastermix composition was identical as described above. To amplify the genes encoding for the *ureC* subunit of the urease enzyme, PCR was performed with primers UreC-F (5'-TGGGCCTTAAAATHCAYGARGAYTGGG-3') and UreC-R (5'-GGTGGTGGCACACCATNANCATRTC-3') as previously described by Reed (2001). A GC clamp (Muyzer *et al.*, 1993), was attached to the 5' end of the UreC-F primer. The length of the expected amplified fragment with the GC clamp was 422 bp. PCR was performed in a 9600 thermal cycler (Perkin-Elmer, Norwalk, CT, USA) as follows: 94 °C for 5 min, followed by 35 cycles of 92 °C for 1 min, 50 °C for 1 min, and 72 °C for 2 min. A final extension was carried out at 72 °C for 10 min. DGGE analysis was performed as described above using polyacrylamide gels with a denaturing gradient ranging from 40 to 60 %. The electrophoresis was run for 16 hours at 60 °C, at 45 V.

DNA sequencing

Putative *ureC* gene fragments and 16 S rRNA gene fragments were cut out of the respective DGGE gels, reamplified by PCR and send for sequencing. DNA sequencing of the PCR fragments was carried out by ITT Biotech-Bioservice (Bielefeld, Germany). Analysis of DNA sequences and homology searches were completed with standard DNA sequencing programs and the BLAST server of the National Center for Biotechnology Information (NCBI) using the BLAST algorithm (Altschul *et al.*, 1997). Phylogenetic trees were constructed using the RDP Phylip Interface (Maidak *et al.*, 2001)

Nucleotide sequence accession numbers

Nucleotide sequences for 16 S rRNA gene fragments have been deposited in GenBank database under accession no. AY157610 to AY157613 respectively. Nucleotide sequences for *UreC* gene fragments under accession no. AY167743 and AY167744.

Sludge analysis

Calcareous sludge was sampled from both reactors after four weeks and six weeks respectively. These samples were analysed for total and volatile suspended solids (TSS and VSS) (Greenberg

et al., 1992), while the sludge settling rate (SSR) and the sludge volume index (SVI) values were also determined. This was done by allowing 1 L sludge to settle for 30 minutes, measuring the rate at which it settled, and then measuring the final sludge volume. The latter was subsequently related to the TSS value. Sludge samples were subsequently dried (50 °C, 48 h) and pulverised. The dried sludge were grounded to the appropriate particle size for XRD analysis, (< 10 µm), using a McCrone micronising mill. The milled samples were then mounted in a sample holder and analysed using a Siemens D-501 diffractometer. Phase identification was done after background subtraction using the Bruker EVA software. The operating parameters are given below.

Instrument and data collection parameters:

Radiation	Cu $K\alpha$ (1.5418 Å)
Temperature	25°C
Specimen	flat-plate, rotating (30 RPM)
Power Setting	40 kV, 40 mA
Soller slits	2° (diffracted beam side)
Divergence slits	1°
Receiving slits	0.05°
Monochromator	secondary, graphite
Detector	scintillation counter
Range of 2θ	15-70°2θ
Step width	0.04°2θ
Time per step	1.5 seconds

Epifluorescence and scanning electron microscopy (SEM)

Fresh sludge samples (50 µL) were stained with Live/Dead™ (Backlight, L-13152, Molecular Probes, Europe) staining solution for 15 – 30 minutes, and subsequently analysed with epifluorescence microscopy using a Axioskop II plus microscope (Zeiss, Germany) equipped with FLUO3 and CY3 filters for separating live (green) and dead (red) stained bacteria respectively. Digital images were captured with a 1-CCD camera using

HPDC software (Hamamatsu Photonics GmbH, Hersching, Germany), and separate ‘live’ and ‘dead’ images from the exact same position were merged using the capturing software. Images were further analysed particle size distribution with digital image analysis (DIA) software (Olympus MicroImage 4.0 (Olympus Optical Co. (Europe))). Dried sludge (28 °C, 14 days) samples were gold-coated and analysed with scanning electron microscopy (SEM) using a JSM 840 instrument (JEOL LTD, Tokyo, Japan).

RESULTS

Reactor performance

After a two-week start-up period, a further two weeks were required for the establishment of optimal reactor performance, defined by the removal of about 80 % of the soluble Ca^{2+} from the wastewater, within eight hours retention time. Anaerobic effluent from a full-scale UASB reactor was used as influent, with considerable variations in most of the wastewater parameters (Table 7.1). Table 7.1 also shows the weekly average effluent data for the two BCC reactors from start-up over a six-week period. Three operational periods are distinguished (week 1, week 2 and week 3 – 6), based on the applied hydraulic retention time (HRT) and urea addition. The first week and second week showed high calcium removal efficiencies, which can be attributed to the high urea load and long hydraulic retention time (HRT) used during this period. After normalising the HRT (week 3), a decrease in reactor efficiency (calcium removal) was first observed, partly due to an accidental under-dosage of urea (Table 7.1). However, the overall performance evolved positively during the subsequent four weeks until a period of optimal precipitation efficiency was established and maintained (week 6, Table 7.1). The total COD decreased with respect to the influent, and this decrease was similar for all three periods. This is, however, ascribed to the sedimentation and co-precipitation of organic mater (e.g. paper

fibres) in the BCC reactors, rather than to microbial degradation. Nitrogen (Kjeldahl and ammonium) increased proportional to the urea additions during the respective periods, while nearly no soluble phosphate could be detected in the effluent. Soluble magnesium removal was not detected in any of the time periods. Week 6 represents the data for optimal performance of the BCC reactors, showing a reasonable low pH, and high calcium removal, both total and soluble.

Table 7.1. Weekly average values for some of the important BCC reactor effluent parameters. All data points except 'pH' in $\text{mg}\cdot\text{L}^{-1}$.

	Influent	Week 1	Week 2	Week 3	Week 4	Week 5	Week 6
UREA	n.a.	1 $\text{g}\cdot\text{L}^{-1}$	0.5 $\text{g}\cdot\text{L}^{-1}$	0.5 $\text{g}\cdot\text{L}^{-1}$	0.5 $\text{g}\cdot\text{L}^{-1}$	0.5 $\text{g}\cdot\text{L}^{-1}$	0.5 $\text{g}\cdot\text{L}^{-1}$
HRT	n.a.	24 h	24 h	8 h	8 h	8 h	8 h
pH	7.1 – 7.4	8.6 ± 0.2	8.3 ± 0.1	7.8 ± 0.2	7.6 ± 0.1	7.3 ± 0.1	7.5 ± 0.1
COD_t	780 – 1200	632 ± 46	597 ± 0	625 ± 6.5	568 ± 1	680 ± 10	695 ± 4
Kjeldahl-N	15 – 48	503 ± 2	286 ± 9	170 ± 6	261 ± 2	250 ± 4	257 ± 10
NH₄⁺-N	4 – 25	486 ± 10	272 ± 9	155 ± 5	236 ± 2	228 ± 2	219 ± 1
P_{total}	15 – 65	7 ± 1	10 ± 4	5 ± 1	3 ± 1	4.5 ± 0	4 ± 0
P_{soluble}	1 – 12	0 ± 0	4 ± 3	3 ± 0	0 ± 0	0 ± 0	2 ± 1
Ca²⁺_{total}	480 – 1000	97 ± 48	54 ± 8	171 ± 23	134 ± 20	185 ± 23	79 ± 11
Ca²⁺_{soluble}	460 – 820	14 ± 5	26 ± 0	159 ± 19	118 ± 17	75 ± 5	79 ± 4
Mg²⁺_{total}	40 – 68	32 ± 2	36 ± 2	57 ± 19	38 ± 2	35 ± 0	33 ± 1
Mg²⁺_{soluble}	34 – 40	32 ± 3	36 ± 2	39 ± 2	36 ± 1	34 ± 0	34 ± 0

n.a. = not applicable

The evolution in reactor performance was also evident from the evolution of urease activity in the reactors (Figure 7.1). The repetitive addition of urea to the inoculum sludge resulted in about a 10-fold increase of the urease activity. At week 1, the urease activity was about $7.2 \text{ mg urea}\cdot\text{L}^{-1}_{\text{reactor}}\cdot\text{h}^{-1}$, meaning that at least 70 h would be required for the hydrolysis of $500 \text{ mg urea}\cdot\text{L}^{-1}_{\text{reactor}}$. At week 6, a urease activity of about $100 \text{ mg (= 1.68 mmol) urea}\cdot\text{L}^{-1}_{\text{reactor}}\cdot\text{h}^{-1}$ was detected, meaning that less than 5 h would be required for complete urea hydrolysis. Whilst numerous bacteria have the urease gene, it is clear that the expression thereof in the activated sludge inoculum was insufficient with regards to

BCC requirements, and that stimulation of this is essential to the optimal working of the reactors.

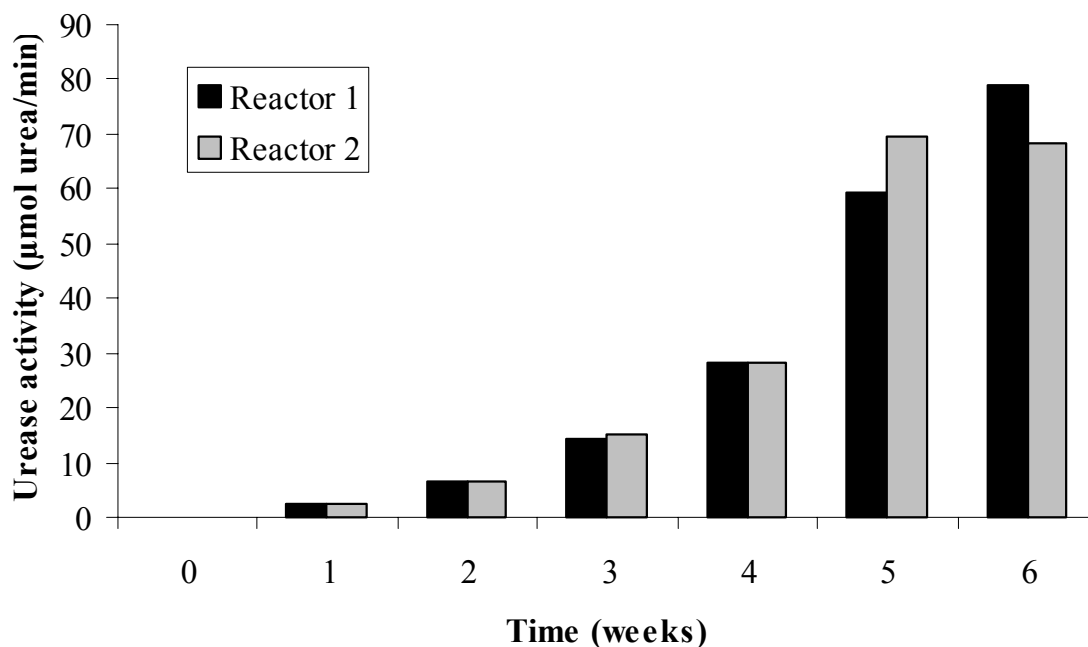


Figure 7.1. Evolution of effective urease activity ($\text{mg urea} \cdot \text{L}^{-1} \text{ reactor} \cdot \text{h}^{-1}$) in the two duplicate BCC reactors ($1 \text{ mmol urea} = 60 \text{ mg}$)

Single reactor cycle analyses

CaCO_3 precipitation from the wastewater was directly proportional to urea hydrolysis, but not dependant on the pH. Figure 7.2a and 7.2b show the evolution of pH, Ca^{2+} , and TAN within a single reactor cycle during a period of optimal performance (week 6; Table 7.1), with urea (Figure 7.2a) and without urea addition as negative control (Figure 7.2b). Ca^{2+} precipitation in the absence of urea addition was limited to about 15 %, while hardly any pH shift or TAN evolution is evident in the control cycle (Figure 7.2b). In the reactor cycle with urea addition (Figure 7.2a), visible pH fluctuations are apparent, but it should be noted that the pH of the bulk solution did not exceed 7.5 during the entire precipitation reaction. NH_4^+ -N evolution proceeded rapidly (3 h) to at least 95 % relative to the initial urea addition, and Ca^{2+} precipitation was about directly proportional to urea hydrolysis.

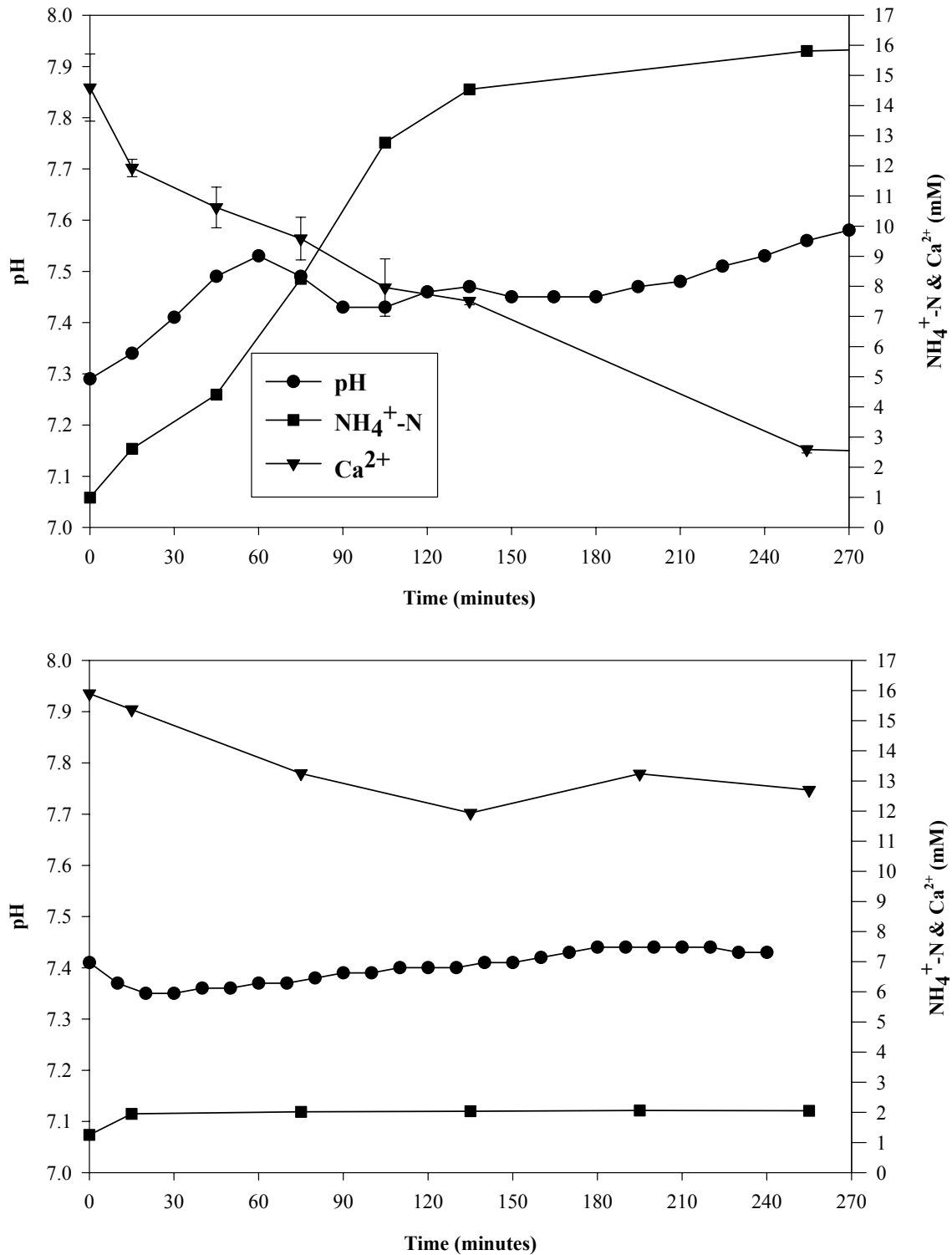


Figure 7.2. Evolution of pH (●), TAN (mM NH₄⁺-N) (■), and Ca²⁺ (mM) (▼) in a single reactor cycle, with (a) and without (b) urea addition.

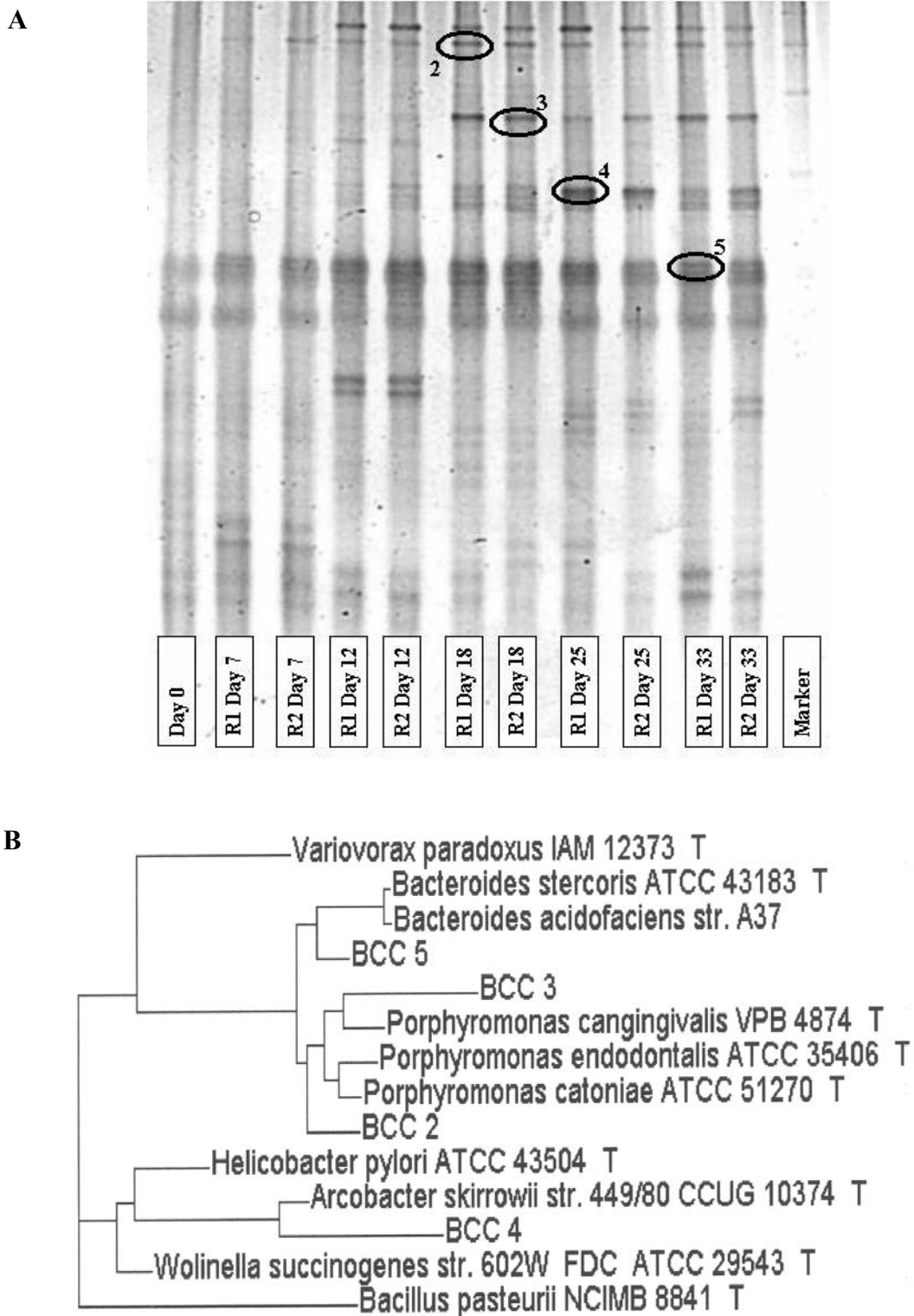


Figure 7.3. (a) DGGE separation of 16S rDNA amplified from the reactors; excised and sequenced bands are indicated (2 – 5). (b) A phylogenetic tree constructed with partial 16S rDNA sequences (BCC 2 – BCC 5). Sequence analysis was done as described in the text; only 94 base positions were included in the calculations.

DGGE analysis and sequencing

The microbial community of the reactors stabilized within a three-week period to a community with about 15 dominant species detectable by DGGE. Especially in the upper half of the gel, a clear development of bands can be seen, representing bacteria that became dominant in time. This development was rapid and persistent from the first week onwards, very few changes occurred in the composition of the dominant bacteria of both reactors. The changes in the bottom of the gel were not further analysed since the appearing and disappearing bands could not be linked to the performance of the reactor. This trend was evident in both reactors. The five major bands were excised but clean sequences could only be obtained for four of the five bands (Figure 7.3a). The closest relatives of cultured bacteria to the excised sequences were confirmed with BLAST software to be *Porphyromonas endodontalis* L16491 (Paster *et al.*, 1994) (BCC 2), *Porphyromonas cangingivalis* g577600 (Collins *et al.*, 1994) (BCC 3), *Arcobacter skirrowii* L14625 (Stanley *et al.*, 1993) (BCC 4), and *Bacteroides stercoris* g1325946 (Ruimy *et al.*, 1996) (BCC 5) (Figure 7.3b).

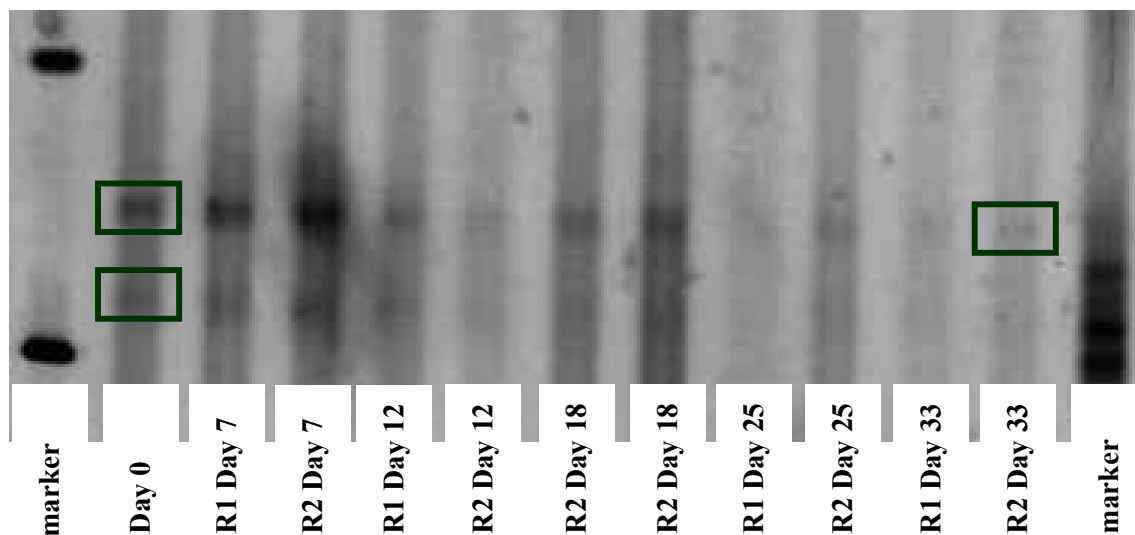


Figure 7.4. DGGE separation of urease rDNA amplified from the reactors; excised and sequenced bands are indicated.

The urease-PCR-DGGE analysis detected only the amplification of two bands in the inoculum sludge, with one of these disappearing subsequently, leaving only a single, dominant band for all the remaining time points in both reactors (Figure 7.4). Both these bands were subsequently sequenced, translated to an amino-acid sequence, and compared with one another and with protein sequences from known isolates. The two bands were clearly different from one another, showing 77 % nucleotide alignment, and only 61 % alignment (76 % positives) in their amino acid sequences. Both bands corresponded with previously sequenced urease genes. The first displayed maximum homology (88 % identity; 92 % positive) with urease genes from the cyanobacteria *Synechococcus sp.* AF035751 (Sakamoto *et al.*, 1998) and *Anabaena variabilis* AF065139 (Collier *et al.*, 1999). The dominant band displayed maximum similarity (64 % identity; 78 % positive) with urease genes from *Sinohizobium meliloti* S69145 (Miksch *et al.*, 1994) and *Yersinia pestis* AF095636 (Sebanne *et al.* 2001).

Sludge analyses

A calcareous sludge developed in the reactor, which functioned as niche for the microbial species, and crystal nucleation sites for CaCO_3 precipitation. A significant increase in TSS was seen, while the VSS remained more or less stable (Table 7.2). The inoculum sludge had a sludge-settling rate (SSR) of about $2 \text{ m}\cdot\text{h}^{-1}$ and the calcareous sludge displayed an SSR increase up to $9 \text{ m}\cdot\text{h}^{-1}$ after six weeks. The SVI portrays the compactability of this calcareous sludge (Table 7.2), and together with the SSR, it shows the calcareous sludge to have excellent settling properties. XRD analysis of the dried sludge revealed a homogenous mineral fraction comprising almost entirely of calcite, with only trace amounts of fluorite (CaF_2) (Figure 7.5). Figure 7.6a and 7.6b show the transformation of the inoculum sludge into calcareous sludge over the experimental period, with the crystalline nature of the BCC sludge being evident from the light microscopy image (Figure 7.6b). Digital image analysis of particle size distribution showed approximately 65 % of the sludge particles having a radius of less than $100 \mu\text{m}$ (data not shown). Commercial Live/Dead reagents stain bacteria with intact cellular membranes (thus alive) green, and cells with damaged membranes red. The Live/Dead staining shows that the surface of the sludge particles is colonised with living bacteria, while dead bacteria can

also be seen (Figures 7.6c – 7.6f). Scanning electron microscopy (SEM) images of the calcareous sludge revealed sludge flocs, which are clearly crystalline in nature, yet, not entirely dense or solid (Figure 7.7a). In fact, a complex, floc structure is evident, including multiple channels and pores. The fossilised remains of bacterial cells, mostly rod-shaped, can be seen as well as large angular crystals (Figure 7.7b).

Table 7.2. Average values for BCC reactor sludge parameters

	Inoculum	Week 2	Week 4	Week 6
TSS ($\text{g}\cdot\text{L}^{-1}$)	24.7	55,0	110,0	152,0
VSS ($\text{g}\cdot\text{L}^{-1}$)	4.9	6.4	4,0	7.2
VSS/TSS (%)	20,0	11.6	3.6	4.7
SVI (mL)	12,0	n.d.	n.d.	2.3

SVI = volume (mL) of 1 g TSS after 30 minutes sedimentation

n.d. = not determined

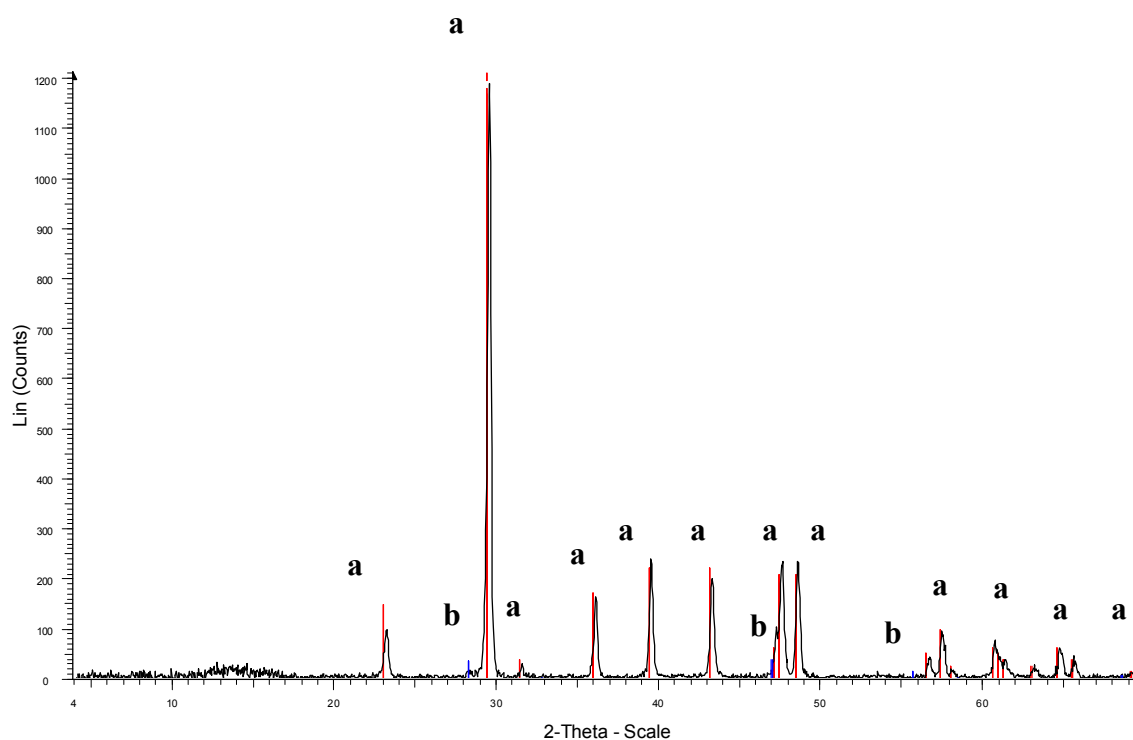


Figure 7.5. An example of the XRD data from the reactor sludge. The crystal forms are indicated: a = calcite, b = vaterite.

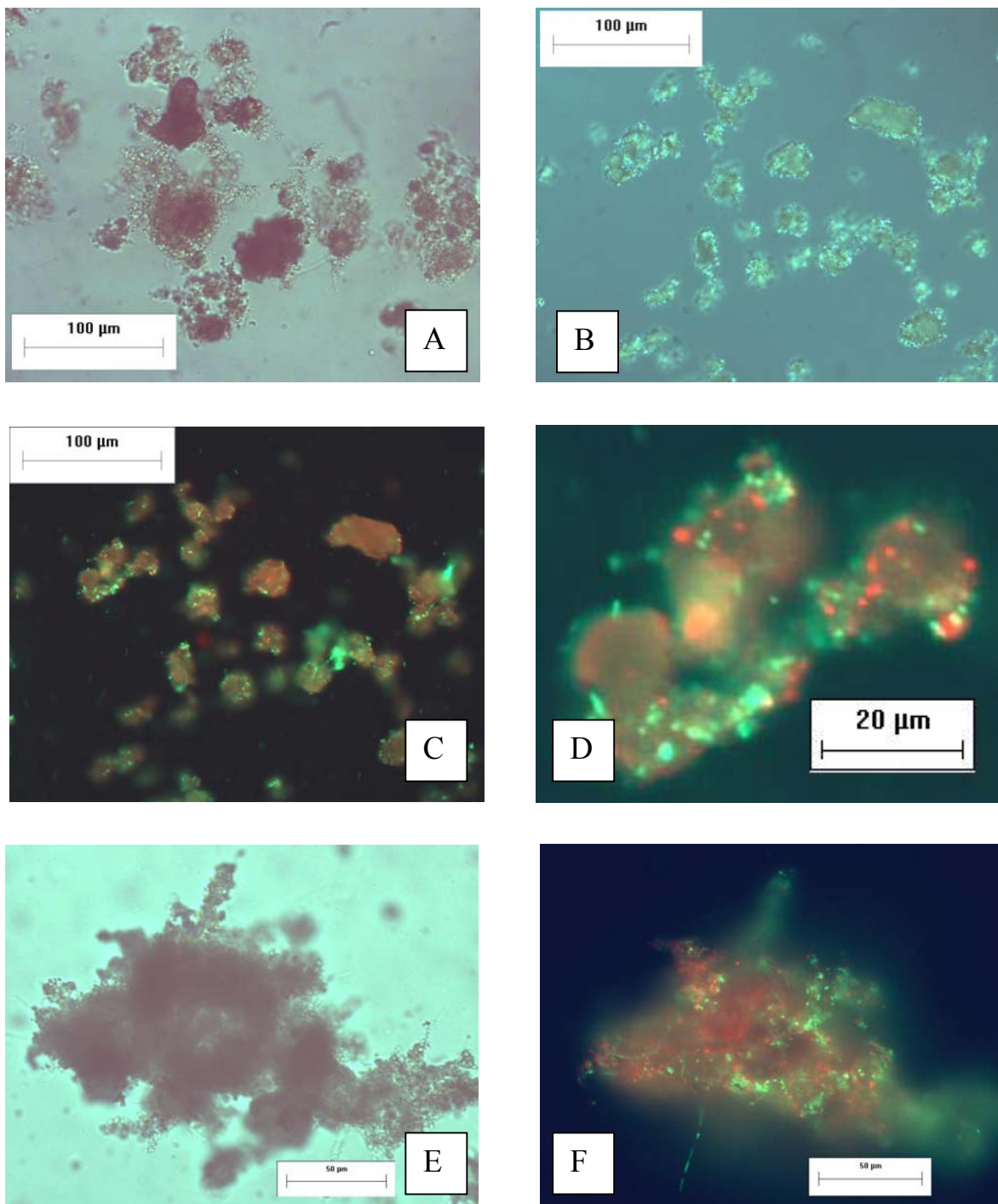


Figure 7.6. Light microscopy images showing the evolution of the organic inoculum sludge (a) to a homogenous calcareous sludge (b); and a merged Live/Dead stained epifluorescent image (c) together with enlargement (d) of the calcareous sludge showing the crystalline flocs colonised with living bacteria as well as the remains of dead bacteria, also shown in (e) and (f).

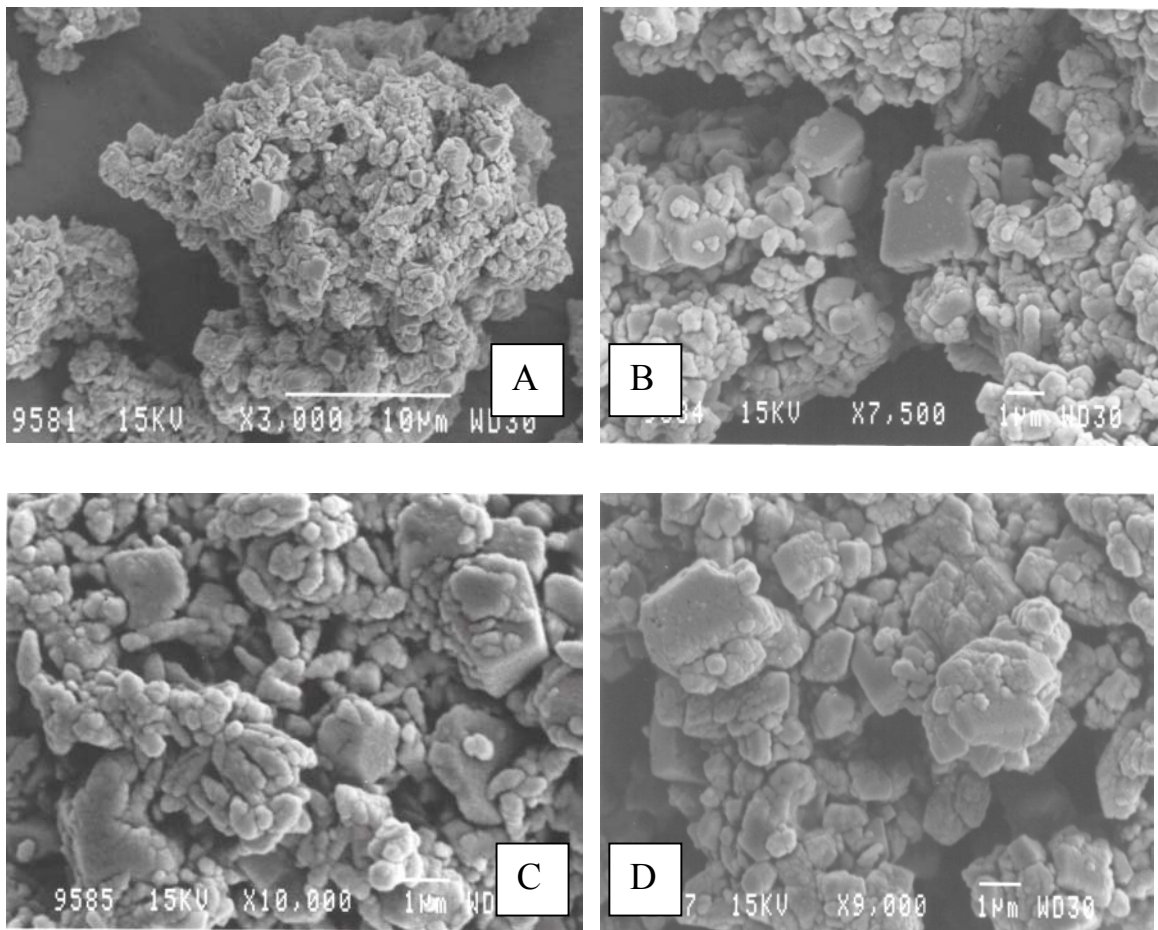


Figure 7.7. SEM photographs of the calcareous sludge flocs, showing channels and pores in the complex floc structure (a) made up by angular crystallites as well as calcified bacterial bodies (b - d).

DISCUSSION

The emphasis of this work was on the characterisation of the bio-catalyst in a bio-catalytic calcification (BCC) reactor in terms of composition and function. A detailed description of BCC reactor performance operational parameters and economic perspectives, is presented

in Chapter 5 and Chapter 6. In these studies it was established that the two main parameters of critical importance for optimal working of BCC reactors are (1) a high actual ureolytic capacity, and (2) the presence of crystal nucleation sites. It was opted to inoculate the reactors with activated sludge from the wastewater plant from the industry, which represents organisms autochthonous to the wastewater being used. Moreover, the sludge already contained some CaCO_3 particles (Figure 7.6a), thus being a possible starting point for nucleation sites to develop. Although the urease enzyme is common to many microorganisms (Reed *et al.*, 2001; Mobley and Hausinger, 1989), Table 7.1 shows that several weeks were still required before optimal calcium removal under standard operational conditions could be achieved. This evolution was directly ascribed to the evolution of the two main parameters mentioned above: the urease activity and the crystal nucleation sites.

Crystal nucleation site development was not specifically quantified, but the definitive increase in TSS (Table 7.2), coupled with the identification of this inorganic component as CaCO_3 (specifically calcite) showed that this was indeed occurring. Considering the wastewater composition, mineral phases that could have been expected include struvite (NH_4MgPO_4), magnesium-calcite and CaCO_3 (Doyle and Parsons, 2002). That only CaCO_3 was detected with XRD is probably due to the large amounts in which this mineral was formed. Of the five known CaCO_3 polymorphs, only the stable forms (aragonite and calcite) could reasonably be expected to form. While aragonite is often detected during biological precipitation, previous studies concerning ureolytic MCP also identified the main crystal type as calcite (Kawaguchi and Decho, 2002; Bachmeier *et al.*, 2000; Bang *et al.*, 2001; Stocks-Fischer *et al.*, 1999). Fluorite precipitation has been reported previously in association with microbial urea hydrolysis in dental plaque biofilms (Wong *et al.*, in press). The presence of trace amounts of fluorite in the BCC sludge is ascribed to impurities in the wastewater. The fact that the BCC reactor system utilises self-developed crystal nucleation sites, rather than commercial alternatives (e.g. silver sand), saves significantly on operational (purchasing) and transport costs. It does, however, also require that this process be studied in detail, so that it can be controlled properly under operational conditions.

The evolution of urease activity was specifically measured, and displayed a 10-fold increase over the experimental period (Figure 7.1). Since the sludge volume was more or less maintained, this increase can be ascribed to the evolution and domination of urease positive micro-organisms in the reactors. Bacteria are known to hydrolyse urea for the purpose of: (1) increasing the environmental pH (Burne and Marquis, 2000; Stocks-Fischer *et al.*, 1999), (2) utilising it as a nitrogen source (Burne and Chen, 2000), and (3) using it as a source of energy (Mobley and Hausinger, 1989). The increase of environmental pH was in our experiments not a likely physiological incentive for the bacteria. The use of urea as nitrogen source is possible, but does not explain the excess amounts which are hydrolysed. Indeed, Table 7.1 clearly shows that most of the hydrolysed urea is converted and released as TAN. This extended hydrolysis thus may relate to the fact that certain organisms utilise urea hydrolysis as a mechanism to generate ATP (Mobley and Hausinger, 1989). In this reaction, ammonia from urea becomes protonated intracellularly, yielding ammonium in the cytoplasm. This results in a pH gradient formation, energisation of the cell membrane, and ATP synthesis. This unique mechanism has been described for a variety of urease positive microorganisms including *Ureaplasma urealyticum* and *Bacillus pasteurii* (Smith *et al.*, 1993; Jahns, 1996; Mobley and Hausinger, 1989). This mechanism would not only be ecologically beneficial to the microbial population, but may also be a key factor in BCC reactor operation and functioning. This mechanism will provide certain bacteria with the ability to survive and rapidly proliferate, thereby becoming the selective factor in the development of the BCC reactor microbial population.

A dynamic evolution in the BCC reactor population was indeed witnessed. Both the *Bacteroides* sp. and the *Porphyromonas* sp. belong to the *Bacteroidales* order, while *Arcobacter* sp. are members of the epsilon subdivision of Proteobacteria. These all represent anaerobic bacterial species, typical to dental cavities and the gastro-intestinal tract (Paster *et al.*, 1994; Stanley *et al.*, 1993). It is not surprising that anaerobic bacteria dominate in the BCC reactors, since anaerobic (UASB) effluent was used as wastewater and the reactors were not specifically aerated. Though these species represent some of the most dominant bacterial species in the BCC reactors, it does not necessarily imply that these are the causative organisms of the hydrolysis/precipitation process. In fact, a comprehensive literature search could not specifically link any of these species with urease

activity, ATP generation through urease activity, or calcium carbonate precipitation. Concerning the latter point, the view is taken in this study that ureolytic MCP apparently does not involve specific calcium precipitating bacteria, but rather microorganisms that selectively express their urease genes under given environmental conditions.

Bacterial urease genes are known to differ considerably in genetic composition, thereby validating the molecular analysis thereof (Mobley and Hausinger, 1989). We attempted to use a new DGGE-based protocol for detecting the urease gene diversity in the microbial population of the reactors. The *UreC* PCR reaction was previously used to differentiate between urease genes from different microbial species (Reed, 2001). Differences in the protein sequences of the detected urease PCR-DGGE bands did show that it was possible to distinguish between different urease genes from environmental samples. Striking was the low diversity of the urease gene fragment. Apparently only one type of urease was dominating the microbial community and probably this type was responsible for the conversion of the urea. The DGGE of the 16S rDNA showed several new bands while the calcium precipitation rate was enhanced, so it is possible that different bacteria possess the same urease gene, or that only one of these strains were responsible for the hydrolysis-precipitation reaction. It is also known that urease genes can be plasmid encoded (Dupuy *et al.*, 1997), and that horizontal gene transfer between the different sludge species could have occurred.

The basic biochemical mechanism of ureolytic MCP is that bacterial urea hydrolysis increases both the pH and the DIC of an environment, thus favouring precipitation (Douglas and Beveridge, 1998; Castanier *et al.*, 1999). Considering the pH (7.35), alkalinity (35 meq·L⁻¹), and Ca²⁺ concentration (15.4 mM) of the anaerobic effluent used in these experiments, over-saturation of CaCO₃ can be roughly calculated as follow (Equations 7.6 and 7.7; Van Haandel and Lettinga, 1994):

$$[\text{CO}_3^{2-}] = \text{Alk}_e \cdot K_2 / [\text{H}^+] = \text{Alk}_e \cdot 10^{(\text{pH} - \text{p}K_2)} = 0.035 \times 10^{(7.35 - 10.33)} = 3.67 \times 10^{-5} \quad (\text{Eq. 7.6})$$

$$[\text{Ca}^{2+}] \cdot [\text{CO}_3^{2-}] / K_{\text{sp}} = (5.64 \times 10^{-7}) / (3.8 \times 10^{-9}) = 149 \quad (\text{Eq. 7.7})$$

$$[\text{Ca}^{2+}] \cdot [\text{CO}_3^{2-}] / K_{\text{sp}} = (5.64 \times 10^{-7}) / (2.0 \times 10^{-7}) = 2.8 \quad (\text{Eq. 7.8})$$

This suggests about 0.1 mM Ca^{2+} to be the maximum tolerable concentration of Ca^{2+} before the onset of precipitation. However, as Figure 7.2b indicates, Ca^{2+} precipitation in the absence of any urea addition is only limited to about 15 %. This is partially explained by the complex nature of real wastewater, for instance the binding of calcium ions to organic matter. Van Haandel and Lettinga (1994) reported experimental findings which showed that the K_s values for CaCO_3 in anaerobic effluent could be as low as 2.0×10^{-7} . Using this value in the calculation above, the corresponding over-saturation is only 2.8 times, suggesting at least 5.44 mM Ca^{2+} remaining in solution (Equation 7.8). Hardly any pH shift is evident in the control cycle. In the reactor cycle with urea addition (Figure 7.2a), pH evolution is governed by the buffer capacity of the wastewater (primarily bicarbonate), as well as by a possible pH increase from urea hydrolysis (Equations 7.3 – 7.5), and by a possible pH decrease from CaCO_3 precipitation (Equations 7.1 and 7.2). Although visible pH fluctuations are apparent, it should be noted that the bulk solution pH hardly exceeds 7.5 during the entire precipitation reaction. NH_4^+ -N evolution confirmed the high ureolytic activity in the reactors: almost all of the added urea was converted completely within about 3 h to NH_4^+ . Typical Michaelis-Menten enzyme kinetics suggest a very high substrate affinity. About 8 mM urea was hydrolysed, while about 12.5 mM Ca^{2+} was precipitated (Figure 7.2a), of which at least 3 mM could be attributed to chemical precipitation (Figure 7.2b). It is thus apparent that Ca^{2+} precipitation is directly proportional to urea hydrolysis, even though little correlation between the pH and the Ca^{2+} evolutions could be detected.

Figure 7.2 linked the biological process (urea hydrolysis) proportionally and in time to the CaCO_3 precipitation event. The Live/Dead staining showed that the surface of the sludge particles, which represent crystal nucleation sites, was colonised with living bacteria, as well as showing some remains of dead bacteria (Figures 7.6c - 7.6f), thereby showing that the calcareous sludge provides a niche for bacteria to attach and proliferate. This was confirmed with SEM analysis. Though intact bacterial cells could not be detected because the dry sludge was viewed without any additional ethanol critical point drying, the fossilised remains of bacterial cells, mostly rod-shaped, could be seen (Figure 7.7). These SEM images displayed some resemblance to SEM images of MCP from natural

environments (Wright, 1999). Cellular incrustation could have involved specific precipitation mechanisms on cellular level, such as the functioning of bacteria as crystal nucleation sites (Stocks-Fischer *et al.*, 1999; Schultze-Lam *et al.*, 1996), and calcium concentration by bacteria (McConnaughey and Whelan, 1997). The SEM analysis also suggested that the precipitation event might well lead to physical capturing and eventual die-off of the organisms. Southam (2000) suggested that cell-surface mineralisation leads to die-off of bacteria, due to the limitation of nutrient and proton transport. It is well documented that bacteria are often captured and fossilised during the precipitation reaction (Trewin and Knoll, 1999). Recently, this phenomenon sparked a debate as to whether mineral precipitates on the ALH84001 meteorite could represent past-life in outer space (McKay *et al.*, 1996).

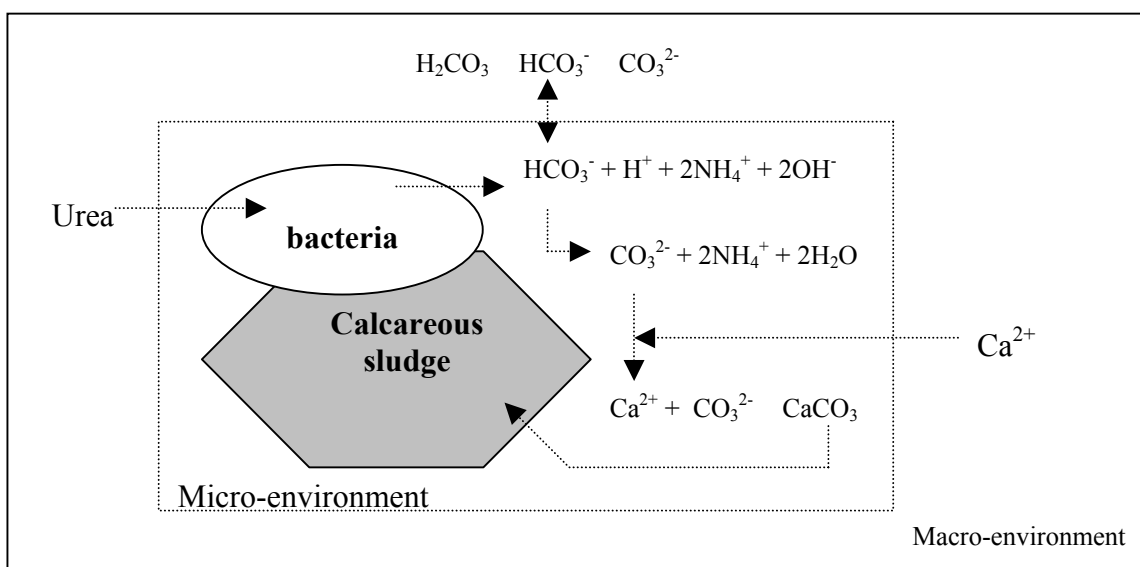


Figure 7.8. Schematic presentation of the hypothesised chain-of-events for ureolytic microbial CaCO_3 precipitation in the BCC reactors as a result of the localisation of ureolytic bacteria on the surface of the crystal nucleation sites.

The above results showed that the BCC reactors require about 4 – 6 weeks start-up before optimal performance is reached, mainly depending on the development of a high urease activity and sufficient crystal nucleation sites. During optimal performance, CaCO_3 precipitation is directly proportional to urea hydrolysis, which is an intracellular

biochemical process. It was furthermore shown that viable microorganisms inhabit the surface of the calcareous sludge flocs, which in this case serves as crystal nucleation sites in the precipitation process. It is proposed that this co-localisation of the biochemical catalysts and the crystal nucleation sites results in the formation of a microenvironment favouring CaCO_3 precipitation (Figure 7.8).

As a result, localised elevated pH levels would cause a shift in the bicarbonate equilibrium, resulting in CO_3^{2-} formation at cellular level, which immediately precipitates as CaCO_3 , because of the presence of crystal nucleation sites. This would explain the near absence of any significant bulk solution pH increase (Figure 7.2). Calcium required for precipitation would be in constant supply as a result of a continuous concentration gradient which results from the precipitation reaction.

CONCLUSION

In conclusion, BCC reactors, combining autochthonous ureolytic bacteria on calcareous sludge flocs, present an efficient process for calcium removal from industrial wastewater. The localisation of the bio-catalyst on the crystal nucleation sites (CNS) allows for the possibility of micro-environment chemistry, which could be a key factor in future implementations of this process. The high degree of adaptability of this process makes BCC reactors an attractive technology for wastewaters elevated in heavy metals, phosphate and radionuclides.

ACKNOWLEDGEMENTS

This research was sponsored by VPK (Oudegem, Belgium), AVECOM nv (Belgium) and by the project grant G.O.A. (1997-2002) of the "Ministerie van de Vlaamse Gemeenschap, Bestuur Wetenschappelijk Onderzoek" (Belgium), and by an equipment grant (epifluorescence microscope) of the Flemish Fund for Scientific Research (FWO-Vlaanderen). Special thanks to Els Jolie and Greet Vandevelde for analytical measurements, and Sofie Dobbelaere, and Thomas Vande Sijpe for critical reading of this manuscript.

[Link to Contents](#) [Link to Chapter 8](#)

GENERAL DISCUSSION AND PERSPECTIVES FOR FUTURE RESEARCH

A GLOBAL PERSPECTIVE ON MICROBIAL CaCO_3 PRECIPITATION

Global warming is by far the largest modern day crisis facing mankind. To meet this challenge, a lot of effort has been made over the last few decades towards the accurate quantification of global carbon stocks, and thorough understanding of the carbon cycle. Within this context, mineral carbonate represents an extremely large pool of sequestered carbon (Lal *et al.*, 2000). Microbiological influences on the precipitation of mineral carbonates have become more and more recognised lately as an integral part of carbon cycling, and, judging from initial reports, the global impact of these processes are probably vastly underestimated (Braissant *et al.*, 2002, Ferris *et al.*, 1994, Castanier *et al.*, 1999). Whalen *et al.* (2002) even suggested that apart from contributing significantly to carbon cycling, biological precipitates could be used as indicators of global change, or other environmental catastrophes. This has been the first major point to cause somewhat of an evolution in the study field of microbial mineral precipitation, away from the predominantly geological characterisation of natural precipitates (Drew *et al.*, 1914).

The second turning point was the study by McKay *et al.* (1996), which suggested a possible connection between carbonaceous deposits on the ALH84001 Martian meteorite and microbiological life in outer space. The impact of this was enormous: even if one were to disregard the notion that it actually presents proof of extraterrestrial life – a heated debate which is still continuing - it still offered a novel tool to study past-life on earth. The key to this is of course whether microorganisms are capable of producing unique, recognisable mineral “fingerprints”, and then also to understand the link between the precipitates, the environmental conditions under which they were deposited, and the microorganisms and biochemical pathways involved. With regards to the meteorite: that particular study have long since evolved to focus on more complex bio-minerals, notable magnetite, but carbonate minerals still remain the base model thereof. The result of all this is that recent literature has indeed focussed more on the role of microbial mineral formation in the eventual production of microbial fossil records (Trewin and Knoll, 1999; McGenity and Sellwood, 1999). In perhaps an even more far-reaching turn-of-events, Vreeland *et al.* (2000) opened the proverbial can-of-worms with their finding that bacterial spores survived inside minerals (in their case the mineral was halite) for millions of years. This will undoubtedly have something of a Jurassic-park effect on future work concerning natural precipitates!

A third factor which has added to the resurging interest in microbial precipitation is the emergence of novel biotechnologies making use of these processes (Ferris and Stehmeier, 1993). It was stated above that the natural impacts of MCP are perhaps vastly underestimated, and the same view is taken concerning the potential impacts of MCP within anthropogenic settings. It is opined herein, that the role of MCP in biofilm formation, and the subsequent impact thereof on industrial processes, has been as neglected as perhaps microbial corrosion of concrete and stainless steel has been in the past (Kielemoes *et al.*, 2002; Monteny *et al.*, 2000). More importantly, though, is the potential for industrial applications which this natural process offers. The two primary points of focus up to now have been the restoration of building structures (sandstone and concrete), and the mineral plugging of groundwater flow (Stocks-Fischer *et al.*, 1999; Ferris and Stehmeier, 1993). But these are only the first steps in the development of many potential applications, which will be discussed later on in this chapter.

WHY DID WE STUDY MCP ?

The study presented here originated from a first investigative study concerning possible microbial remedial technologies for global warming, specifically gaseous carbon dioxide (CO₂) trapping and removal. Apart from the fact that biological mineral precipitation was a fascinating natural phenomenon to study as such, the possibility of capturing and storing CO₂ in mineral form presented a very promising approach to this problem. Although this concept perhaps precedes its time somewhat, that view is still held, and some perspectives on this are also presented later on.

The identification of a local industry with specific problems concerning calcium-rich wastewater, presented a more immediate problem to focus on. Together with the fact that the wastewater industry entails by far the largest industrial market for biotechnological applications, it became the primary challenge of this work. As is the case with any young research field, it presents the obvious problem of where to start, and what to focus upon. The study was narrowed down to ureolytic CaCO₃ precipitation, for the following reasons:

- (1) Urea hydrolysis satisfies simultaneously both the requirements for CaCO₃ precipitation: a pH increase and a DIC increase.
- (2) Urease-positive bacteria are very common, which broadens the application and integration possibilities, and allows for *in situ* treatment with autochthonous bacteria.
- (3) Urea is a natural, cheap and easily available chemical, leaving no hazardous by-products upon hydrolysis.

The study was furthermore separated into two sections. The first part (Chapters 3 and 4) dealt with some of the fundamental principles governing the precipitation process, and the second part (Chapters 5 to 7) dealt with the development of a biotechnology for the removal of calcium from wastewater using ureolytic MCP.

PERSPECTIVES ON THE MAJOR FINDINGS

Three major findings dominated the results from Chapter 3, concerning the fundamental mechanisms of ureolytic MCP.

(1) The observation of strain-specific calcification

Strain-specific calcification refers to the ability of different bacterial strains/species to produce recognisably different CaCO₃ precipitates when cultivated under exactly similar conditions. In our case, “different” did not relate to the crystal phase (e.g. calcite, aragonite, vaterite), but in fact to visual morphological differences. Single colonies of bacteria, precipitating CaCO₃ within, were used to study this phenomenon. This approach had the advantage that it allowed one to study the reaction within a unique micro-environment created by the bacterial colonies (Rivadeneira *et al.*, 1994). It was convincingly showed that the biochemical reaction (urea hydrolysis) was predominantly responsible for the observed differences. Nonetheless, one can not help but recognize that a missing element from this study was an assessment of the role of the organic matrix in the different crystal formations. The work of Hunter (1996), Kawaguchi and Decho (2002), and Brown *et al.* (2002), discussed in Chapter 2, seems to suggest that this is a key factor in species-specific precipitation. The importance of this finding is that species-specific precipitation could be a useful tool in the study of microbial fossil records.

(2) The apparent detection of urease isozymes

To our knowledge, denaturing gradient gel electrophoresis (DGGE) was used for the very first time to analyse diversity in urease genes. This technique detected multiple bands for single strains, which suggested the presence of urease isozymes within a single organism. This is extremely significant, since Burne and Chen (2000) recently remarked that although urease isoforms within single organisms are known, no molecular explanation for this has yet been provided. Prof. Robert Hausinger¹ shared this view during personal communication (see also Mobley and Hausinger (1989) and Mobley *et al.* (1995)). The importance of microbial ureases during pathogenesis, including regulation and control of

¹ hausinge@pilot.msu.edu

expression, has been the focus of numerous studies, and this result will undoubtedly have made a positive contribution to the molecular knowledge of these enzymes.

(3) *The effect of soluble calcium on urease activity*

Probably the most significant finding from Chapter 3 was that urease activity of intact live bacterial cells were positively stimulated by the presence of calcium ions, but also that this was only the case for some strains, and not for others. This finding was the first proof of an apparent link between the precipitation-catalysing reaction (urea hydrolysis) and the environment (calcium ions). From this, the suggestion arises that CaCO₃ precipitation is not merely an unrelated side-event resulting from microbial metabolism (Knorre and Krumbein, 2000).

(4) *Calcium toxicity and ATP*

Is microbial calcification an ATP-driven reaction? This should be the essential question arising from Chapter 4. Though much of the work presented in this chapter is based on hypotheses, it was conclusively shown that calcium ions presented a toxic environment to bacteria under alkaline conditions. Precipitation is a direct form of detoxification, since it lowers the calcium concentration and lowers the pH. The link between Chapter 4 and the final result from Chapter 3 is vital: some alkaliphilic bacteria can use urea as source of ATP (Jahns, 1996), and ATP is required for the active expulsion of Ca²⁺ ions from cells (McConnaughey and Whelan, 1997). Thus, under conditions of alkaline calcium stress, some bacteria should respond by displaying increased urease activity to produce ATP for detoxification. This response was indeed witnessed (Figure 3.7).

(5) *Ureolytic MCP can be used for the removal of Ca²⁺ from industrial wastewater*

The primary aim of this research was the development of a reactor-based biotechnological process for the removal of calcium ions from industrial wastewater. This goal was accomplished, of which a pilot plant currently under design and construction bears testimony (Figure 8.1). This is done in collaboration with the companies AVECOM, BIOTIM and VPK. Chapter 5 and 6 showed that bio-catalytic calcification is efficient, easy to operate, easily integrated into a wastewater treatment system, and economically competitive with existing chemical based technologies. The aspect of this process, which

has received the least attention, is the possible drawbacks of this technology, specifically with regards to further downstream wastewater treatment. In this regard, two main problematic areas were identified:

- (1) The need to remove the additional nitrogen load (brought about by the urea hydrolysis). This is undeniably the greatest drawback of the BCC process. However, extensive nitrification/denitrification tests have already been conducted by AVECOM, which showed that limited addition of an extra COD source (either acetate or raw wastewater from the industry) was required to achieve sufficient denitrification. Alternatively, a significant part of the urea dosage can potentially be substituted with aeration (CO_2 stripping) though this would require some further investigation. Nitrogen removal technologies are currently under investigation which perform simultaneous nitrification/denitrification without the need of an additional carbon source.

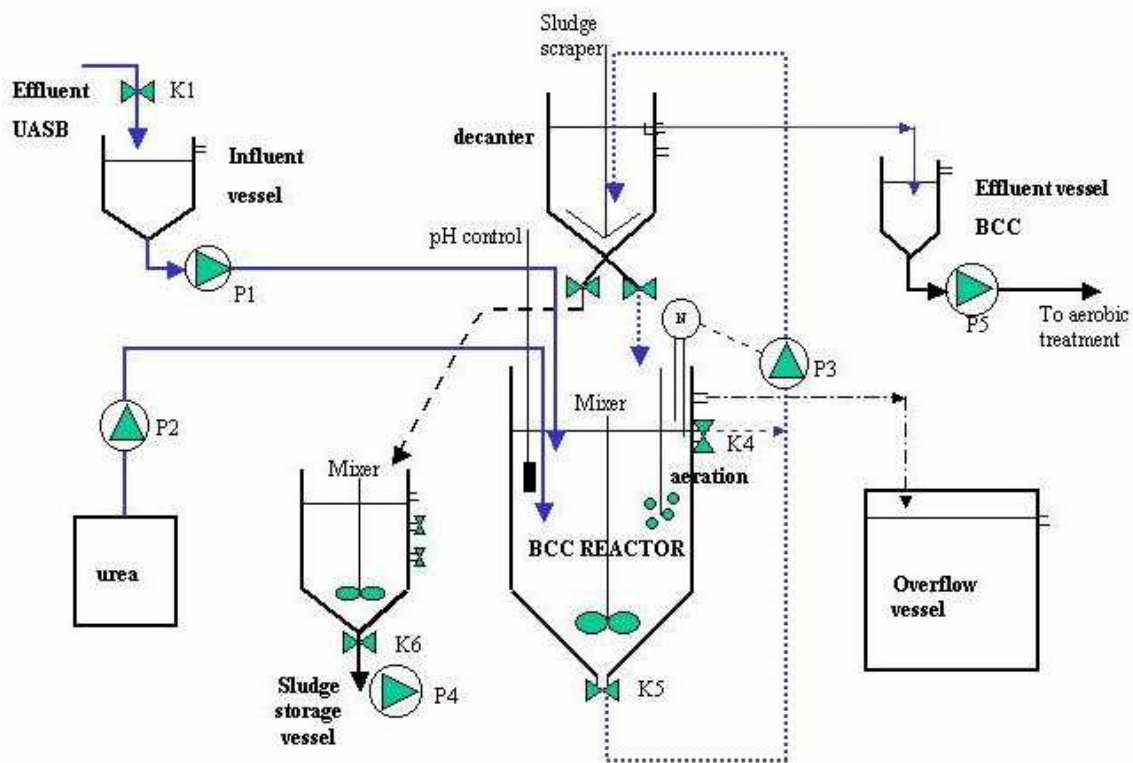


Figure 8.1. The designed proposal of the BCC pilot plant (courtesy of AVECOM N.V.)

- (2) The second possible adverse effect of BCC treatment regards the settling characteristics of the downstream activated sludge system. Currently, a large fraction of Ca^{2+} precipitates in the sludge during aeration, which results in a heavy, compact, and fast-settling sludge. If the BCC system removes the calcium, the sludge characteristics will obviously change. This is an unavoidable event, and only the long-term operation of the pilot-plant will allow sufficient assessment of this.



Figure 8.2. *CaCO₃ scaling-damage on a concrete pipeline which is part of downstream processing of calcium-rich wastewater from a paper-recycling facility.*

(6) *Is the key to the BCC process micro-environment chemistry?*

Chapter 7 took a closer look at the microbiology, biochemistry and ecology of the BCC process. The concluding hypothesis from this chapter is that micro-environment chemistry is driving the precipitation process, and that this is brought about by the fact that the biocatalyst (urea hydrolyzing bacteria) colonise the crystal nucleation sites (calcareous

sludge). In other words, the major components of the crystallisation process is linked in time and space. This could be the essential key advantage of the BCC process above chemical technologies.

BIOTECHNOLOGICAL POTENTIALS FOR MCP

(1) Wastewater treatment

Industries faced with the problem of Ca^{2+} -rich effluents are limited. The first and foremost challenge is therefore the extension of the BCC reactor process towards the removal of other wastewater pollutants. A logic choice would be phosphate, since biological phosphate precipitation as struvite or hydroxy-apatite (HAP) via urea hydrolysis is already well documented (Mobley and Hausinger, 1989) and many industries worldwide are dealing with excess phosphate in wastewater (Jaffer *et al.*, 2002). Moreover, global mineral phosphate stocks are being depleted at an alarming rate, which have resulted in an increased interest in technologies for phosphate recovery (Jaffer *et al.*, 2002). Recovery in one of the mineral forms mentioned above is ideal in this regard, as struvite is recognised as an excellent slow-release fertiliser. An additional advantage is that the added nitrogen would be removed as well, taking much strain of further down-stream processing. A new project along these lines is currently being initiated at LabMET. An interesting alternative potential application field for this process is the selective point-of-source treatment of human urine, which is of specific interest in the development of closed life support systems (CLSS) used for long-term space travel. This process also has a very large potential market in the treatment of wastewater contaminated with various types of “unusual” pollutants. Boughriet *et al.* (2000) saw co-precipitation as an economical tool for the removal of aromatic carboxylic acids, humic and fulvic acids, amino and fatty acids, and divalent heavy metals. The latter has already been investigated by Fujita *et al.* (2001) and removal potential include divalent heavy metals such as Cu^{2+} , Mn^{2+} , Cd^{2+} , Sr^{2+} , UO_2^{2+} , Pb^{2+} to name a few.

(2) Greenhouse gas emissions

On several occasions in this dissertation, reference was made to the possible use of MCP as a novel tool for carbon sequestration. Mineral carbonate presents a more sustainable

sequestration than for example biomass, while it also presents a tradable commodity (Yan, 1999). For CO₂ sequestration, photosynthetic MCP (see Chapter 2 for details) is by far the most interesting option, since this process precipitates CaCO₃ while CO₂ is simultaneously taken up by the precipitating biomass, and double efficiency is achieved this way. A recent American project has focussed on the direct sequestration of CO₂ produced during electricity production. In the proposed system, hot CO₂ gas would be dissolved in water, and treated in a photosynthetic reactor using cyanobacteria from a thermal hot-spring, which are of course adapted to hot CO₂-rich environments (Arp *et al.*, 1999). Microbial driven calcification is also a very common phenomenon in thermal hot-springs (Arp *et al.*, 1999), and the combination of this process with the above stated system could offer a significant optimisation potential. Monger and Gallegos (2000), however, raised a significant point concerning CO₂ sequestration through CaCO₃: only if the calcium used during the precipitation is not directly derived from carbonaceous minerals, is the sequestration meaningful. Otherwise, no net CO₂ removal can be obtained.

(3) Surface precipitation: nanotechnology potentials

Many multicellular organisms in nature produce hard minerals such as teeth and bones and shells, using inorganic minerals to build highly organised, highly controlled, complex structures. These bio-minerals are composite materials consisting of an inorganic component and an organic matrix – the latter being the decisive component in the characteristics of the end-product (Klaus-Joerger *et al.*, 2001). The current surface-precipitation applications of MCP are large-scale precipitation on concrete or sandstone structures (Castanier *et al.*, 1999). Not denying the success of these technologies, one must also realise that the application thereof is limited by practical and especially economical constraints. Progress in this field, might require a paradigm shift with regards to the possible uses of bio-minerals on surfaces. Mineral precipitation could be useful in altering the aesthetic, physical (strength, porosity), acoustic, insulation, and radiation resistance characteristics of a number of surfaces, certainly not limited to sandstone alone. On the other hand, one should not only consider precipitation, but also the inhibition thereof, as a possible technology. In this regard, multi-national companies such as Bayer® are already developing kitchen products resistant against carbonate scaling, with the active component based on organic macromolecules found in mollusc shells. Similarly, such products can

find numerous applications in medical research, in combating catheter encrustation and mineral precipitation in the urinary tract (stone formation) (Burne and Chen, 2000). But many of these applications are still limited by the possible scale thereof, and it is opined herein that the real field of microbial precipitation is nanotechnology. The development of nano-structured materials is becoming widespread, with specific applications in areas of biomedical sciences, optics, magnetics, and energy sciences (Klaus-Joerger *et al.*, 2001). Lowe (2000) commented that the unique ability of biological systems to control the structure, phase, orientation and nanostructural topography of inorganic crystals make them ideal for nanotechnological applications. While CaCO₃ is often not the mineral of interest in applications, this mineral remains the best model to use (Lowe, 2000).

(4) MCP in biofilm formation and development

Most of the biological mineral precipitation processes described above is in fact biofilm-related precipitation. Both Prof. Bill Costerton (Montana State University) and Prof. Hans-Kurt Flemming (Gerhard-Mercator University Duisburg), share the opinion that the role of mineral precipitation in biofilms are poorly understood, both with regards to the biofilm formation/development, and the industrial impact thereof (personal communication). For example, mineral precipitation can assist the formation of biofilms on “difficult” surfaces such as polished stainless steel, or it can be used as detoxification protection against smart materials such as Cu²⁺ treated surfaces. The controlling function (if any) of microbes in these processes, is an interesting challenge for future research. [Link to Contents](#)

In conclusion, Albert Einstein said “*the supreme task (of the scientist) is to arrive at those universal elementary laws from which the cosmos can be build up by pure deduction. There is no logical path to these laws; only intuition, resting on sympathetic understanding of experience, can reach them...*” The deduction is that there remains a lot of experience to be gained in the field of microbiological CaCO₃ precipitation.

BIBLIOGRAPHY

- Abdelouas, A., Lu, Y.M., Lutze, W. and Nuttall, H.E. (1998). Reduction of U(VI) to U(IV) by indigenous bacteria in contaminated ground water. *Journal of Contaminant Hydrology*, **35**(1-3): 217-233.
- Adolphe, J.P., Loubierre, J.F., Paradas, J., Soleihavoup, F. (1990). Procédé de traitement biologique d'une surface artificielle. European patent, No. 90400G97.0
- Altschul, S.F., Madden, T.L., Schaffer, A.A., Zhang, J., Zhang, Z., Miller, W. and Lipman, D.J. (1997). Gapped BLAST and PSI-BLAST: a new generation of protein database search programs. *Nucleic Acids Research*, **25**: 3389-3402.
- Anderson, S., Appanna, V.D., Huang, J. and Viswanatha, T. (1992). A novel role for calcite in calcium homeostasis. *FEBS Letters*, **308**: 94-96.
- Arp, G., Thiel, V., Reimer, A., Michaelis, W. and Reitner, J. (1999). Biofilm exopolymers control microbialite formation at thermal springs discharging into the alkaline Pyramid Lake, Nevada, USA. *Sedimentary Geology*, **126**(1-4): 159-176.
- Bachmeier, K.L., Williams, A.E., Warmington, J.R. and Bang, S.S. (2002). Urease activity in microbiologically-induced calcite precipitation. *Journal of Biotechnology*, **93**(2): 171-181.
- Bang, S.S., Galinat, J.K. and Ramakrishnan, V. (2001). Calcite precipitation induced by polyurethane-immobilized *Bacillus pasteurii*. *Enzyme and Microbial Technology*, **28**(4-5): 404-409.
- Battistoni, P., De Angelis, A., Pavan, P., Prisciandaro, M. and Cecchi, F. (2001). Phosphorus removal from a real anaerobic supernatant by struvite crystallization. *Water Research*, **35**(9): 2167-2178.
- Bichler, K-H., Eipper, E., Naber, K., Braun, V., Zimmermann, R. and Lahme, S. (2002). Urinary infection stones. *International Journal of Antimicrobial Agents*, **19**(6): 488-498.
- Boon, N., De Windt, W., Verstraete, W. and Top, E.M. (2002). Evaluation of nested PCR-DGGE (denaturing gradient gel electrophoresis) with group-specific 16S rRNA

- primers for the analysis of bacterial communities from different wastewater treatment plants. *FEMS Microbiology Ecology*, **39**: 101-112.
- Boon, N., Goris, J., De Vos, P., Verstraete, W. and Top E.M. (2000). Bioaugmentation of activated sludge by an indigenous 3-chloroaniline degrading *Comamonas testosteroni* strain, I2gfp. *Applied Environmental Microbiology*, **66**: 2906-2913.
- Boon, N., Goris, J., De Vos, P., Verstraete, W. and Top E.M. (2001). Genetic diversity among 3-chloroaniline and aniline degrading strains of the Comamonadaceae. *Applied Environmental Microbiology*, **67**: 1107-1115.
- Booth, I.R., Jones, M.A., McLaggan, D., Nikolaev, Y., Ness, L., Wood, C.M., Miller, S., Töttemeyer, S. and Ferguson, G.P. (1996). Bacterial Ion Channels. In: W.N. Konings, H.R. Kaback, and J.S. Lolkema (Eds.). *Handbook of Biological Physics*, 693-730. Elsevier Amsterdam.
- Boquet, E., Boronat, A. and Ramos-Cormenzana, A. (1973). Production of calcite (calcium carbonate) crystals by soil bacteria is a general phenomenon. *Nature (London)*, **246**: 527-529.
- Boughriet, A., Laureyns, J., Douez, C., Nacer, A. and Langelin, H.R. (2000). SEM and IR and Micro-Raman spectroscopy of solids from uranyl/vaterite/water systems. *Microscopy and Analysis*, **67**: 7-9.
- Boulos, L., Prévost, M., Barbeau, B., Coallier, J. and Desjardins, R. (1999). LIVE/DEAD[®] BacLight^(TM): application of a new rapid staining method for direct enumeration of viable and total bacteria in drinking water. *Journal of Microbiological Methods*, **37**(1): 77-86.
- Bradbury, J. (1998). Nanobacteria may lie at the heart of kidney stones. *The Lancet*, **352**(9122): 121.
- Bradford, M.M. (1976). A rapid and sensitive method for quantitation of microgram quantities of protein utilizing the principle of protein-dye binding. *Annals of Biochemistry*, **72**: 248-254.
- Braissant, O., Verrecchia, E.P. and Aragno, M. (2002). Is the contribution of bacteria to terrestrial carbon budget greatly underestimated? *Naturwissenschaften*, **89**(8): 366-370.
- Brown, S., Sarikaya, M. and Johnson, E. 2000. A genetic analysis of crystal growth. *Journal of Molecular Biology*, **299**(3): 725-735.

-
- Burne, R.A. and Chen Y.Y. (2000). Bacterial ureases in infectious diseases. *Microbes and Infection*, **2**: 533-542.
- Burne, R.A. and Marquis, R.E. (2000). Alkali production by oral bacteria and protection against dental caries. *FEMS Microbiology Letters*, **193**(1): 1-6.
- Camoin, G.F. (1999) Microbial mediation in carbonate diagenesis (editorial). *Sedimentary Geology*, **126**: 1- 4.
- Castanier, S., Le Metayer-Levrel, G. and Loubiere, J.F. 1995. Nouvelles compositions pour mortier biologique, procédé de recouvrement d'une surface ou de comblement d'une cavité a l'aide des compositions. French patent, No. 9505861.
- Castanier, S., Le Métayer-Levrel, G. and Perthuisot, J.P. (1999). Ca-carbonates precipitation and limestone genesis – the microbiologist point of view. *Sedimentary Geology*, **126**: 9-23.
- Collier, J.L., Brahmsha, B. and Palenik, B. (1999). The marine cyanobacterium *Synechococcus* sp. WH7805 requires urease (urea amidohydrolase, EC 3.5.1.5) to utilize urea as a nitrogen source: molecular-genetic and biochemical analysis of the enzyme. *Microbiology* **145**: 447-459.
- Collins, M.D., Love, D.N., Karjalainen, J., Kanervo, A., Forsblom, B., Willems, A., Stubbs, S., Sarkiala, E., Bailey, G.D., Wigney, D.I. and Jousimies-Somer, H. (1994). Phylogenetic analysis of members of the genus *Porphyromonas* and description of *Porphyromonas cangingivalis* sp. nov. and *Porphyromonas cansulci* sp. nov. *International Journal of Systematical Bacteriology*, **44**: 674-679.
- Cooke, A.J., Rowe, R.K., Rittmann, B.E. and Fleming, I.R. (1999). Modeling biochemically driven mineral precipitation in anaerobic biofilms. *Water Science and Technology*, **30**(7): 57-64.
- Dawes, I.W. and Sutherland, I.W. (1993). *Microbial physiology*, 2nd edition. Blackwell Scientific Publications. Oxford, UK.
- Decho, A.W. (2000). Exopolymer microdomains as a structuring agent for heterogeneity within microbial biofilms. In: R. E. Riding and S. M. Awramik (Eds.), *Microbial sediments*, 25-31. Springer-Verlag, Berlin Heidelberg.
- Deer, W.A., Howie, R.A. and Zussman, J. (1966). *An introduction to the rock forming minerals*. Longman Group Limited, London.

- Desrosiers, M.G., Gately, L.J., Gambel, A.M. and Menick, D.R. (1996). Purification and characterisation of the Ca²⁺-ATPase of *Flavobacterium odoratum*. *Journal of Biological Chemistry*, **271**(7): 3945-3951.
- Douglas, S. and Beveridge, T.J. (1998). Mineral formation by bacteria in natural microbial communities. *FEMS Microbiology Ecology*, **26**(2): 79-88.
- Doyle, J.D. and Parsons, S.A. (2002). Struvite formation, control and recovery, *Water Research*, **36**(16): 3925-3940.
- Drew, G.H. (1914). On the precipitation of calcium carbonate in the sea by marine bacteria. Carnegie Publication No. **182**: 7-45, Washington.
- Dupuy, B., Daube, G., Popoff, M.R. and Cole, S.T. (1997) Clostridium perfringens urease genes are plasmid borne. *Infection and Immunity*, **65**(6): 2313-2320.
- Erlich, H.L. (1998). Geomicrobiology: its significance for geology. *Earth-Science Reviews* **45**: 45-60.
- Eswaran, H., Reich, P.F., Kimble, J.M., Beinroth, F.H., Padmanbhan, E. and Moncharoen, P. (2000). Global carbon stocks. In: R. Lal, J. Kimble, H. Eswaran, and B.A. Stewart (Eds.), *Global climate change and pedogenic carbonates*. Lewis publishers, New York.
- Feldmann, M. (1997). Geomicrobial processes in the subsurface: a tribute to Johannes Neher's work. *FEMS Microbiology Reviews*, **20**: 181-189.
- Felske, A., Akkermans, A.D.L. and De Vos, W.M. (1998). In situ detection of an uncultured predominant Bacillus in Dutch grassland soils. *Applied and Environmental Microbiology*, **64**: 4588-4590.
- Felske, A., Wolterink, A., Van Lis, R., De Vos, W.M. and Akkermans, A.D.L. (1999). Searching for predominant soil bacteria: 16S rDNA cloning versus strain cultivation. *FEMS Microbiology Ecology*, **30**: 137-145.
- Ferrer, R.M., Quevedo-Sarmiento, J., Rivadeneyra, M.A., Bejar, V., Delgado, R. and Ramos-Cormenzana, A. (1988). Calcium carbonate precipitation by two groups of moderately halophilic microorganisms at different temperatures and salt concentrations. *Current Microbiology*, **17**: 221-227.
- Ferris, F.G. and Stehmeier, L.G. (1993). Bacteriogenic mineral plugging. US Patent 5.143.155.

- Ferris, F.G., Thompson, J.B. and Beveridge, T.J. (1997). Modern freshwater microbialites from Kelly lake, British Columbia, Canada. *Palaios*, **12**(3): 213-219.
- Ferris, F.G., Wiese, R.G. and Fyfe, W.S. (1994). Precipitation of carbonate minerals by microorganisms – implications for silicate weathering and the global carbon-dioxide budget. *Geomicrobiology Journal*, **12**(1): 1-13.
- Folk, R. (1999). Nannobacteria and the precipitation of carbonate in unusual environments. *Sedimentary Geology*, **126**(1-4): 47-55.
- Fujita, Y., Ferris, F.G., Lawson, R.D., Colwell, F.S. and Smith, R.W. (2000). Calcium carbonate precipitation by ureolytic subsurface bacteria. *Geomicrobiology Journal*, **17**: 305-318.
- Gollapudi, U.K., Knutson, C.L., Bang, S.S. and Islam, M.R. (1995). A new method for controlling leaching through permeable channels. *Chemosphere*, **30**: 695-705.
- Greenberg, A.E., Clesceri, L.S. and Eaton, A.D. (Ed.) (1992). Standard methods for the examination of water and wastewater, 18th ed. American Public Health Association, Washington, D.C.
- Griffiths, R.I., Whiteley, A.S., O'Donnell, A.G. and Bailey, M.J. (2000). Rapid method for coextraction of DNA and RNA from natural environments for analysis of ribosomal DNA- and rRNA-based microbial community composition. *Applied Environmental Microbiology*, **66**: 5488-5491.
- Guellil, A., Thomas, F., Block, J.C., Bersillon, J.C. and Ginestet, P. (2001). Transfer of organic matter between wastewater and activated sludge flocks. *Water Research*, **35**(1): 143-150.
- Habets, L.H.A. and Knelissen, H.J. (1997). In line biological water regeneration in a zero discharge recycle paper mill. *Water Science and Technology*, **35**: 41-48.
- Hedelin, H. (2002). Uropathogens and urinary tract concretion formation and catheter encrustations. *International Journal of Antimicrobial Agents*, **19**(6): 484-487.
- Herbaud, M-L., Guiseppi, A., Denizot, F., Haiech, J. and Kilhoffer, M-C. (1998). Calcium signalling in *Bacillus subtilis*. *Biochimica et Biophysica Acta – Molecular Cell Research*, **1448**(2): 212-226.
- Holland, I.B., Jones, H.E., Cambell, A.K. and Jacq, A. (1999). An assessment of the role of intracellular free Ca²⁺ in *Echerichia coli*. *Biochimie*, **81**: 901-907.

- Hunter, G.K. (1996). Interfacial aspects of biomineralization. *Current Opinion in Solid State and Materials Science*, **1**(3): 430-435.
- Jaffer, Y., Clark, T.A., Pearce, P. and Parsons, S.A. (2002). Potential phosphorus recovery by struvite formation. *Water Research*, **36**(7): 1834-1842.
- Jahns, T. (1996). Ammonium/urea-dependent generation of a proton electrochemical potential and synthesis of ATP in *Bacillus pasteurii*. *Journal of Bacteriology*, **178**(2): 403-409.
- Jukes, T.H. and Cantor, C.R. (1969). Evolution of protein molecules. In: H.N. Munro (ed.), *Mammalian protein metabolism*, 21-132. Academic Press, Inc., New York, N.Y.
- Katkova, V.I. and Rakin, V.I. (1994). Bacterial genesis of calcite. *Journal of Crystal Growth*, **142**(1-2): 271-274.
- Kaufman, E.N., Little, M.H. and Selvaraj, P.J. (1996). Recycling of FGD gypsum to calcium carbonate and elemental sulphur using mixed sulphate-reducing bacteria with sewage digest as carbon source. *Journal of Chemical Technology and Biotechnology*, **66**(4): 365-374.
- Kawaguchi, T. and Decho, A.W. (2002). A laboratory investigation of cyanobacterial extracellular polymeric secretions (EPS) in influencing CaCO₃ polymorphism. *Journal of Crystal Growth*, **240**(1-2): 230-235.
- Kielemoes, J., Bultinck, I., Storms, H., Boon, N. and Verstraete, W. (2002). Occurrence of manganese-oxidizing microorganisms and manganese deposition during biofilm formation on stainless steel in a brackish surface water. *FEMS Microbiology Ecology*, **39**(1): 41-55.
- Kile, D.E., Eberl, D.D., Hoch, A.R. and Reddy, M.M. (2000). An assessment of calcite crystal growth mechanisms based on crystal size distributions. *Geochimica et Cosmochimica Acta*, **64**(17): 2937-2950.
- Klaus-Joerger, T., Joerger, R., Olsson, E. and Granqvist, C.G. (2001). Bacteria as workers in the living factory: metal accumulating bacteria and their potential for material science. *Trends in Biotechnology*, **19**: 15-20.
- Knorre, H. and Krumbein, W. (2000). Bacterial calcification. In: R. E. Riding and S. M. Awramik (Eds.), *Microbial sediments*, 25-31. Springer-Verlag, Berlin Heidelberg.
- Kowalchuk, G.A., Bodelier, Heilig, P.L.E., Stephen, G.H.J. and Laanbroek, H.J. (1998). Community analysis of ammonia-oxidising bacteria, in relation to oxygen

- availability in soils and root-oxygenated sediments, using PCR, DGGE and oligonucleotide probe hybridisation. *FEMS Microbiology Ecology*, **27**: 339-350.
- Kramer, G., Klingler, H.C., and Steiner, G.E. (2000). Role of bacteria in the development of kidney stones (review article). *Current Opinion in Urology*, **10**(1): 35-38.
- Lal, R., Kimble, J., Eswaran, H. and Stewart, B.A. (Eds.) (2000). Global climate change and pedogenic carbonates. Lewis publishers, New York.
- Langelier, W.F. (1937). The analytical control of anti-corrosion water treatment. *Journal of the American Water Works Association*, **28**: 1500 – 1521.
- Le Métayer-Levrel, G., Castanier, S., Oriol, G., Loubière, J-F. and Perthuisot, J-P. (1999). Applications of bacterial carbonatogenesis to the protection and regeneration of limestone in buildings and prehistoric patrimony. *Sedimentary Geology* **126** (1-4): 25-34.
- Lloyd, J.R. and Lovley, D.R. (2001). Microbial detoxification of metals and radionuclides. *Current Opinion in Biotechnology*, **12**: 248-253.
- Lowe, C.R. (2000). Nanobiotechnology: the fabrication and applications of chemical and biological nanostructures. *Current Opinion in Structural Biology*, **10**(4): 428-434.
- Machel, H.G. (2001). Bacterial and thermochemical sulfate reduction in diagenetic settings – old and new insights. *Sedimentary Geology*, **140**(1-2): 143-175.
- Maidak, B.L., Cole, J.R., Lilburn, T.G., Parker, C.T. Jr., Saxman, P.R., Farris, R.J., Garrity, G.M., Olsen, G.J., Schmidt, T.M. and Tiedje, J.M. (2001). The RDP-II (Ribosomal Database Project). *Nucleic Acids Research*, **29**(1): 173-174.
- Maliva, R.G., Missimer, T.M., Leo, K.C., Statom, R.A., Dupraz, C., Lynn, M. and Dickson, J.A.D. (2000). Unusual calcite stromatolites and pisoids from a landfill leachate collection system. *Geology*, **28**(10): 931-934.
- McConnaughey, T.A. and Whelan, F.F. (1997). Calcification generates protons for nutrient and bicarbonate uptake. *Earth-Science Reviews*, **42**: 95-117.
- McGenity, T.J. and Sellwood, B.W. (1999). New approaches to studying the microbial precipitation of carbonate minerals. *Sedimentary Geology*, **126**: 5-8.
- McKay, D.S., Gibson, E.K. Jr., Thomas-Keprta, K., Vali, H., Romanek, C.S., Clemett, S.J., Chillier, X.D.F., Maechling, C.R. and Zare, R.N. (1996). Search for past life on Mars: possible relic biogenic activity in Martian meteorite ALH84001. *Science*, **273**: 924-930.

- Merz-Preiß. (2000). Calcification in cyanobacteria. In: R. E. Riding and S. M. Awramik (Eds.), *Microbial sediments*, 50-57. Springer-Verlag, Berlin Heidelberg.
- Miksch, G., Arnold, W., Lentzsch, P., Priefer, U.B. and Puhler, A. (1994), A 4.6 kb DNA region of *Rhizobium meliloti* involved in determining urease and hydrogenase activities carries the structural genes for urease (ureA, ureB, ureC) interrupted by other open reading frames. *Molecular Genetics and Genomics*, **242**(5): 539-550.
- Mobley, H.L.T. and Hausinger, R.P. (1989). Microbial ureases: significance, regulation and molecular characterisation. *Microbiological reviews*, **53**(1): 85-108.
- Mobley, H.L.T., Island, M.D. and Hausinger, R.P. (1995). Molecular biology of microbial ureases. *Microbiological Reviews*, **59**: 451-480.
- Monger, H.C. and Gallegos, R.A. (2000). Biotic and abiotic processes and rates of pedogenic carbonate accumulation. In: R. Lal, J. Kimble, H. Eswaran, and B.A. Stewart (Eds.). *Global climate change and pedogenic carbonates*, Lewis publishers, New York..
- Monteny, J., Vincke, E., Beeldens, A., De Belie, N., Taerwe, L., Van Gemert, D. and Verstraete, W. (2000). Chemical, microbiological, and *in situ* test methods for biogenic sulfuric acid corrosion of concrete. *Cement and Concrete Research*, **30**(4): 623-634.
- Morita, R.Y. (1980). Calcite precipitation by marine bacteria. *Geomicrobiology Journal*, **2**: 63-82.
- Morizot, A., Neville, A. and Hodgkiess, T. (1999). Studies of the deposition of CaCO₃ on a stainless steel surface by a novel electrochemical technique. *Journal of Crystal Growth*, **198/199**: 738-743.
- Morse, J.W. and Arvidson, R.S. (2002). The dissolution kinetics of major sedimentary carbonate minerals. *Earth-Science Reviews*, **58**(1-2): 51-84.
- Muyzer, G., De Waal, E.C. and Uitterlinden, A. (1993). Profiling of complex microbial populations using denaturing gradient gel electrophoresis analysis of polymerase chain reaction-amplified genes coding for 16S rRNA. *Applied Environmental Microbiology*, **59**: 695-700.
- Nebel, B.J. and Wright, R.T. (1998). Environmental Science, 6th edition. Prentice Hall Inc. New Jersey, USA.
- Nilsson, Ö. and Sternbeck, J. (1999). A mechanistic model for calcite crystal growth using surface speciation. *Geochimica et Cosmochimica Acta*, **63**(2): 217-225.

- Norris, V., Grant, S., Freestone, P., Canvin, J., Sheikh, F.N., Toth, I., Trinei, M., Modha, K. and Norman, N. (1996). Calcium signalling in bacteria. *Journal of Bacteriology*, **178**(13): 3677-3682.
- Novitsky, J.A. (1981). Calcium-carbonate precipitation by marine bacteria. *Geomicrobiology Journal*, **2**(4): 375-388.
- Øvreas, L., Forney, L., Daae, F.L. and Torsvik, V. (1997). Distribution of bacterioplankton in meromictic lake Saelevannet, as determined by denaturing gradient gel electrophoresis of PCR-amplified gene fragments coding for 16S rRNA. *Applied Environmental Microbiology*, **63**: 3367-3373.
- Parraga, J., Rivadeneyra, M.A., Delgado, R., Iniguez, J., Soriano, M. and Delgado, G. (1998). Study of biomineral formation by bacteria from soil solution equilibria. *Reactive & Functional Polymers*, **36**: 265-271.
- Paster, B.J., Dewhirst, F.E., Olsen, I. and Fraser, G.J. (1994). Phylogeny of *Bacteroides*, *Prevotella*, and *Porphyromonas* spp. and related bacteria. *Journal of Bacteriology*, **176**: 725-732.
- Peckman, J., Paul, J. and Thiel, V. (1999). Bacterially mediated formation of diagenetic aragonite and native sulphur in Zechstein carbonates (Upper Permian, Central Germany). *Sedimentary Geology*, **126**: 205-222.
- Peiffer, W.E., Desrosiers, M.G. and Menick, D.R. (1996). Cloning and expression of the unique Ca^{2+} -ATPase from *Flavobacterium odoratum*. *Journal of Biological Chemistry*, **271**: 5095-5100.
- Plant, L.J. and House, W.A. (2002). Precipitation of calcite in the presence of inorganic phosphate. *Colloids and Surfaces A: Physicochemical and Engineering Aspects*, **203**: 143-153.
- Ramachandran, S.K., Ramakrishnan, V. and Bang, S.S. (2001). Remediation of concrete using micro-organisms. *ACI Materials Journal*, **98**(1): 3-9.
- Raeymaekers, L., Wuytack, E.Y., Willems, I., Michiels, C.W. and Wuytack, F. (2002). Expression of a P-type Ca^{2+} -transport ATPase in *Bacillus subtilis* during sporulation. *Cell Calcium*, **32**(2): 93-103.
- Reed, K.E. (2001). Restriction enzyme mapping of bacterial urease genes: using degenerate primers to expand experimental outcomes. *Biochemistry and Molecular Biology Education*, **29**: 239-244.

-
- Riding, R.E. and Awramik, S.M. (Eds.) (2000). *Microbial Sediments*. Springer-Verlag, Berlin Heidelberg, New York.
- Rivadeneira, M.A., Delgado, R., Del Moral, A., Ferrer, R.M. and Ramos-Cormenzana, A. (1994). Precipitation of calcium carbonate by *Vibrio* spp. from an inland saltern. *FEMS Microbiology Ecology*, **13**: 197-204.
- Rivadeneira, M.A., Delgado, G., Ramos-Cormenzana, A. and Delgado, R. (1998). Biomineralisation of carbonates by *Halomonas eurihalina* in solid and liquid media with different salinities: crystal formation sequence. *Research in Microbiology*, **149**: 277-287.
- Rivadeneira, M.A., Delgado, G., Soriano, M., Ramos-Cormenzana, A. and Delgado, R. (2000). Precipitation of carbonates by *Nesterenkonia halobia* in liquid media. *Chemosphere*, **41**: 617-624.
- Rodriguez-Navarro, C., Sebastian, E., Rodriguez-Gallego, M. (1997). An urban model for dolomite precipitation: authentic dolomite on weathered building stones. *Sedimentary Geology*, **109**: 1-11.
- Ruimy, R., Podglajen, I., Breuil, J., Christen, R. and Collatz, E. (1996). A recent fixation of *cfiA* genes in a monophyletic cluster of *Bacteroides fragilis* is correlated with the presence of multiple insertion elements. *Journal of Bacteriology*, **178**(7): 1914-1918.
- Saitou, N. and Nei, M. (1987). The neighbour-joining method: a new method for reconstructing phylogenetic trees. *Molecular Biology and Evolution*, **4**: 406-425.
- Sakamoto, T., Delgado, V.B. and Bryant, D.A. (1998). Growth on urea can trigger death and peroxidation of the cyanobacterium *Synechococcus* sp. strain PCC 7002. *Applied Environmental Microbiology*, **64**(7): 2361-2366.
- Sawyer, C.N., McCarty, P.L. and Parkin, G.F. (1994). *Chemistry for environmental engineering*, 4th Edition. McGraw-Hill Inc. New York, 658 pages.
- Schultze-Lam, S., Fortin, D., Davis, B.S. and Beveridge, T.J. (1996). Mineralisation of bacterial surfaces. *Chemical Geology*, **132**: 171-181.
- Sebbane, F., Devalckenaere, A., Foulon, J., Carniel, E. and Simonet, M. (2001). Silencing and reactivation of urease in *Yersinia pestis* is determined by one G residue at a specific position in the *ureD* gene. *Infection and Immunity*, **69**(1): 170-176.

- Smith, D.G.E., Russel, W.C., Ingledew, W.J. and Thirkell, D. (1993). Hydrolysis of urea by *Ureaplasma urealyticum* generates a transmembrane potential with resultant ATP synthesis. *Journal of Bacteriology*, **175**: 3253-3258.
- Sondi, I. and Matijevic, E. (2001). Homogeneous precipitation of calcium carbonates by enzyme catalyzed reaction. *Journal of Colloid and Interface Science*, **238**: 208-214.
- Southam, G. (2000). Bacteria surface-mediated mineral formation. In: D. R. Lovley (ed.), *Environmental microbe-metal interactions*. ASM Press, Washington D.C.
- Stanley, J., Linton, D., Burnens, A.P., Dewhirst, F.E., Owen, R.J., Porter, A., On, S.L. and Costas, M. (1993). *Helicobacter canis* sp. nov., a new species from dogs: An integrated study of phenotype and genotype. *Journal of General Microbiology*, **139**: 2495-2504.
- Stocks-Fisher, S., Galinat, J. K. and Bang, S.S. (1999). Microbiological precipitation of CaCO₃. *Soil Biology & Biochemistry*, **31**: 1563-1571.
- Stolz, J.F. (2000). Structure of microbial mats and biofilms. In: R. E. Riding and S. M. Awramik (Eds.), *Microbial sediments*, 1-9. Springer-Verlag, Berlin Heidelberg.
- Stumm, W. and Morgan, J.J. (1981). *Aquatic Chemistry*, 2nd Edition. John Wiley, New York.
- Suzuki, K., Tanaka, Y., Osada, T. and Waki, M. (2002). Removal of phosphate, magnesium and calcium from swine wastewater through crystallisation enhanced by aeration. *Water Research*, **36**: 2991-2998.
- Tiano, P., Biagiotti, L. and Mastromei, G. (1999). Bacterial bio-mediated calcite precipitation for monumental stones conservation: methods of evaluation. *Journal of Microbiological Methods*, **36**: 139-145.
- Trewin, N.H. and Knoll, A.H. (1999). Preservation of Devonian chemotrophic filamentous bacteria in calcite veins. *Palaios*, **14**: 288-294.
- Urzi, C., Garcia-Valles, M., Vendrell, M. And Pernice, A. (1999). Biomineralisation processes on rock and monument surfaces observed in field and in laboratory conditions. *Geomicrobiology Journal*, **16**(1): 39-54.
- Valls, M. and De Lorenzo, V. (2002). Exploiting the genetic and biochemical capacities of bacteria for the remediation of heavy metal pollution. *FEMS Microbiology Reviews*, **26**: 327-338.

- Van Haandel, A.C. and Lettinga, G.L. (1994). Anaerobic sewage treatment. A practical guide for regions with a hot climate. John Wiley & Sons, Chichester.
- Van Langerak, E.P.A., Gonzalez-Gil, G., Van Aelst, A., Van Lier, J.B., Hamelers, H.V.M. and Lettinga, G. (1998). Effects of high calcium concentrations on the development of methanogenic sludge in upflow anaerobic sludge bed (UASB) reactors. *Water Research*, **32**: 1255-1263.
- Van Langerak, E.P.A., Hamelers, H.V.M. and Lettinga, G. (1997). Influent calcium removal by crystallization reusing anaerobic effluent alkalinity. *Water Science and Technology*, **36**: 341-348.
- Vauterin, L., Yang, P., Hoste, B., Vancanneyt, M., Civerolo, E.L., Swings, J., and Kersters, K. (1991). Differentiation of *Xanthomonas campestris* pv. citri strains by sodium dodecyl sulphate-polyacrylamide gel electrophoresis of proteins, fatty acid analysis, and DNA-DNA hybridisation. *International Journal of Systematic Bacteriology*, **41**: 535-542.
- Vecht, A. and Ireland, T.G. (2000). The role of vaterite and aragonite in the formation of pseudo-biogenic carbonate structures: implications for Martian exobiology. *Geochimica et Cosmochimica Acta*, **66**: 2719-2725.
- Vreeland, R.H., Rosenzweig, W.D. and Powers, D.W. (2000). Isolation of a 250 million-year-old halotolerant bacterium from a primary salt crystal. *Nature*, **407**: 897-900.
- Warren, L.A., Maurice, P.A., Parmar, N. and Ferris, F.G. (2001). Microbially mediated calcium carbonate precipitation: Implications for interpreting calcite precipitation and for solid-phase capture of inorganic contaminants. *Geomicrobiology Journal*, **18**: 93-115.
- Warren, L.A. and Haack, E.A. (2001). Biochemical controls on metal behaviour in freshwater environments. *Earth-Science Reviews*, **54**: 261-320.
- Warscheid, T. and Braams, J. (2000). Biodeterioration of stone: a review. *International Biodeterioration and Biodegradation*, **46**(4): 343 – 368.
- Warthmann, R., Van Lith, Y., Vasconcelos, C., McKenzie, J.A. and Karpoff, A.M. (2000). Bacterial induced dolomite precipitation in anoxic culture experiments. *Geology*, **28**(12): 1091-1094.
- Watube, N. and Wilbur, K.M. (1960). Influence of the organic matrix on crystal types in molluscs. *Nature*, **188**: 334.

- Westfall, F. (1999). The nature of fossil bacteria: A guide to the search for extraterrestrial life. *Journal of Geophysical Research – Planets*, **104**: 16437-16451.
- Whalen, M.T., Day, J., Eberli, G.P. and Homewood, P.W. (2002). Microbial carbonates as indicators of environmental change and biotic crises in carbonate systems: examples from the Late Devonian, Alberta basin, Canada. *Palaeogeography, Palaeoclimatology, Palaeoecology*, **181**: 127-151.
- Wong, L., Sissons, C.H., Pearce, E.I.F. and Cutress, T.W. (In Press) Calcium phosphate deposition in human dental plaque microcosm biofilms induced by a ureolytic pH-rise procedure. *Archives of Oral Biology*.
- Wright, D.T. (1999). The role of sulphate-reducing bacteria and cyanobacteria in dolomite formation in distal ephemeral lakes of the Coorong region, South Australia. *Sedimentary Geology*, **126**(1-4): 147-157.
- Yan, X. (1999). Assessment of calcareous alga *Corallina pilulifera* as elemental provider. *Biomass & Bioenergy*, **16**: 357-360.
- Yates, K.K. and Robbins, L.L. (1999). Radioisotope tracer studies of inorganic carbon and Ca in microbiologically derived CaCO₃. *Geochimica and Cosmochimica Acta*, **63**(1): 129-136.
- You, S.H., Tseng, D.H. and Guo, G.L. (2001). A case study on the wastewater reclamation and reuse in the semiconductor industry. *Resources, Conservation and Recycling*, **32**: 73-81.
- Yu, H.Q., Tay, J.H. and Fang, H.H. (2001). The roles of calcium in sludge granulation during UASB reactor start-up. *Water Research*, **35**: 1052-1060.

FREDERIK HAMMES

Laboratory of Microbial Ecology and
Technology (LabMET); Coupure Links;
653; B-9000 Gent; Belgium

fhammes@hotmail.com

PERSONAL

Date of birth: 1975-10-15
Gender: Male
Marital status: Not married
Nationality: South African
Languages: Afrikaans, English, Dutch/Flemish

EDUCATION

1998 - 2002 Ghent University (Ghent, Belgium)

Ph.D. research (Microbial Ecology & Technology)
Ureolytic microbial calcium carbonate (CaCO₃)
precipitation
Promoters: Prof. W. Verstraete, Prof. S. Siciliano

2000 - 2002 Ghent University (Ghent, Belgium)

Ph.D. study program
(Program requiring a selection of academic courses,
publications in peer-reviewed journals, conference
attending etc.)

1997 - 1998 Ghent University (Ghent, Belgium)

GAS Milieuwetenschappen en Technologieën
(Course-orientated M.Sc. level degree in Environmental
Science and Technology)
Thesis: Biofilm formation and development on stainless
steel (Promoter: Prof. W. Verstraete)

Graduated with distinction

Awarded the SIDMAR environmental award for best research thesis for the academic year 1997 - 1998

1994 - 1997 University of Pretoria (Pretoria, South Africa)

B.Sc. (Microbiology)

1989 - 1993 Hoërskool F.H. Odendaal (Pretoria, South Africa)

Matriculated with distinctions in Mathematics, Science, Biology and Latin

WORK EXPERIENCE

1998-2002 Collaborator of several research projects commissioned by Jansens Pharmaceutica, Dredging n.v., The European Space Agency (ESA), OWS, Avecom and Procter & Gamble

- **Procter&Gamble and OWS n.v. (Belgium):** Research project on the washing-removal of heavy metals from contaminated soils using EDDS as chelating agent. The project involved standard chemical laboratory procedures as well as innovative research opportunities, within a rather large team of stakeholders.
- **Procter&Gamble (Belgium):** Management of a research project on the microbiological susceptibility of activated carbon based drinking water filter systems. This project involved standard water-microbiological testing over a 3-month period.
- **Dredging n.v. (Belgium):** Management of the final year of a four-year project on possible uses of dredging sludge. This also encompassed the management of two thesis students and a technician working on the project.
- **Jansens Pharmaceutica (Belgium):** Biological treatment of the pesticide Imazalil in an activated carbon biomembrane reactor. Primarily reactor-operation and basic analysis.
- **European Space Agency (ESA):** Primarily consultant based project on the potential conversion of space developed Biological Life Support Systems (BLS Technologies for terrestrial applications in domestic wastewater treatment systems.

1998-2002 Tutored 2 bio-engineer students, 1 GAS student, 1 master's student and 1 laboratory technician, during training and completion of their theses.

SPECIFIC SKILLS

General laboratory practice and management

- Including basic classic microbiological techniques, standard wastewater analysis, spectrophotometric analysis, flame atomic adsorption spectrometry, etc.

Lab-scale reactor design

- Hands-on experience with design and operation of sequential batch reactors (SBR), set-up and operation of lab-scale anaerobic reactors (UASB), and set-up and operation of flow-cells for biofilm development

Microscopy

- Four years extensive experience of light microscopy and fluorescence microscopy including activated and anaerobic sludge analysis, biofilm analysis and Live/Dead and other fluorescent staining techniques
- Extensive experience in use of digital image analysis software for both light and fluorescent microscopy images

Molecular microbiology

- Hands-on knowledge of polymerase chain reaction (PCR) techniques
- Hands-on knowledge of denaturing gradient gel electrophoresis (DGGE)
- Basic know-how of sequence analysis software and constructing of phylogenetic trees

Software

- Microsoft Office
- SigmaPlot
- MicroImage (Digital Image Analysis)

SCIENTIFIC OUTPUT

Publications

J. KIELEMOES, F. HAMMES and W. VERSTRAETE. 1998. Selective biofilm formation and development on stainless steel. Proc. Part I of the 12th Forum for Applied Biotechnology 1998, 24-25 September 1998, Belgium. Pp. 1137-1145. Med. Fac. Landbouww. Univ. Gent, 63/4a, 1998, Pp. 1137-1145.

J. KIELEMOES, F. HAMMES and W. VERSTRAETE. 1998. Measurement of microbial colonisation of two types of stainless steel. Environmental Technology 21, 831 - 843.

F. HAMMES, Y. KALOGO and W. VERSTRAETE. 2000. Anaerobic digestion technologies for closing the domestic water, carbon and nutrient cycles. Water Sc. Technol. 41, 203-211.

J. KIELEMOES, F. HAMMES and W. VERSTRAETE. 2000. Measurement of microbial colonisation of two types of stainless steel. Environmental Technology 21, 831-843.

Y. KALOGO, F. ROSILLON, F. HAMMES and W. VERSTRAETE. 2000. Effect of a water extract of Moringa oleifera seeds on the hydrolic microbial species diversity of a UASB reactor treating domestic wastewater. Letters in Applied Microbiology 31, 259 - 264.

P. VANDEVIVERE, F. HAMMES, W. VERSTRAETE, T. FEIJTEL and D. SCHOWANEK. 2001. Metal decontamination of soil, sediment, and sewage sludge by means of transition metal chelant [S,S]-EDDS. J. Env. Eng. 127, 802-811.

M.A. SEKA, Y. KALOGO, F. HAMMES, J. KIELEMOES and W. VERSTRAETE. 2001. Chlorine-susceptible and chlorine-resistant type 021N bacteria occurring in bulking activated sludges. Appl. Environ. Microbiol. 67, 5303-5307.

F. HAMMES and W. VERSTRAETE. 2002. Key roles of pH and calcium metabolism in microbial carbonate precipitation. Re/Views I Environmental Science & Bio/Technology 1, 3-7.

F. HAMMES, A. SEKA, S. DE KNIF and W. VERSTRAETE. A novel approach to calcium removal from calcium-rich industrial wastewater. Water Research (*In press*).

F. HAMMES, A. SEKA, K. VAN HEGE, T. VAN DE WIELE, J. VANDERDEELEN, S.D. SICILIANO and W. VERSTRAETE. Calcium removal from industrial wastewater by bio-catalytic CaCO₃ precipitation. *Submitted to the Journal of Chemical Technology and Biotechnology.*

F. HAMMES, N. BOON, G. CLEMENT, J. DE VILLIERS, S.D. SICILIANO and W. VERSTRAETE. A bio-catalytic calcification (BCC) reactor as model for ureolytic microbial CaCO₃ precipitation. *Submitted to Applied Microbiology and Biotechnology (October 2002).*

F. HAMMES, N. BOON, J. DE VILLIERS, S.D. SICILIANO and W. VERSTRAETE. Strain-specific ureolytic microbial calcium carbonate (CaCO₃) precipitation by different isolates from the *Bacillus sphaericus* group. *Submitted to Applied and Environmental Microbiology (October 2002).*

Participation in symposia, conferences, posters etc.

J. KIELEMOES, F. HAMMES and W. VERSTRAETE. 1998. Initial biofilm formation and development on stainless steel. First COST (European co-operation in the field of scientific and technical research) 520 workshop concerning biofouling and materials. 26 - 29 August 1998, Trento, Italy. (*poster presentation*)

J. KIELEMOES, F. HAMMES and W. VERSTRAETE. 1998. Heterogeneity and microbiologically driven corrosion. Twelve forum of Applied Biotechnology (FAB), 24 - 25 September, Bruges, Belgium. (*poster presentation*)

J. KIELEMOES, F. HAMMES and W. VERSTRAETE. 1998. Selective biofilm formation and development on stainless steel. Fourth PhD symposium of the Faculty of Applied Biological Sciences, Ghent University, 7 October 1998, Ghent, Belgium. (*poster presentation*)

A. SEKA, F. HAMMES, J. KIELEMOES and W. VERSTRAETE. 1999. New method for assessment of biocide efficacy on filamentous bulking sludge. Thirteenth Forum of Applied Biotechnology (FAB), September 1999, Ghent, Belgium. (*Poster presentation*)

F. HAMMES, Y. KALOGO and W. VERSTRAETE. 2000. Anaerobic digestion technologies for closing the domestic water, carbon and nutrient cycles. *Water Sc. Technol.* 41, 203-211.

F. HAMMES, D. DEMEY, V. HERMANS and W. VERSTRAETE. 1999. Status & future needs: biological techniques (introductory lecture). In: ESA Workshop on Advanced Life Support. pp. 175-180. ESTEC, Noordwijk (The Netherlands), 13-14 April 1999.

F. HAMMES, N. BOON and W. VERSTRAETE. 2001. Calcium interaction with bacteria at alkaline pH regimes. In: Abstracts "9th International Symposium on Microbial Ecology (ISME-9)", Amsterdam, The Netherlands. p. 137.

F. HAMMES and W. VERSTRAETE. 2001. Bacterial calcium metabolism as the key to microbial carbonate precipitation (MCP). 13th Forum for Applied Biotechnology(FAB), Het Pand, Ghent, Belgium. 22-23 September 1999. (*poster presentation*) (* Awarded best-poster of the conference)

F. HAMMES and W. VERSTRAETE. 2001. Bio-catalytic calcification technology for calcium removal from industrial wastewater. 13th Forum for Applied Biotechnology(FAB), Het Pand, Ghent, Belgium. 22-23 September 1999. (*poster presentation*)

F. HAMMES, E. VINCKE and W. VERSTRAETE. 2002. Microorganisms and concrete: friends or enemies. Concrete for a Sustainable Agriculture - Agro-, Aqua- and Community Applications. Het Pand, Ghent, Belgium. 21-24 April 2002.

AWARDS

SIDMAR ENVIRONMENTAL AWARD

- Awarded for best M.Sc. thesis of the academic year 1997 - 1998 for the study program GAS Milieuwetenschappen en Technologiën.

ALTRAN AWARD

- LabMET was awarded the second prize in the annual ALTRAN AWARDS FOR INNOVATION (July 1999). Frederik Hammes coordinated and managed the project writing for this.

13th FORUM OF APPLIED BIOTECHNOLOGY

- Awarded first prize for best poster at the conference (Ghent, Belgium. 22-23 September 1999)